14 Electrocardiography

DAVID M. MIRVIS AND ARY L. GOLDBERGER

The technology and the clinical value of the electrocardiogram (ECG or, as sometimes referred to, EKG) have continuously evolved since the invention of the string galvanometer by Einthoven in 1901. The ECG soon became the most commonly used cardiac diagnostic test, and it remains the fundamental method to assess the heart's electrical activity. This chapter provides an overview of the pathophysiology, the diagnostic criteria, and the utility of the most common ECG diagnoses in adults.

FUNDAMENTAL PRINCIPLES

The ECG is the outcome of a complex series of physiologic and technologic processes. First, transmembrane ionic currents are generated by ion fluxes across cell membranes and between adjacent cells. These currents are synchronized during cardiac activation and recovery sequences to generate a physiologically meaningful, time-varying electrical field in and around the heart.

Electrodes placed in specific locations on the extremities and torso detect the currents reaching the skin. These electrodes are configured to produce *leads*. The outputs of these leads are then amplified, filtered, digitized, and displayed to produce an ECG recording. These signals are typically analyzed by signal processing and pattern recognition software to provide a preliminary interpretation that is then subject to careful clinician review.

Genesis of Cardiac Electrical Fields

Ionic Currents and Cardiac Electrical Fields During Activation. Transmembrane ionic currents (see Chapter 62) are ultimately responsible for the potentials recorded as an ECG. As sites along a cardiac fiber are activated, the polarity of the transmembrane potential converts from negative (with the inside of the cell negative relative to the outside) to positive (with the inside of the cell positive relative to the outside of the cell), as represented in the typical cardiac action potential. Thus, sites on a cardiac fiber that have undergone excitation have positive transmembrane potentials, whereas more distal sites remaining in a resting state have negative transmembrane potentials (see Fig. 62.1).

This reversal of polarity along a fiber creates a flow of positively charged intracellular current from the already activated to the more distal, inactivated portions of the fiber. As activation of multiple adjacent fibers proceeds in synchrony, an activation *wavefront* is produced that moves in the direction of activation and that generates an electrical field characterized by positive potentials ahead and negative potentials behind it (see Fig. 62.7).

An electrode senses positive potential when an activation front is moving toward it and senses negative potentials when the activation front is moving away from it. The magnitude of the potential recorded by an electrode at any site is (1) directly proportional to the average rate of change of intracellular potential as determined by the action potential shape; (2) directly proportional to the size of the wavefront; (3) inversely proportional to the square of the distance from the activation front to the recording site; and (4) directly proportional to the cosine of the angle between the direction of activation spread and a line drawn from the site of activation to the recording site. Thus, if activation proceeds directly toward an electrode such that the angle between the direction of activation and the location of the electrode equals zero (and its cosine equals 1), the voltage sensed by the electrode will be maximal. In contrast, if activation proceeds in a direction perpendicular to that direction (cosine = 0), the sensed potential will be zero.

Cardiac Electrical Field Generation During Recovery. The cardiac electrical field during recovery differs in several important ways from that during activation. First, the gradient of intercellular potentials and thus the direction of current flow during recovery are the opposite of those described for activation. As a cell undergoes recovery, its intracellular potential becomes progressively more negative. For a cardiac fiber, the intracellular potential of the region whose recovery has progressed further (usually modelled as the region activated first) is more negative than that of the adjacent, less recovered region. Intracellular currents then flow from the less recovered toward the more recovered portion of the fiber. That is, recovery wavefronts will have an orientation opposite that of activation wavefronts.

Second, the strengths of the recovery wavefronts during recovery are lower than during activation. As noted, the strength of a wavefront is proportional to the rate of change in transmembrane potential. Rates of change in transmembrane potential during the recovery phases are considerably slower than during activation, and the strength of the resulting wavefront is lower.

Third, the rate of movement of the recovery wavefronts is much slower than that of activation fronts. Activation is rapid and occurs over only a small short length of the fiber. Recovery, by contrast, lasts 100 msec or longer and occurs simultaneously over extensive portions of the heart. Hence, the overall duration of the recovery waveforms will be longer than that of activation.

These features result in ECG differences between activation and recovery patterns. All other factors being equal (an assumption often not true, as described later), waveforms generated during recovery of a fiber with uniform recovery properties would be of opposite polarity, lower amplitude, and longer duration than those generated by activation.

Role of Transmission Factors. The activation and recovery fields are significantly perturbed by the complex three-dimensional physical environment in which they are generated. These *transmission factors* include the biophysical characteristics of the heart itself as well as those of the surrounding organs and tissues.

An important *cardiac factor* is the presence of connective tissue between cardiac fibers that disrupts efficient electrical coupling of adjacent fibers. Waveforms generated in fibers with little or no intervening connective tissue are narrow in width and smooth in contour, whereas those recorded from tissues with abnormal fibrosis are prolonged and may exhibit prominent notching.

Extracardiac factors include the effects of all the tissues and structures that lie between the activation region and the body surface, including intracardiac blood, lungs, skeletal muscle, subcutaneous fat, and skin. These tissues alter the intensity and the orientation of the wavefronts as they travel across them.

Physical factors reflect basic laws of physics. Potential magnitudes change in proportion to the square of the distance between the heart and recording electrode. In humans, the right ventricle (RV) and anteroseptal aspect of the left ventricle (LV) are closer to the anterior chest wall than are other parts of that chamber. Therefore, ECG potentials will be higher on the anterior than on the posterior chest, and the amplitudes of waveforms projected from the anterior LV to the chest wall will be greater than those generated by posterior LV regions.

An additional physical factor affecting the recording of cardiac signals is *cancellation*. When two or more wavefronts are simultaneously active, as is common during activation, the vectoral components of the wavefronts may augment (if oriented in the same directions) or cancel

(if oriented in opposite directions) each other when viewed from remote electrode positions. The magnitude of this effect is substantial. During the inscription of the QRS wave, as much as 90% of cardiac activity is obscured by cancellation effects.

As a result of these factors, surface recordings have an amplitude of only 1% of the amplitude of transmembrane potentials, are smoothed in detail so that they have only a general spatial relationship to the underlying cardiac events, and preferentially reflect electrical activity in some cardiac regions over others.

Recording Electrodes and Leads Systems

Electrode Characteristics. The standard clinical ECG is recorded from electrodes placed on each of the four extremities and from six placed on the chest.[1] These electrodes are connected to form *leads* that record the potential difference between two electrodes. One electrode is designated as the positive input. The potential at the other (negative) electrode is subtracted from the potential at the positive electrode to yield the *bipolar potential*. The actual potential at either electrode is not known; only the difference between them is recorded.

In some cases, as described later, multiple electrodes are electrically connected together to form the negative member of the bipolar pair. This electrode network is commonly referred to as a *compound* or *reference electrode*. The lead then records the potential difference between a single electrode serving as the positive input (the *exploring electrode*) and the potential in the reference electrode.

The clinical ECG is performed using 12 leads: three standard *limb leads* (leads I, II, and III), six *precordial leads* (leads V_1 through V_6), and three *augmented limb leads* (leads aVR, aVL, and aVF). Specifics of electrode placement and definitions of the positive and negative inputs for each lead are presented in Table 14.1.

Standard Limb Leads. The standard limb leads record the potential differences between two limbs, as detailed in Table 14.1 and illustrated in Figure 14.1(top). Lead I registers the potential difference between the left arm (positive electrode) and right arm (negative electrode); lead II displays the potential difference between the left leg (positive electrode) and right arm (negative electrode); and lead III records the potential difference between the left leg (positive electrode) and left arm (negative electrode). The electrode on the right leg serves as an electronic reference that reduces noise and is not included in these lead configurations. Limb electrodes should be placed near the wrists and ankles or, at a minimum, distal to the shoulders and hips.

The electrical connections for each of these leads can be represented as a vector oriented from its negative toward its positive pole. These vectors form a triangle, known as the *Einthoven triangle*, in which the potential in lead II equals the sum of potentials sensed in leads I and III, that is:

$$I + III = II.$$

Precordial Leads and the Wilson Central Terminal. The precordial leads register the potential at each of the six specific torso sites (see Fig. 14.1, bottom left panel) in relation to a reference potential. An exploring electrode is placed at each of six specific precordial sites and connected to the positive input of the recording system (see Fig. 14.1, bottom right). The negative input is the mean value of the potentials recorded at each of the three limb electrodes, referred to as the *Wilson central terminal* (WCT).

The potential in each V lead can be expressed as:

$$V_i = E_i - WCT$$

where

$$WCT = (LA + LL + RA) / 3$$

and V_i is the potential recorded in precordial lead i, E_i is the voltage sensed at the exploring electrode for lead V_i, and WCT is the potential in the composite Wilson central terminal, and LA, LL, and RA are the potentials in the left arm, left leg, and right arm, respectively.

The potential recorded by the WCT is considered to remain relatively constant during the cardiac cycle, and the output of a precordial lead is determined predominantly by time-dependent changes in the potential recorded at that precordial site.* The potentials registered by these leads preferentially reflect activity in cardiac regions underlying the exploring electrode, with lesser although meaningful contribution by potentials generated from more distant cardiac sources.

*The precordial and the augmented limb leads are commonly referred to as "unipolar" leads. However, a true unipolar lead registers the potential at one site in relation to an absolute zero potential. Referring to these leads as unipolar is based on the assumption that the WCT represents a constant, true zero potential. In reality, the potential in the WCT is neither zero nor constant during the cardiac cycle. Hence, these leads are in reality bipolar leads with the WCT serving as the compound negative pole.

Augmented Limb Leads. The three augmented limb leads are designated aVR, aVL, and aVF. For lead aVR, the exploring electrode (Fig. 14.2) that forms the positive input is the right arm electrode, for lead aVL it is the left arm electrode, and for aVF it is the left leg electrode. The reference potential for these leads is formed by connecting the two limb electrodes not used as the exploring electrode. For lead aVL, for example, the exploring electrode is on the left arm, and the reference electrode is the combined output of the electrodes on the right arm and the left foot.

Thus,

$$aVR = RA - (LA + LL) / 2$$

$$aVL = LA - (RA + LL) / 2$$

and

$$aVF = LL - (RA + LA) / 2$$

This modified reference system produces a signal that is larger than if the full WCT were included. When the WCT was used, the output was small, in part because the same electrode potential was included in both the exploring and the reference potential inputs. Eliminating this duplication results in a theoretical 50% increase in amplitude.

Other Lead Systems. Expanded lead systems (see Table 14.1, bottom) include recordings from additional electrodes placed on the right

TABLE 14.1 Location of Electrodes and Lead Connections for the Standard 12-Lead Electrocardiogram and Additional Leads

LEAD TYPE	POSITIVE INPUT	NEGATIVE INPUT
Standard Limb Leads*		
I	Left arm	Right arm
II	Left leg	Right arm
III	Left leg	Left arm
Augmented Limb Leads		
aVR	Right arm	Left arm plus left leg
aVL	Left arm	Right arm plus left leg
aVF	Left leg	Left arm plus right arm
Precordial Leads†		
V_1	Right sternal margin, fourth intercostal space	Wilson central terminal
V_2	Left sternal margin, fourth intercostal space	Wilson central terminal
V_3	Midway between V_2 and V_4	Wilson central terminal
V_4	Left midclavicular line, 5th intercostal space	Wilson central terminal
V_5	Left anterior axillary line at same horizontal plane as for V_4 electrode	Wilson central terminal
V_6	Left midaxillary line at same horizontal plane as for V_4 electrode	Wilson central terminal
V_7	Posterior axillary line at same horizontal plane as for V_4 electrode	Wilson central terminal
V_8	Posterior scapular line at same horizontal plane as for V_4 electrode	Wilson central terminal
V_9	Left border of spine at same horizontal plane as for V_4 electrode	Wilson central terminal

*Limb electrodes should be placed near the wrists and ankles or, at a minimum, distal to the shoulders and hips.
†The right-sided precordial leads V_3R to V_6R are placed in mirror-image positions on the right side of the chest. (See text for further details.)
From Kligfield P, Gettes LS, Bailey JJ, et al. Recommendations for the standardization and interpretation of the electrocardiogram: part I: the electrocardiogram and its technology a scientific statement from the American Heart Association Electrocardiography and Arrhythmias Committee, Council on Clinical Cardiology; the American College of Cardiology Foundation; and the Heart Rhythm Society endorsed by the International Society for Computerized Electrocardiology. *J Am Coll Cardiol.* 2007;49:1109–1127.
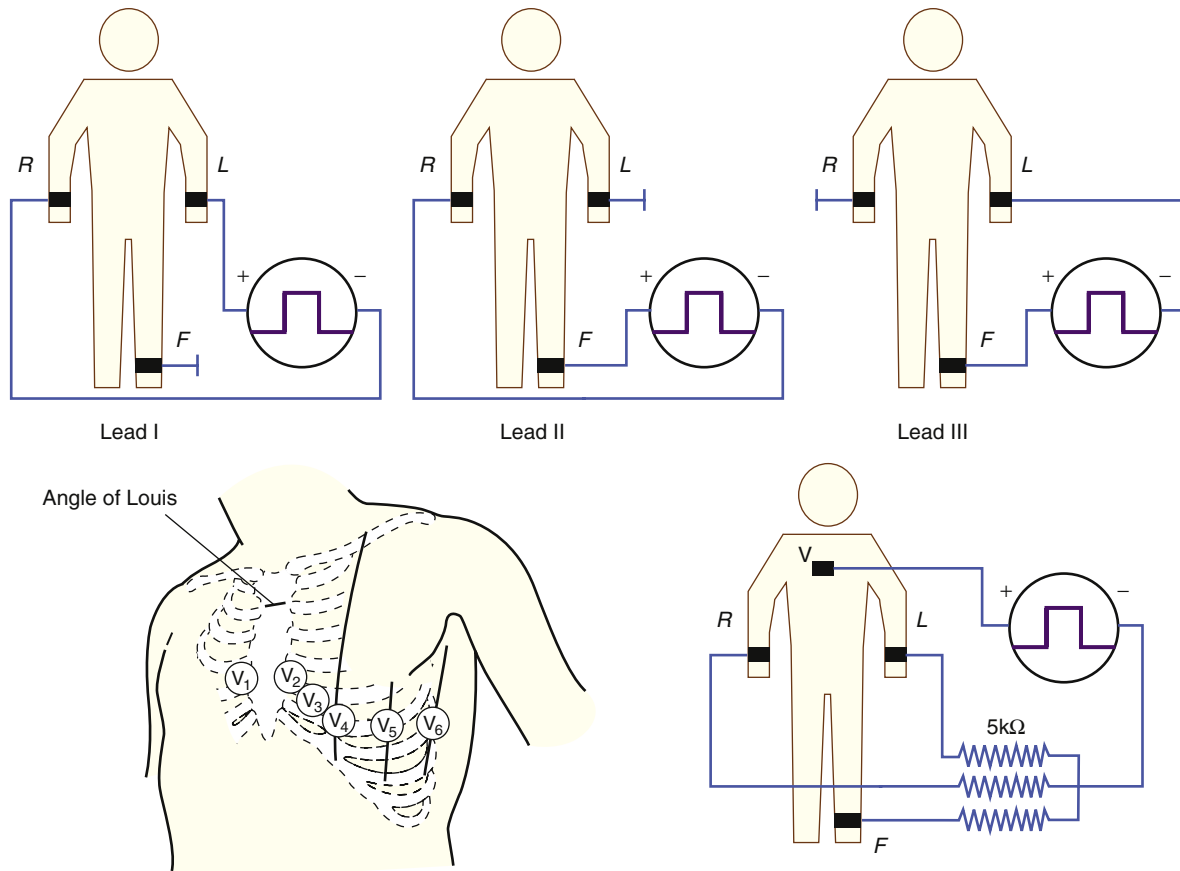
FIGURE 14.1 **Top,** Electrode connections for recording the standard limb leads I, II, and III and the augmented limb leads aVR, aVL, and aVF, with electrodes on the right arm, left arm, and left foot. **Bottom,** Electrode locations and electrical connections for recording a precordial lead. *Left,* The positions of the exploring electrode (V) for the six precordial leads. *Right,* Connections to form the Wilson central terminal for recording a precordial (V) lead. When constructing the Wilson central terminal, 5000-ohm resistors (5 kΩ) are connected to each limb electrode.
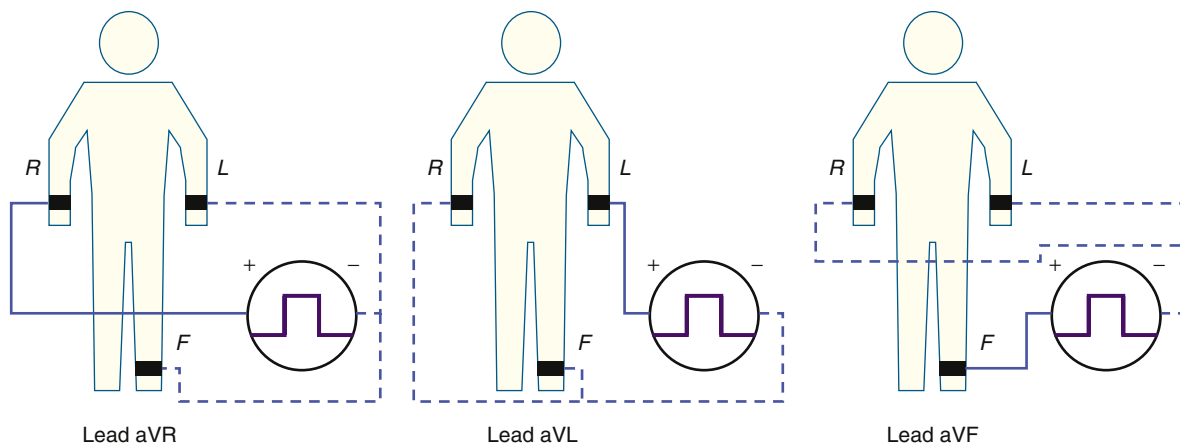
FIGURE 14.2 Electrode locations and electrical connections for recording the augmented limb leads aVR, aVL, and aVF. *Dotted lines* indicate connections to generate the reference electrode potential.

precordium to assess RV abnormalities such as RV myocardial infarction (MI). The right-sided precordial leads V_3R to V_6R are placed in mirror-image positions on the right side of the chest. Electrodes added on the left posterior torso (e.g., V_7 at the posterior axillary line at the level of V_4 and V8 at the posterior scapular line at the level of V_4) may detect acute posterolateral MI, and some placed higher on the anterior torso than normal may help detect abnormalities such as the Brugada pattern and its variants (see Chapters 63 and 70).

Other lead sets have sought to minimize movement artifacts during exercise and long-term monitoring (see Chapters 32 and 61) by placing limb electrodes on the torso rather than near the ankles and wrists. The resulting waveforms may differ substantially from those recorded from the standard ECG sites, with altered QRS and ST-T wave patterns in all 12 leads. These differences may impact the diagnostic accuracy of criteria of, for example, ventricular hypertrophy and MI.[1] Thus, these

alternative lead sets should not be used to record a diagnostic ECG. Less frequently used but important lead systems include those designed to record a *vectorcardiogram* (VCG), which depicts the orientation and strength of a single cardiac vector representing overall cardiac activity throughout the cardiac cycle.

Hexaxial Reference Frame and the Electrical Axis
The three standard limb and the three augmented limb leads are aligned in the *frontal plane* of the torso. The six precordial leads are aligned in the *horizontal plane* of the chest.

Each ECG lead can be represented as a vector, the *lead vector*. The lead vectors for leads I, II, and III are directed from the negative electrode toward the positive one, e.g., from the right arm to the left arm for lead I (Fig. 14.3, *left*). For an augmented limb and for a precordial lead, the lead vector passes through the midpoint of the axis connecting
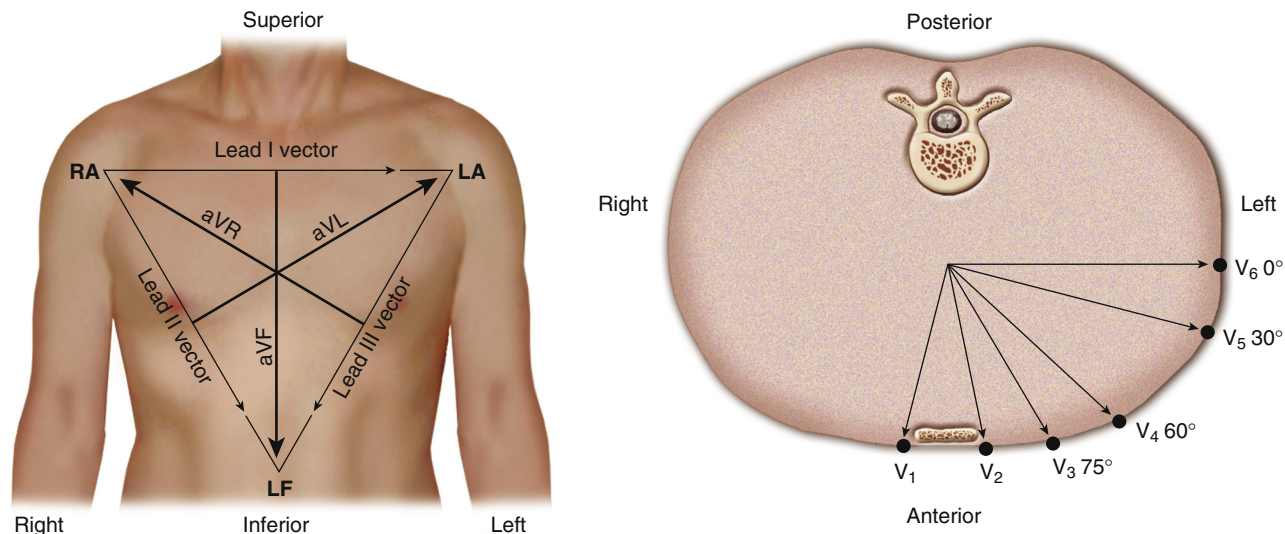
FIGURE 14.3 Lead vectors for the three standard limb leads, the three augmented limb leads (*left*), and the six unipolar precordial leads (*right*). *LA,* Left arm; *LF,* left foot; *RA,* right arm.

the electrodes that comprise the reference electrode and points to the location of the exploring electrode. That is, for lead aVL, the vector points from the midpoint of the axis connecting the right arm and left leg electrodes toward the left arm (see Fig. 14.3, *left*). For each precordial lead, the lead vector in the horizontal plane points from the center of the triangle formed by the three standard limb leads to the precordial electrode site (see Fig. 14.3, *right*).

Instantaneous cardiac activity also can be approximated as a single vector, the *heart vector,* that represents the vectoral sum of the activity of all active wavefronts. This vector's location, orientation, and intensity vary from instant to instant as cardiac activation proceeds.

The amplitude of the recorded waveform in a lead equals the length the projection of the heart vector onto the lead vector. This relation may be expressed mathematically as:

$$V_L = H \cos \theta$$

where V_L is the recorded voltage in lead L, H is the strength (length) of the heart vector, and Θ is the angle between the heart vector H and the lead vector. Thus, when the direction of activation (i.e., the direction of the heart vector) and that of the lead vector are parallel ($\Theta = 0$ degrees and cosine $\Theta = 1$), the recorded voltage is maximal; when the activation is perpendicular to the lead axis, the recorded potential equals zero ($\Theta = 90$ degrees and cosine $\Theta = 0$).
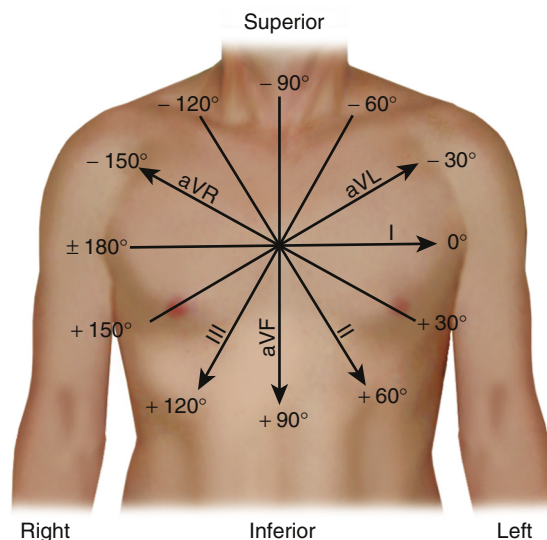
The lead axes of the six frontal plane leads can be superimposed to produce the *hexaxial reference system*. As depicted in Figure 14.4, the six lead axes divide the frontal plane into 12 segments, each subtending 30 degrees. This presentation allows calculation of the *mean electrical axis* of the heart representing the direction of activation in a theoretical "average" cardiac fiber.

The process for computing the mean electrical axis during ventricular activation in the frontal plane is illustrated in Figure 14.5. First, the mean electrical force (i.e., the heart vector) as projected onto each lead is estimated by computing the area under the QRS waveform, measured as mV-ms, in that lead. Areas above the baseline (usually the TP segment as discussed later) are assigned a positive polarity and those below the baseline are assigned a negative polarity. The overall area equals the sum of the positive and the negative areas.

Second, the area under the QRS in each lead (typically, two are chosen) is represented as a vector oriented along the appropriate lead axis in the hexaxial reference system. Third, the mean electrical axis is computed as the resultant or vector sum of the (two) vectors.

A mean electrical axis in the frontal plane directed toward the positive end of the lead axis of lead I, that is, oriented directly away from the right arm and toward the left arm, is designated as having an axis of 0 degrees. Axes oriented in a clockwise direction relative to this zero level are assigned positive values, and those oriented in a counterclockwise direction are assigned negative values (see Fig. 14.4).

The mean electrical axis in the horizontal plane can be computed in an analogous manner by using the areas under and lead axes of the six precordial leads (see Fig. 14.3, *right*). A horizontal plane axis located

FIGURE 14.4 The hexaxial reference system constructed from the lead axes of the six frontal plane leads. The lead axes of the six frontal plane leads have been rearranged so that their centers overlie one another. Positive ends of each axis are labeled with the name of the lead.
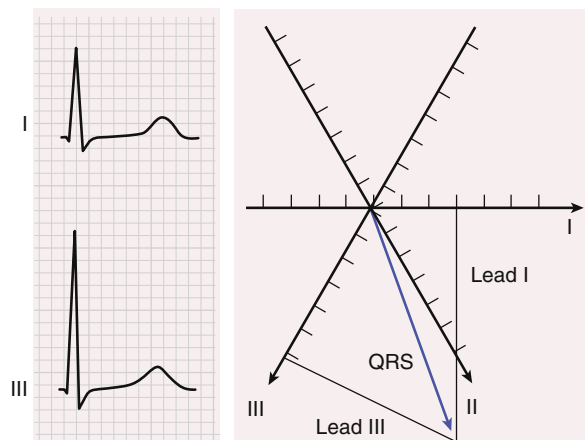
FIGURE 14.5 Calculation of the mean electrical axis during ventricular depolarization from the areas under the QRS complex in leads I and III. Magnitudes of the areas of the two leads are plotted as vectors on the appropriate lead axes, and the mean QRS axis is the sum of these two vectors. (From Mirvis DM. *Electrocardiography: A Physiologic Approach*. St Louis: Mosby–Year Book; 1993.)

along the lead axis of lead V_6 is assigned a value of 0 degrees; axes directed more anteriorly have positive values.

This approach can also be applied to compute the mean electrical axis for other phases of cardiac activity. Thus, the mean force during atrial activation is represented by the areas under the P wave and the mean force during ventricular recovery by the areas under the ST-T wave.

Electrocardiographic Processing and Display Systems

ECG recording using computerized systems includes: (1) signal acquisition, (2) data transformation, waveform recognition, and feature extraction, (3) diagnostic classification, and (4) display of the final ECG. Technical requirements for processing an ECG have been developed by various medical and engineering organizations.[1,2]

Signal Acquisition. Recorded signals are amplified, converted into digital form, and filtered to reduce noise. The standard amplifier gain for routine electrocardiography is 1000. Lower (e.g., 500, or *half-standard*) or higher (e.g., 2000, or *double-standard*) gains may be used to compensate for unusually large or small signals, respectively.

Analog signals are converted to a digital form at rates of 1000 samples per second (1000 Hz) to as high as 15,000 Hz. Too low a sampling rate may miss brief high-frequency signals such as notches in QRS complexes or pacemaker spikes. Too fast a sampling rate may introduce artifacts, including high-frequency noise, and will generate large amounts of data necessitating extensive digital storage capacity.

ECG potentials are filtered to reduce distorting signals. Low-pass filters reduce the distortions caused by high-frequency interference from, for example, muscle tremor and nearby electrical devices. High-pass filters reduce the effects of body motion or respiration. For routine electrocardiography, the standards set by professional groups require an overall bandwidth of 0.05 to 150 Hz for adults.[1] Narrower filter settings, such as 1 to 30 Hz, as typically used in rhythm monitoring, will reduce baseline wander related to motion and respiration but will distort both the QRS complex and the ST-T wave.

ECG amplifiers are *capacitor coupled*, with a capacitor stage between the input and output. The ECG may be modeled as a time-varying or alternating current (AC) signal producing the waveforms superimposed on a fixed direct current (DC) baseline. Capacitor-coupling permits the flow of AC signals, which account for the waveform shape, while blocking the nonphysiologic DC potentials such as those produced by the electrode interfaces. The elimination of the DC potential from the final product, however, means that ECG potentials are not to be calibrated against an external reference level (e.g., a ground potential). Rather, ECG potentials are measured in relation to another portion of the waveform that serves as a baseline. The *TP segment,* which begins at the end of the T wave of one cardiac cycle and ends with the onset of the P wave of the next cycle (as detailed later), is usually the most appropriate internal ECG baseline, e.g., for measuring ST-segment deviation.

Data Transformation, Waveform Identification, and Feature Extraction. The multiple cardiac cycles that are recorded for each lead and are typically overlaid electronically to form a single representative beat for each lead. This reduces the effects of minor beat-to-beat variation in the waveforms and random noise. The averaged waveforms from each lead are overlaid on each other to measure waveform intervals.[1]

Diagnostic Classification. These measurements are then compared with specific diagnostic criteria. For many diagnoses, ECG criteria are based on statistical correlations between anatomic or physiologic findings and ECG measurements in large populations (e.g., criteria for ECG diagnosis of ventricular hypertrophy). For such population-based criteria, the diagnosis is not absolute but represents a statistical probability that a structural or physiologic abnormality exists based on the presence or absence of a specified set of ECG findings. Because different populations may be studied and different ECG and structural measurements may be used as the reference standard, numerous different criteria with highly varying accuracies have been developed for common clinical conditions.

In other cases, the criteria are derived mainly from physiologic constructs and constitute the sole basis for a diagnosis, with no anatomic or functional correlation. For example, the criteria for intraventricular conduction defects are diagnostic without reference to an anatomic standard.

Display. Cardiac potentials are most often displayed as the classic *scalar* ECG, which depicts the potentials recorded from each lead as a function of time. Amplitudes are displayed on a scale of 0.1 mV/mm (for *standard gain*) on the vertical axis and time as 40 msec/mm on the horizontal scale. Leads generally are displayed in three groups—the three standard limb leads, followed by the three augmented limb leads, followed by the six precordial leads.
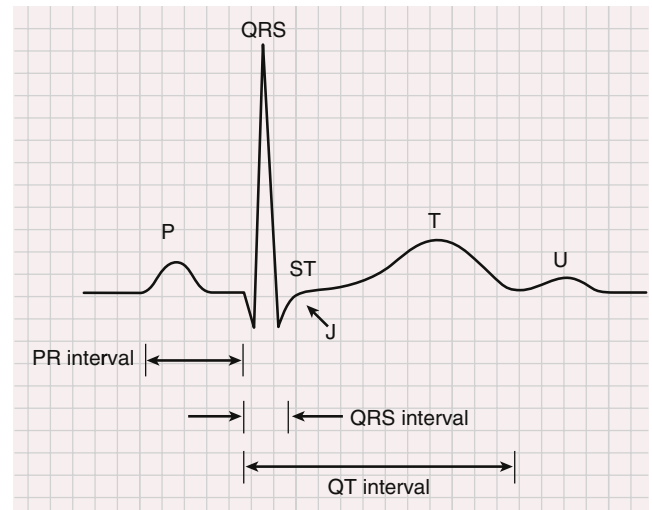
FIGURE 14.6 The waves and intervals of a normal electrocardiogram. (From Goldberger AL, Goldberger ZD, Shvilkin A. *Goldberger's Clinical Electrocardiography: A Simplified Approach*. 9th ed. Philadelphia: Elsevier; 2017.)

Alternative display formats have been proposed. One is the *Cabrera display* in which the six limb leads are displayed in the sequence of the frontal plane reference frame[3] and in which the polarity of lead aVR is inverted. In this scheme, waveforms are ordered as follows: lead aVL, lead I, inverted lead aVR, lead II, lead aVF, and lead III. Advantages of this system may include facilitating estimation of the electrical axis by presenting the leads in the order in which they appear on the frontal plane reference frame (see Fig. 14.4) and demonstrating the relevance of abnormalities in lead aVR by reversing its polarity.

THE NORMAL ELECTROCARDIOGRAM

The waveforms and intervals that make up the standard ECG are displayed schematically in Figure 14.6, and a normal 12-lead ECG is shown in Figure 14.7. The *P wave* is generated by activation of the atria, the *PR interval* corresponds to the duration of atrioventricular (AV) conduction, the *QRS complex* is produced by the activation of the two ventricles, and the *ST-T wave* reflects ventricular recovery.

Table 14.2 lists the classic normal values for the various intervals and waveforms. The range of normal values of these measurements reflects the substantial intraindividual and interindividual variability in ECG patterns. Intraindividual differences may occur between ECGs recorded days, hours, or even minutes apart because of technical issues (e.g., changes in electrode position) or the physiologic effects of changes in, for example, posture, temperature, or heart rate.

Variability between individuals may reflect differences in age, gender, race, body habitus, and physiology. For example, in the Atherosclerosis Risk in Communities (ARIC) study,[4] the upper limits for ST-segment elevation in leads V_1 and V_2 were 50 μV higher in white men than in white women and almost 100 μV higher in African American men than in white men.

Atrial Activation and the P Wave
Atrial Activation and the Normal P Wave

Atrial activation begins with impulse generation in the atrial pacemaker complex in or near the sinoatrial node (see Chapter 62). Once the impulse leaves this pacemaker site, atrial activation proceeds anteriorly and inferiorly toward the lower portion of the right atrium (RA) and the AV node.

The left atrium (LA) is normally activated after the onset of RA activation primarily by propagation across *Bachmann's bundle*, which extends from the anterior RA to the LA near the right upper pulmonary vein. Activation then continues in both atria during much of the middle
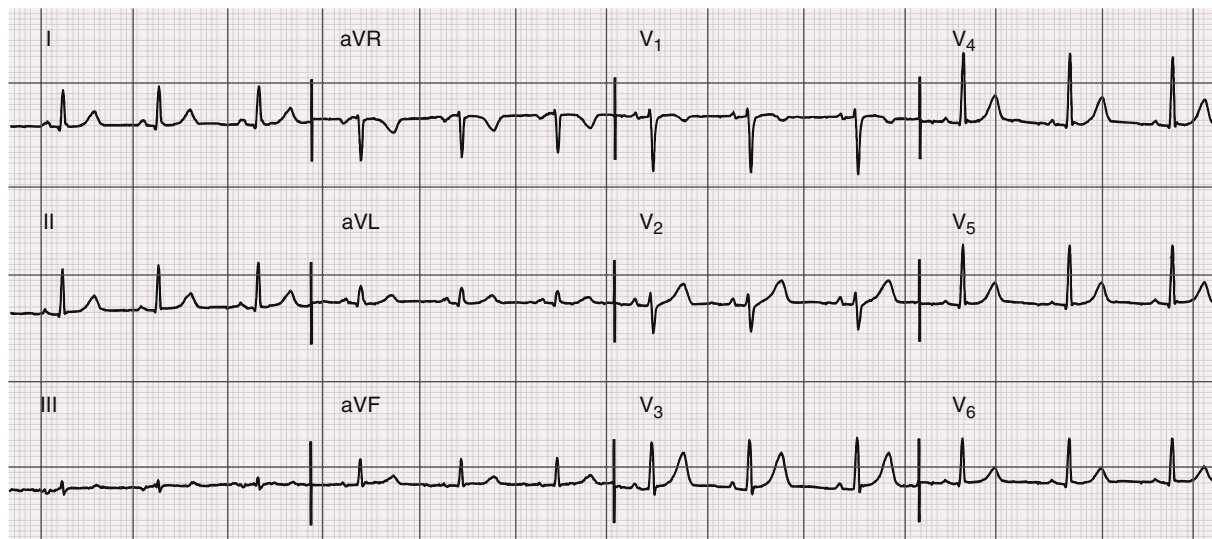
FIGURE 14.7 Normal ECG recorded from a 48-year-old woman. *Vertical lines* are spaced at 40-msec intervals. *Horizontal lines* represent voltage amplitude, with lines spaced at 0.1-mV intervals. Every fifth line on each axis is darkened. The heart rate is approximately 76 beats/min (with physiologic variations due to respiratory sinus arrhythmia); the PR interval, QRS, and QTc durations measure approximately 140, 84, and 400 msec, respectively; and the mean QRS axis is approximately +35 degrees.

TABLE 14.2 Normal Upper Limits for Durations of Electrocardiogram Waves and Intervals in Adults

WAVE OR INTERVAL	DURATION (MSEC)
P wave duration	<120
PR interval	<200
QRS duration	<110–120*
QT interval$_c$ (corrected)	≤440–450*

*See text for further discussion.
References: Rautaharju PM, Surawicz B, Gettes LS, et al. Recommendations for the standardization and interpretation of the electrocardiogram. Part IV. The ST segment, T and U waves. *J Am Coll Cardiol*. 2009;53:982–991; and Kligfield P, Gettes LS, Bailey JJ, et al. Recommendations for the standardization and interpretation of the electrocardiogram: part I: the electrocardiogram and its technology *J Am Coll Cardiol*. 2007;49:1109–1127.

of the atrial activation period, with LA activation continuing after the end of RA activation.

The normal P wave reflects these activation patterns. P waves are positive in lead II and usually positive in leads I, aVL, and aVF, reflecting the inferior and leftward direction of normal activation. This corresponds to a mean frontal plane P wave axis of approximately 60 degrees. The pattern in leads aVL and III may be upright or downward, depending on the exact orientation of the mean P wave axis.

In the horizontal plane, early activation of the RA generates a P wave that is oriented primarily anteriorly. Later, activation shifts leftward and posteriorly as it proceeds over the LA. Thus, the P wave in the right precordial leads is typically upright. In lead V$_1$ and occasionally in lead V$_2$, the P wave may be biphasic with an initial positive deflection followed by a later, smaller negative wave. In the more lateral leads, the P wave is upright and reflects continual right-to-left spread of the activation fronts.

The upper limit for a normal P wave duration is conventionally set at 120 msec, as measured in the lead with the widest P wave. The amplitude in the limb leads normally is less than 0.25 mV, and a terminal negative deflection in the right precordial leads is normally less than 0.1 mV in depth.

Atrial Repolarization

The potentials generated by atrial repolarization are not usually seen on the surface ECG because of their low amplitude (usually <100 μV) and because they may be superimposed on the much higher-amplitude QRS complex. A repolarization wave (the T_a wave) may be observed as a low-amplitude wave with a polarity opposite that of the P wave during AV block, and it may be accentuated during exercise testing (see Chapter 32), with acute pericarditis (see Chapter 86), or atrial infarction (see Chapter 37).

Heart Rate Variability

Analysis of beat-to-beat changes in heart rate and related dynamics, termed *heart rate variability* (see Chapters 61 and 102), can provide insight into neuroautonomic control mechanisms and their perturbations with aging, disease, and drug effects. For example, relatively high-frequency (0.15 to 0.4 Hz) fluctuations are mediated primarily by vagus nerve traffic, such that heart rate increases during inspiration and decreases during expiration. Attenuation of this respiratory sinus arrhythmia at rest is a marker of physiologic aging and also occurs with diabetes mellitus, congestive heart failure, and a wide range of other conditions that alter autonomic tone modulation. Of note, false-positive increases in high-frequency variability, attributable to abnormal sinoatrial function and loss of vagal modulation, may occur with aging and chronic heart disease. This finding has been termed *heart rate fragmentation*.[5] Relatively lower-frequency (0.05 to 0.15 Hz) physiologic oscillations in heart rate appear to be jointly regulated by sympathetic and parasympathetic interactions. A variety of complementary signal-processing techniques have been developed to analyze heart rate variability and its interactions with other physiologic signals, including time domain statistics, frequency domain techniques based on spectral methods, and newer computational tools derived from nonlinear dynamics and complex systems theory. In addition, fluctuations in beat-to-beat QT intervals may also exhibit meaningful variability.

Atrioventricular Node Conduction and the PR Segment

The *PR segment* is the usually isoelectric region beginning with the end of the P wave and ending with the onset of the QRS complex. It forms part of the *PR interval* that extends from the onset of the P wave to the onset of the QRS complex. The normal PR interval measures 120 to 200 ms in duration in adults and is best determined from the lead with the shortest interval.

The PR segment includes atrial repolarization and slow conduction within the AV node plus the more rapid conduction through the ventricular conduction system. The segment ends when enough ventricular myocardium has been activated to initiate the QRS complex.

The potentials generated by the conduction system structures, like most atrial repolarization potentials, are too small to be detected on the body surface at amplifier gains used in clinical electrocardiography. Signals from elements of the conduction system can be

recorded from intracardiac recording electrodes placed, for example, against the base of the interventricular septum (see Chapters 61 and 64).

Ventricular Activation and the QRS Complex

Normal ventricular activation is a complex process that depends on interactions between the physiology and anatomy of both the specialized ventricular conducting system and the ventricular myocardium.

Ventricular Activation. Ventricular activation is the net product of two events: endocardial activation, followed by transmural activation of the two ventricles. *Endocardial* activation is guided by the anatomic distribution and physiology of the His-Purkinje system. The rapid conduction within the broadly dispersed ramifications of this treelike (*fractal*) system results in the synchronized activation of multiple endocardial sites and the depolarization of most of the endocardial surfaces of both ventricles within several milliseconds.

The sequence of LV endocardial activation, depicted in Figure 14.8, begins at three sites on the left side of the septum: (1) the anterior paraseptal wall, (2) the posterior paraseptal wall, and (3) the center of the left side of the septum. These loci generally correspond to the sites of insertion of the fascicles of the left bundle branch (LBB). Septal activation thus begins on the left side and spreads across the septum from left to right and from apex to base.

Wavefronts then sweep from the initial sites of activation in anterior and inferior and then superior directions to activate the anterior and

lateral walls of the LV. The last areas of the LV to be activated are the posterobasal regions.

Excitation of the RV endocardium begins near the insertion point of the right bundle branch (RBB) near the base of the anterior papillary muscle and spreads to the free wall. The final areas to be activated are the pulmonary conus and the posterobasal RV areas.

Thus, in both ventricles, the overall endocardial excitation pattern begins on septal surfaces, sweeps down toward the apex and then around the free walls to the basal regions, in an apex-to-base direction.

Activation then moves across the ventricular wall from endocardium to epicardium. Excitation of the endocardium begins at sites of Purkinje–ventricular muscle junctions and proceeds by muscle cell–to–muscle cell conduction toward the epicardium. Multiple regions of both ventricles are usually activated simultaneously, resulting in substantial cancellation of the electrical forces that are generated, as previously described.

Normal QRS Complex

QRS patterns are described by the sequence of waves constituting the complex. An initial negative deflection is called the *Q wave*, the first positive wave is the *R wave*, and the first negative wave after a positive wave is the *S wave*. A second upright wave following an S wave, when present, is an *R′ wave*, i.e., an *R-prime wave*. A monophasic negative complex is referred to as a *QS complex*. Tall waves are denoted by uppercase letters and smaller ones by lowercase letters. For example, the QRS complex may be described as qRS if it consists of an initial small negative wave (q) followed by a tall upright one (R) and a deep negative one (S). In an RSr′ complex, initial tall R and S waves are followed by a small positive wave (r′).
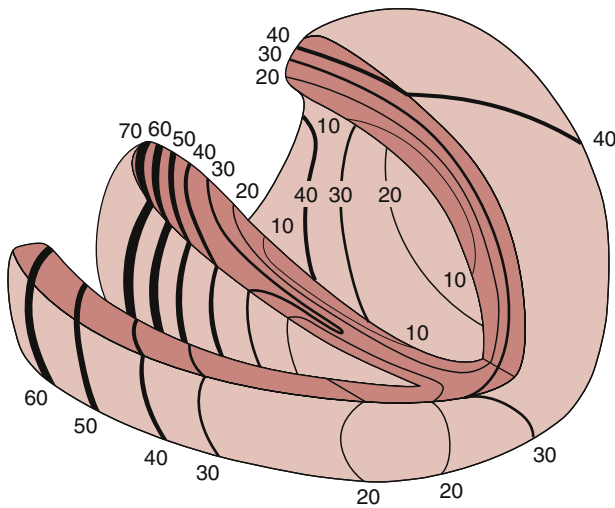
In each case, the deflection must cross the baseline to be designated a discrete wave. Changes in waveform patterns that do not cross the baseline result in *notches* or *slurs*. A notch is an abrupt change in waveform direction that does not cross the baseline. A slur exists when there is a distinct change in the slope or rate of change in waveform amplitude. The significance of these patterns is discussed later.

Early QRS Patterns. The complex pattern of activation described earlier may be simplified into two forces, the first representing septal activation and the second representing LV free wall activation (Fig. 14.9). Because RV muscle mass is considerably smaller than that of the LV, most of the electrical activity it generates is canceled by the much greater forces from the LV so that it contributes little to normal QRS complexes. Thus, the normal QRS can be represented by septal and LV activity with little meaningful oversimplification.

Initial activation forces of the interventricular septum are oriented from left to right in the frontal plane and anteriorly in the horizontal plane, corresponding to the anatomic position of the septum within the chest. These wavefronts produce initial positive waves in leads with axes directed to the right (e.g., lead aVR) or anteriorly (e.g., lead V_1). Leads with axes directed to the left (e.g., leads I, aVL, V_5, and V_6) will register initial negative waves known as *septal q waves* (discussed later). These initial forces are normally of low amplitude and are brief (<30 msec in duration).

FIGURE 14.8 Activation sequence of the normal right and left ventricles. Portions of the left and right ventricles have been removed so that the endocardial surfaces of the ventricles and the interventricular septum can be seen. *Isochrone lines* connect sites that are activated at equal instants after the earliest evidence of ventricular activation. (From Durrer D. Electrical aspects of human cardiac activity: a clinical-physiological approach to excitation and stimulation. *Cardiovasc Res*. 1968;2:1–12.)

Mid- and Late QRS Patterns. Subsequent parts of the QRS complex reflect ongoing activation of, mainly, the free walls of the LV and RV. The complex interrelationships among cardiac position, conduction system function, and ventricular geometry result in a wide range of normal QRS patterns in the limb leads. The QRS pattern in leads II, III, and aVF may be predominantly upright, with qR complexes, or these leads may show rS or RS patterns. Lead I may record a qR pattern or an isoelectric RS pattern. These variations are discussed later in relation to lead axes.

Normal QRS patterns in the precordial leads follow an orderly progression from right (V_1) to left (V_6). In leads V_1 and V_2, initial r waves generated by septal activation are followed by S waves (an rS pattern), reflecting leftward and posterior activation of the LV free wall proceeding away from the precordial electrode.

FIGURE 14.9 Ventricular depolarization shown as two sequential vectors representing septal (*left*) and left ventricular free wall (*right*) activation. QRS waveforms generated by each stage of activation in leads V_1 and V_6 are shown.

In midprecordial leads V_3 and V_4, the fronts first approach the exploring electrode and then move leftward and posteriorly, away from the exploring electrode. This sequence generates an R or r wave as it moves toward the electrode, followed by an S wave as it moves away from the electrode to produce rS or RS complexes.

As the exploring electrode moves further to the left to V_5 and V_6, the R wave becomes more dominant and the S wave becomes smaller (or totally lost by leads V_5 and V_6) because of the longer time period during which the activation front moves toward the positive end of the electrode. In the leftmost leads (i.e., leads V_5 and V_6), the normal pattern also includes the septal q wave, to produce a qR (or qRs) morphology.

Thus, in the precordial leads, the QRS complex usually is characterized by a consistent progression from an rS complex in the right precordial leads, to an RS pattern in the midprecordial leads, and to a qR pattern in the left precordial leads. The site at which the pattern changes from a dominant S wave to a dominant R wave pattern—the *transition zone*—normally occurs between lead V_3 and V_4. Transition zones that are shifted to the right (e.g., to lead V_2) are *early transitions* (previously referred to as *"counterclockwise rotation"*), and those shifted leftward (e.g., to V_5 or V_6) are *delayed transitions* (previously referred to as *"clockwise rotation"*). These patterns may have diagnostic significance in detecting, for example, ventricular hypertrophy, conduction defects, and MI, as discussed later.

Normal variability in patterns is related to demographic and physiologic factors. QRS amplitudes are greater (within the normal range) in men than in women and higher in African Americans than in those of other races. Higher-than-normal amplitudes are characteristic of chamber hypertrophy and conduction defects, as discussed later. Low-amplitude QRS complexes, that is, complexes with overall amplitudes of less than 0.5 mV in all frontal plane leads and less than 1.0 mV in the precordial leads, may occur as a normal variant or as a result of cardiac (e.g., infiltrative cardiomyopathies, myocarditis) or extracardiac (e.g., pericardial effusion, chronic obstructive pulmonary disease, pneumothorax) conditions, as discussed later in this and in other chapters.

Electrical Axis. The wide range of normal QRS patterns in the limb leads can be interpreted by referring to the hexaxial reference system in Figure 14.4. The normal mean QRS axis in adults lies between −30 degrees and +90 to 100 degrees, with physiologically vertical/inferior axes most prevalent in young adults. If the mean axis is near 90 degrees, that is, directed toward the left foot, the QRS complex in leads II, III, and aVF will be predominantly upright with qR complexes; lead I will record an isoelectric RS pattern because the heart vector lies perpendicular to its lead axis. If the mean axis is nearer 0 degrees, that is, directed toward the left arm, the patterns will be reversed; leads I and aVL will register a predominantly upright qR pattern, and leads II, III, and aVF will show rS or RS patterns. This variation largely reflects physiologic differences in the conduction system; the anatomic position of the heart within the torso has a minor role.

In adults, mean QRS axes more positive than +90 to 100 degrees (usually with an rS pattern in lead I) represent right axis deviation. Axes more negative than −30 degrees (with an rS pattern in lead II) represent left axis deviation. Mean axes lying between −90 degrees and −180 degrees (or, equivalently, between +180 and +270 degrees) are referred to as extreme axis deviations or, alternatively, as right superior axis deviations. The term indeterminate axis refers to the condition in which all six extremity leads show biphasic (QR or RS) patterns, indicating a mean electrical axis that is perpendicular to the frontal plane. This finding may occur as a normal variant or may be seen in a variety of pathologic conditions discussed later.

The Intrinsicoid Deflection. As previously described, an electrode overlying the ventricular free wall will record a rising R wave as transmural activation proceeds toward it. The peak of the R wave occurs when the activation front reaches the epicardium. After that, the full thickness of the wall under the electrode will be in an active state and the electrode will register negative potentials as activation proceeds in remote cardiac areas. This sudden reversal of potential produces a sharp downslope after the peak of the R wave, the *intrinsicoid deflection,* that approximates the timing of activation of the epicardium under the electrode. Thus, the time from the onset of the QRS to the intrinsicoid deflection (the *R-peak time*) has been interpreted as a measure of the duration of transmural spread of excitation.

Ventricular Recovery and the ST-T Wave

Genesis of Ventricular Recovery Potentials. The ST-T wave reflects activity during the plateau phase and the later repolarization phases of the cardiac action potential. ST-T wave patterns depend on the interaction of two factors: (1) the direction of intracellular current flow in cardiac fibers during repolarization, and (2) the sequence of recovery within the ventricles.

Differences in recovery times occur between regions of the LV and across the ventricular wall. In general, the repolarization sequence is the opposite of the activation sequence; that is, regions activated later have shorter action potentials than areas activated early. Thus, action potential durations are shorter in the anterobasal region than in the posteroapical region of the LV. Similarly, action potential durations are shorter in the epicardium than in the endocardium.

In each case, the shortening of recovery time is greater than the delay in onset of activation, so that repolarization ends first in areas activated last. The resulting repolarization current flow will then be directed away from the basal LV toward the apex and away from the endocardium toward the epicardium. That is, repolarization current flow will be in the same direction as during activation. The result is that normal QRS and ST-T patterns are *concordant*, with the ST-T wave having the same polarity as the QRS complex.

Evidence suggests that the regional differences in action potential duration are the major cause of ST-T wave, with lesser contribution by transmural differences.[6] In addition, some evidence suggests a role for so-called M or midmyocardial cells in the genesis of the ST-T wave.[7] These cells have longer action potentials than either endocardial or epicardial cells and repolarize last. Thus, at the end of the ST-T segment, repolarization currents flow from the epicardium toward the mid-wall, contributing to the downslope of the T wave.

The Normal ST-T Wave

The normal ST-T wave begins as a low-amplitude, slowly changing wave (the *ST segment*) that gradually evolves into a larger wave, the *T wave*. The onset of the ST-T wave, the *junction* or *J point*, is normally at or near the isoelectric baseline (typically the PR segment) of the ECG (see Fig. 14.6). The level of the ST segment generally is measured at the J point or, in some applications such as exercise testing, 40 or 80 msec after the J point (see Chapter 15).

The polarity of the normal ST-T wave generally is the same as the net polarity of the preceding QRS complex; that is, they are concordant. T waves usually are upright in leads I, II, aVL, and aVF and in the lateral precordial leads, and they have an amplitude of 1.5 mV or less. T waves are normally negative in lead aVR and variable in leads III, V_1, and V_2 (see later).

The amplitude of the normal J point and ST segment varies with race, sex, and age.[4] They typically are greatest in lead V_2, and they are higher in young men than in young women and in African Americans than in whites. Recommendations[1] for the upper limits of normal J point elevation in leads V_2 and V_3 are 0.2 mV for men age 40 or older, 0.25 mV for men younger than 40, and 0.15 mV for women. In other leads, the recommended upper limit is 0.1 mV for men and women. Higher levels, however, are common in normal persons especially among athletes. As many as 30% of athletes had ST elevation exceeding 0.2 mV in the anterior precordial leads.

The QT Interval

The QT interval extends from the onset of the QRS complex to the end of the T wave. Thus, it includes the total duration of ventricular activation and recovery and, in a general sense, corresponds to the duration of the ventricular action potential.

Accurately measuring the QT interval is challenging. Difficulties include precisely identifying the beginning of the QRS complex and especially the end of the T wave[8]; determining which lead or leads to use; and adjusting the measured interval for rate, QRS duration, and gender. These factors also make determining diagnostic thresholds and comparing QT intervals in the same person over time, such as during drug treatment, complex.

Because the onset of the QRS and the end of the T wave do not occur simultaneously in every lead, the QT interval duration will vary from lead to lead by as much as 50 to 65 msec (*QT dispersion*). In automated ECG systems, the QT interval typically is measured from a composite of all leads, beginning with the earliest onset of the QRS in any lead and terminating with the latest end of the T wave in any lead. When the interval is measured from a single lead, the lead in which the interval is the longest (most frequently lead V_2 or V_3) and in which a prominent U wave is absent (often aVR and aVL) is preferred.

Measurement of the *JT interval* (beginning at the end of the QRS complex rather than from its onset) has been proposed for patients with wide QRS complexes to adjust for the inclusion of the prolonged QRS duration in the overall QT interval.

The normal QT interval is rate dependent, decreasing as heart rate increases. This corresponds to rate-related changes in the duration of the normal ventricular action potential. Numerous formulae have been proposed to correct the measured QT interval for this rate effect.[1] The most commonly used formula is based on one proposed by Bazett in 1920. The result is the *corrected QT interval*, or *QTc*, defined by the following equation:

$$QTc = QT / \sqrt{RR}$$

where the QT and RR intervals are measured in seconds. A joint report of the American Heart Association (AHA), American College of Cardiology (ACC), and other professional organizations[1] suggested that the upper limit for QTc be set at 460 msec for women and 450 msec for men, and that the lower limit be set at 390 msec.

This formula has limited accuracy in correcting for the effects of heart rate on the QT interval. Large database studies have shown that the QTc interval based on the Bazett correction remains significantly affected by heart rate and that as many as 30% of normal ECGs may be diagnosed as having a prolonged QT interval when this formula is used.

Another commonly used correction is *Fridericia's formula* in which the adjusted QT interval is a function of the cube root of the RR interval. The AHA/ACC joint committee suggested using linear or power function regression equations.[1] One linear formula (proposed by Hodges) that has been shown to be relatively insensitive to heart rate, is:

$$QTc = QT + 1.75 \ (HR - 60)$$

where HR is heart rate (beats/min) and the intervals are computed as units of seconds. Other approaches include regression analyses based on the specific population studied or computing individual-specific corrections to assess serial changes such as during drug therapy.

The normal QT interval may be modified by numerous influences in addition to heart rate. These include gender (with longer intervals in women than in men), age (with increasing T intervals with increasing age), circadian rhythm (with longer intervals during sleep), and changes in autonomic tone (with decreasing intervals with increasing sympathetic tone and increasing intervals with higher parasympathetic activity). The impact of autonomic tone is demonstrated by, for example, the greater effect of increasing heart rate by exercise than with atrial pacing.

Abnormal QT prolongation occurs in numerous cardiac and noncardiac syndromes, during treatment with cardiac and noncardiac drugs, with electrolyte and metabolic abnormalities, and as a result of several gene mutations impacting ion channels (see Chapter 63). It is associated with tachyarrhythmias and sudden death (see Chapters 65–68 and 70). In the Multi-Ethnic Study of Atherosclerosis (MESA), each 10 msec increase in QT_C was associated with a 25%, 11%, and 19% increase in the development of heart failure, cardiovascular events, and stroke, respectively, during an 8-year follow-up.[9] Short QT intervals (defined by one consensus statement as <390 msec) are uncommon but identify a channelopathy with a very high risk of ventricular arrhythmias, atrial fibrillation, syncope, and sudden cardiac death (see Chapter 63).

The QRST Angle and the Ventricular Gradient

The *spatial QRST angle* is the angle, in three-dimensional space, between the vector representing the mean QRS force and the vector representing the mean ST-T force. The angle between the two vectors in the frontal plane represents a reasonable simplification and normally is less than 90 degrees for women and 107 degrees for men. If the two vectors representing mean activation and mean recovery forces are added, a third vector known as the *ventricular gradient* is created that represents the net area under the QRST complex.

These and related measures seek to quantify the level of global electrical heterogeneity in the ventricles. As described earlier, activation and repolarization forces are, in concept, concordant in direction and equal in magnitude. Thus, vectors representing the areas under the QRS complex (corresponding to the strength and orientation of overall activation forces) and under the ST-T (corresponding to overall recovery forces) should be equal and have the same orientation. That is, if the action potentials of all cells had uniform shapes and if depolarization and repolarization occurred in all regions in the same directions, the QRST angle and the ventricular gradient would equal zero.

The greater the differences in global electrical heterogeneity, the larger will be the QRST angle and the ventricular gradient. Abnormal levels of heterogeneity may occur in many conditions, including ischemia and hypertrophy, and may lead to arrhythmias, as discussed in Chapter 62. In an analysis of two large general population studies, a prediction model for sudden cardiac death demonstrated that these and related measurements were significantly and independently associated with sudden death during and after adjustment for other risk factors.[10]

Other Repolarization Waves

The U Wave

The T wave may be followed by an additional low-amplitude wave known as the *U wave*. This wave is usually less than 0.1 to 0.15 mV in amplitude, less than 160 to 200 msec in duration, and of the same polarity as the preceding T wave. Often, the U wave may merge with the end of the T wave to produce what appears to be a notched T wave, leading to what may be called a *QT(U) wave*. The U wave is generally largest in the leads V_2 and V_3 and is most often seen at slow heart rates and in patients with hypertension or hypokalemia. Its electrophysiologic basis is uncertain. Suggestions include delayed repolarization in areas of the ventricle that undergo late mechanical relaxation, late repolarization of the Purkinje fibers, and long action potentials of midmyocardial M cells. Negative U waves are uncommon and are strongly associated with adverse cardiac events.

The J Wave

A *J wave* is a dome- or hump-shaped wave or notch that appears at the end of or after the QRS complex and that has the same polarity as the preceding QRS complex. It may be prominent as a normal variant (see later), in certain pathologic conditions such as systemic hypothermia (sometimes referred to as an *Osborn wave*, described later), and in a set of conditions commonly referred to as the *J wave syndromes* that include the *Brugada patterns* (see Chapters 63 and 67) and the *early repolarization pattern* (discussed later and in Chapter 63). The origin of the J wave has been putatively associated with a prominent notch found in phase 1 of epicardial action potentials but not in those on the endocardium, creating a transmural potential gradient at the end of the QRS complex and beginning of the ST-T wave, leading to QRS notching and ST elevation.[7] A role of increased vagal tone has also been implicated in persons without structural heart disease, because benign early repolarization patterns are most apparent at slower heart rates.

Another wave occurring at the onset of repolarization is the *epsilon wave*. This uncommon wave (or set of waves) appears as a low-amplitude, high-frequency spike (or spikes) between the end of the QRS and the onset of the T wave, usually in the right precordial leads. It has been related to markedly delayed activation of islands of functional tissue interspersed among fatty or scarred tissue and, for example, is one diagnostic hallmark of arrhythmogenic right ventricular cardiomyopathy (see Chapter 52).

Normal Variants

Numerous variations in these normal ECG patterns frequently occur in persons without heart disease. The presence of such findings without coexistent cardiac pathology is particularly common among young persons and athletes (see Chapter 32). These variations are important to recognize because they may be mistaken for significant abnormalities, leading to erroneous and potentially harmful diagnoses of heart disease.

The absence of septal q waves, with QS complexes in the right precordial leads or with initial R waves in leads I, V_5, and V_6, is a common normal variant that is not generally associated with any specific cardiac disease. Recent studies using cardiac magnetic resonance (CMR)
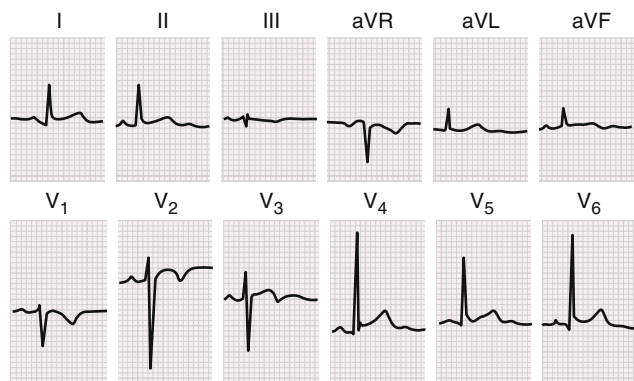
FIGURE 14.10 Normal tracing with a juvenile T wave inversion pattern in leads V_1, V_2, and V_3, as well as early repolarization pattern manifested by ST-segment elevation in leads I, II, aVF, V_4, V_5, and V_6. J point notching is also present in lead V_4. (Courtesy Dr. C. Fisch.)

FIGURE 14.11 Normal variant with the "benign early repolarization" pattern of a J point notch and ST-segment elevation. The ST-segment elevation and a J point notch are most marked in the midprecordial lead V_4. Reciprocal ST-segment depression and PR-segment depression are absent (except in lead aVR). (From Goldberger AL, Goldberger ZD, Shvilkin A. *Goldberger's Clinical Electrocardiography: A Simplified Approach*. 9th ed. Philadelphia: Elsevier; 2017.)

imaging have, however, suggested that this finding may reflect septal scarring of ischemic or nonischemic origin.[11]

The presence of rSr′ patterns in leads V_1 and V_2 with a normal QRS duration may commonly be found in subjects without cardiac disease, including up to half of trained athletes (see Chapter 32). It may be artefactually produced by placing electrodes of leads V_1 and V_2 higher on the chest than standard. In patients with pectus excavatum, the pattern may result from changes in heart position caused by the skeletal deformity. Pathologic conditions with this pattern, discussed later, include bundle branch blocks, Brugada patterns, RV hypertrophy, preexcitation syndromes, and hyperkalemia.

T wave inversion in leads V_1 to V_3 (sometimes referred to as the *persistent juvenile pattern*) (Fig. 14.10) is common among children and adolescents and in 1% to 3% of apparently healthy adults. It is more prevalent in women than in men, in African Americans than in other racial or ethnic groups, and in as many as 30% of athletes. T wave inversion of 2 mm or greater in two leads from V_{2-6}, in leads II and aVF, or in leads I and aVL suggests underlying pathology.
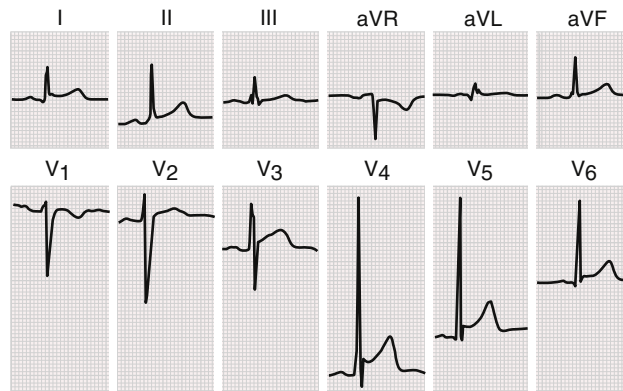
Another common and important variant is the so-called benign *early repolarization pattern* (see Chapter 63). Differing diagnostic criteria have been proposed. The AHA suggested that the term be applied as an umbrella term including cases with ST-segment elevation without chest pain, with terminal QRS slurring, or with terminal QRS notching.[12]

Recent recommendations by another expert panel[7] have suggested that this ECG diagnosis may be made if (1) there is a prominent notch or J wave at the end of QRS complex or slur on the downstroke of the R wave, (2) the peak of the notch or J wave is 0.1 mV or greater in amplitude in two or more contiguous leads, excluding V_1 to V_3 (to avoid cases of Brugada pattern), and (3) the QRS duration is normal. Although commonly associated with these findings, ST-segment elevation is not required.

The elevated ST segment, when present, typically has a rapidly upsloping shape and is most prominent in the right and midprecordial leads (Fig. 14.11). Its appearance is labile, being most prominent under conditions of increased vagal tone and decreasing with exercise. This pattern occurs in as many as 30% of the general population and is most prevalent in young adults, especially African American men and in athletes.

Although most commonly a benign variant, subsets of subjects with the early repolarization phenotype have been described as tachyarrhythmias and sudden death may occur. Potentially malignant subsets of early repolarization syndrome include those with J wave patterns in multiple leads and the inferior leads, J wave amplitudes of greater than 0.2 mV, or horizontal or downsloping ST-segment elevation (see Chapters 63 and 70).[7] Specific diagnostic criteria for this syndrome, including clinical and family history criteria and genetic markers, have been proposed.[7]

Cardiac mapping studies have documented the electrophysiologic bases for these ECG findings in patients with early repolarization syndromes.[13] These include localized areas with prominent epicardial J

waves followed by significantly shortened repolarization phases. The heterogeneous distribution of these regions results in large and localized repolarization potential gradients that may be arrhythmogenic.

It is important to distinguish the early repolarization pattern from other clinically important diagnoses. These include anterior MI, pericarditis, and cardiomyopathies and the Brugada patterns (see Chapter 63). QRS notches due to intraventricular conduction defects and myocardial scarring that are most common in the middle portions of the downslope of the R wave. The distinction between benign and pathologic early repolarization variants is an ongoing subject of research and some controversy.

An important set of normal variations, including benign early repolarization, are those that commonly occur in athletes (see Chapter 32). Prolonged, regular exercise can produce significant electrophysiologic changes that commonly cause variant ECG patterns. Although these changes reflect physiologic rather than pathologic effects, they may mimic the ECG patterns of various diseases and thus result in high rates of false-positive interpretations. To account for these variants, different ECG criteria separating normal from abnormal tracings have been proposed for use in athletes.[14] These include considering increased QRS voltage, IRBBB, and right-sided T wave inversions, among other findings, to be normal variants.

THE ABNORMAL ELECTROCARDIOGRAM

The prevalence of abnormal ECGs in the general population is substantial and increases progressively with age and in certain population groups. For example, in the ARIC study of 4856 disease-free persons with normal ECGs at enrollment, 53.4% developed an abnormal ECG over the subsequent 10 years.[15] Many of these abnormalities have prognostic as well as diagnostic import. In the ARIC study, enrollees with a continuously normal ECG had a 41% lower risk of cardiovascular disease during a 13 year follow-up than did those who developed abnormal tracings.[15] Even minor ECG abnormalities (e.g., isolated ST-T wave changes) have prognostic significance; among subjects free of baseline cardiovascular disease at enrollment in the Third National Health and Nutrition Examination Survey (NHANES), each additional minor ECG abnormality was associated with a 13% increase in cardiovascular death during a 14-year follow-up.[1]

Chamber Enlargement and Hypertrophy
Atrial Abnormalities
Various pathophysiologic events can produce P wave abnormalities reflecting changes in (1) the origin of the initiating sinus node impulse, (2) conduction within the atria and from the RA to the LA, or (3) the size and shape of the atria. These may result in abnormal patterns of interatrial block, left atrial abnormalities, and right atrial abnormalities.

Abnormal Atrial Activation and Conduction. Small shifts in the site of initial activation within or near the sinoatrial node or to ectopic sites within the atria can lead to major changes in the pattern of atrial activation and in the morphology of P waves. These shifts may occur as *escape rhythms* if the normal SA nodal pacemaker fails or as *accelerated atrial rhythms* if the automaticity of an ectopic site is enhanced (see Chapter 65). Physiologic changes may also alter the P wave shapes; exercise, for example, may produce a more vertical mean P wave axis.

P wave patterns may suggest the site of impulse formation and the path of subsequent activation. A negative P wave in lead I suggests activation beginning in the LA, and an inverted P wave in the inferior leads generally corresponds to a posterior atrial activation site. However, predicting the specific location of origin from a P wave pattern is highly variable. Accordingly, these patterns, as a group, may be referred to as *atrial rhythms* rather than assigned anatomic terms inferring a specific site of origin.

Interatrial block (sometimes termed intra-atrial block [IAB]) refers to conduction delay within and between the atria that alters the duration and pattern of P waves.[16] In milder cases of delay, conduction from the RA to the LA is delayed, but the overall sequence of activation is preserved. The increased lag in LA activation relative to that of the RA increases P wave duration beyond 120 msec. P waves typically have two humps in lead II, with the first representing RA and the second reflecting LA activation.

With more advanced IAB, the normal conduction paths are blocked. The sinus node impulses reach the LA only after passing inferiorly toward the AV junction, across the mid-lower portion of the interatrial septum, and then superiorly through the LA. In these cases, P waves are wide and biphasic (an initial positive wave followed by a negative deflection) in the inferior and anterior leads. IAB may also be intermittent, varying from beat to beat.

Interatrial block is uncommon in the general population. Among over 14,000 persons in the general population enrolled in the ARIC trial, interatrial block was found in 0.5% at enrollment and an additional 1.3% developed IAB in during an average 5.9-year follow-up.[17] Rates among patients with cardiac disease or in hospitalized cohorts may, however, reach 60%. It is often, but not always, associated with ECG findings of LA enlargement, and evidence of anatomic LA remodeling and reduced atrial pump function.[18] IAB is associated with a threefold increase in the risk of developing atrial tachyarrhythmias and fibrillation (*Bayés syndrome*), and increases in the risk for ischemic strokes and cardiac death.

Left Atrial Abnormality

Anatomic abnormalities of the LA that alter the P waves include atrial dilation, atrial muscular hypertrophy, elevated intra-atrial pressures, and, as discussed earlier, conduction slowing. Because these pathophysiologic abnormalities often coexist and produce similar ECG effects, the resulting patterns are often referred to as *left atrial abnormality*.

DIAGNOSTIC CRITERIA. Abnormalities in LA structure and function produce wide and notched P waves, with prominent terminal negative deflections (P terminal forces) in the right precordial leads. The most common criteria for diagnosing left atrial abnormality are listed in Table 14.3 and illustrated in Figures 14.12 and 14.13.

Mechanisms for the Electrocardiogram Abnormalities. Prolonged activation time of the LA produces prolonged P wave duration, notching of P waves that is most prominent in inferolateral leads, and increased amplitude of the terminal negative P wave terminal force in the right precordial leads. As described earlier, the ECG changes described for LA abnormalities are very similar to those described for IAB and may reflect IAB caused by the structural changes induced by atrial hemodynamic abnormalities, sometimes referred to as "atriopathies."[18]

Diagnostic Accuracy. Studies correlating these ECG criteria with LA volumes determined by CMR[1] have demonstrated the limited accuracy of the criteria. A prolonged P wave duration has a high sensitivity (84%) but low specificity (35%). By contrast, bifid P waves and increased negative terminal P wave amplitude in lead V_1 have low sensitivities (8% and 37%, respectively) and high specificities (90% and 88%, respectively).

Clinical Significance. Because of the similarities in the ECG features of IAB and LA abnormality, the clinical significance of the two sets of abnormalities is similar. The finding of LA abnormality is associated with more severe cardiac dysfunction in patients with ischemic heart disease

TABLE 14.3 Common Diagnostic Criteria for Left and Right Atrial Abnormalities

LEFT ATRIAL ABNORMALITY	RIGHT ATRIAL ABNORMALITY*
Prolonged P wave duration to >120 msec in lead II	Peaked P waves with amplitudes in lead II to >0.25 mV
Prominent notching of P wave, usually most obvious in lead II, with interval between notches of >40 msec	Prominent initial positivity in lead V_1 or V_2 >0.15 mV
Ratio between duration of P wave in lead II and duration of PR segment >1.6	Increased area under initial positive portion of P wave in lead V_1 to >0.06 mm-sec
Increased duration and depth of terminal-negative portion of P wave in lead V_1 (P terminal force) so that the area subtended by it is >0.04 mm-sec	Rightward shift of mean P wave axis to >+75 degrees
Leftward shift of mean P wave axis to between −30 and −45 degrees	

*In addition to criteria based on P wave morphologies, right atrial abnormality is suggested by QRS changes as described in the text.
Reference: Hancock EW, Deal BJ, Mirvis DM, et al. Recommendations for the standardization and interpretation of the electrocardiogram. Part V. ECG changes associated with cardiac chamber hypertrophy. *J Am Coll Cardiol*. 2009;53:992–1002.
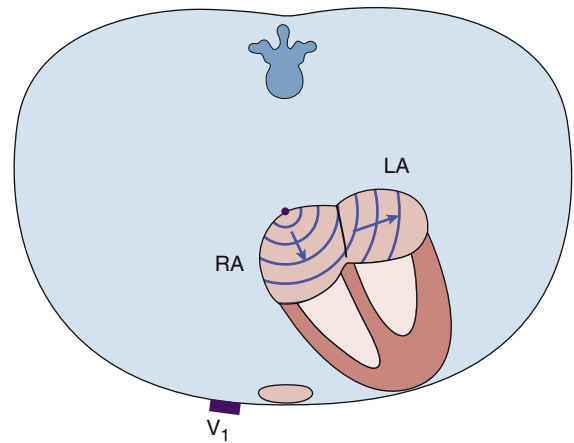
FIGURE 14.12 Top, Atrial depolarization. **Bottom,** P wave patterns associated with normal atrial activation (*left*) and with right atrial (*middle*) and left atrial (*right*) abnormalities. (Modified from Park MK, Guntheroth WG. *How to Read Pediatric ECGs*. 4th ed. St Louis: Mosby; 2006.)

(see Chapter 40) and with mitral or aortic valve disease (see Chapters 72, 73 and 75, 76). Patients with LA abnormalities also have a higher-than-normal incidence of atrial tachyarrhythmias, cerebrovascular accidents (CVAs), and all-cause and cardiovascular mortality (see Chapter 66). For example, in the ARIC study of over 14,000 persons followed for a mean of 22 years, LA abnormality defined by an abnormal P wave terminal force in V_1 was associated with an adjusted hazard rate for nonlacunar strokes of 1.49.[19]

Biatrial abnormality

FIGURE 14.13 Biatrial abnormality, with tall P waves in lead II (right atrial abnormality) and an abnormally large terminal negative component of the P wave in lead V₁ (left atrial abnormality). The P wave is also notched in lead V₅ as part of this pattern.

Right Atrial Abnormality

The ECG features of right atrial abnormality are illustrated in Figures 14.12 and 14.13. As in the case of LA abnormality, the term *right atrial abnormality* is preferred rather than designations such as "right atrial enlargement" that suggest a particular underlying pathophysiology.

> **Diagnostic Criteria.** P wave amplitudes in the limb and right precordial leads typically are abnormally high; P wave duration remains normal. Criteria commonly used to diagnose RA abnormality are listed in Table 14.3. In addition, RA abnormality is suggested by a qR-type pattern in the right precordial leads without evidence of MI or by low-amplitude QRS complexes in lead V₁ together with a threefold or greater increase in lead V₂.
>
> **Mechanisms for the Electrocardiogram Abnormalities.** Greater RA mass and size generate greater electrical forces early during atrial activation, producing taller P waves in limb leads and increasing the initial P wave deflection in leads such as lead V₁ that face the right heart. Because RA activation occurs early during the P wave, P wave duration is not prolonged, in contrast to the pattern with LA enlargement. Downward displacement of the heart may be responsible for the increase in P-terminal force and tall P waves in patients with emphysema.
>
> **Diagnostic Accuracy.** Imaging studies have shown that the ECG features of RA abnormality have limited sensitivity (7% to 10%) but high specificity (96% to 100%) for detecting anatomic RA enlargement.[1]
>
> **Clinical Significance.** Patients with chronic obstructive pulmonary disease and this ECG pattern (often referred to as P pulmonale) have more severe pulmonary dysfunction and significantly reduced survival, than do others (see Chapters 87 and 88). However, comparison of ECG and hemodynamic parameters has not demonstrated a close correlation between P wave patterns and RA hypertension.
>
> **Other Atrial Abnormalities.** Patients with biatrial abnormalities may have ECG patterns reflecting each defect. These include large, biphasic P waves in lead V₁ and tall, broad P waves in leads II, III, and aVF (see Fig. 14.13).

Left Ventricular Hypertrophy

Left ventricular hypertrophy (LVH) diagnosed by ECG occurs in 1% to 5% of the general population and in as many as one-third of patients with hypertension. QRS changes include greater than normal amplitudes of R waves in leads facing the LV (i.e., leads I, aVL, V₅, and V₆), and deeper than normal S waves in leads overlying the opposite side of the heart (i.e., V₁ and V₂). These changes are often associated with left axis deviation, notching or slurring of R waves, and patterns suggesting intraventricular conduction defects (Fig. 14.14). The ST segment may be normal or somewhat elevated in leads with tall R waves.

In many patients, the ST segment is depressed and followed by an inverted T wave (Fig. 14.15) in leads I, II, aVL, and V₅–V₆. The depressed ST segment is typically either flat or sloped downward from a depressed J point followed by an asymmetrically inverted T wave (the so-called *strain pattern*). These repolarization changes usually occur in patients with QRS changes but may appear alone. Additional abnormalities may include prolongation of the QT interval and evidence of LA abnormality.

These ECG features are most typical of LVH induced by pressure overload of the LV such as with hypertension (see Chapter 26). Volume overload may produce a somewhat different pattern, with tall upright T waves and narrow (<25 msec) but deep (≥0.2 mV) Q waves in leads I, aVL, and V₄₋₆ (Fig. 14.16) (see Chapter 73). These distinctions have limited value in identifying hemodynamic conditions.

QRS in hypertrophy
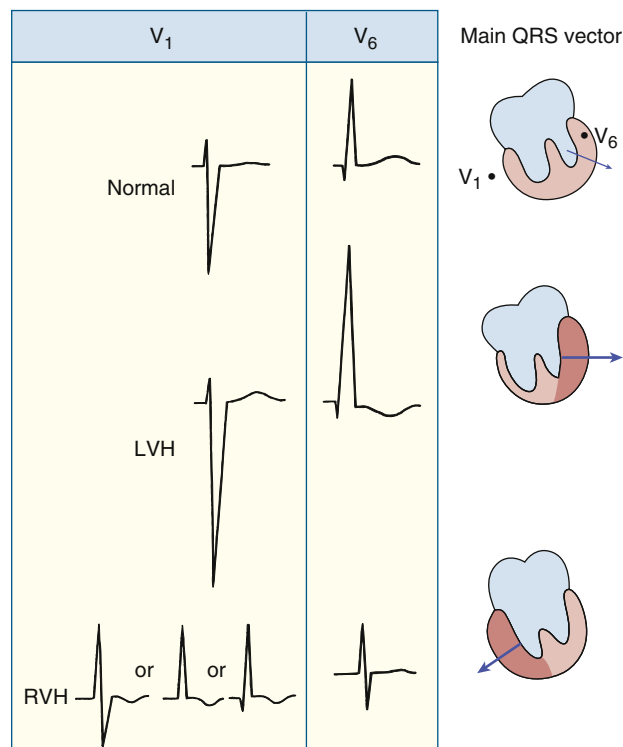
FIGURE 14.14 Left ventricular hypertrophy increases the amplitude of electrical forces directed to the left and posteriorly. In addition, repolarization abnormalities can cause ST-segment depression and T wave inversion in leads with a prominent R wave. Right ventricular hypertrophy can shift the QRS vector to the right, usually with an R, RS, or qR complex in lead V₁, especially when caused by severe pressure overload. T wave inversions may be present in the left precordial leads. (From Goldberger AL, Goldberger ZD, Shvilkin A. *Goldberger's Clinical Electrocardiography: A Simplified Approach*. 9th ed. Philadelphia: Elsevier; 2017.)
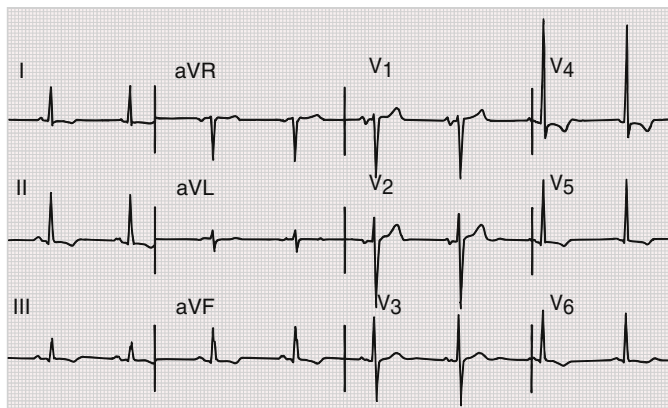
FIGURE 14.15 Marked left ventricular hypertrophy pattern with prominent precordial lead QRS voltages, ST-segment depression, and T wave inversion (compare with Fig. 14.16). Left atrial abnormality also is present.
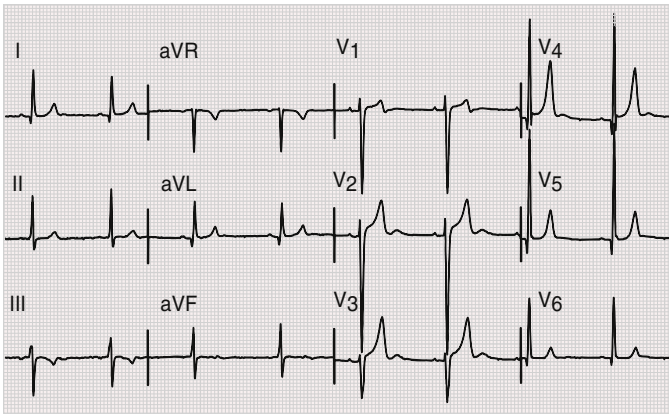
FIGURE 14.16 Left ventricular hypertrophy pattern with prominent Q waves and positive anterior T waves on an electrocardiogram from a patient with severe aortic regurgitation.

Mechanisms for the Electrocardiogram Abnormalities. ECG changes of LVH result from interrelated structural, biochemical, and bioelectric changes.[20] Structural abnormalities include (1) an increase size of myocytes leading to an increase in mass and in the size of activation fronts moving across the thickened wall to generate higher body surface voltages, (2) thickened walls that require more time to fully activate, and (3) changes in the interstitium including fibrosis, inflammation, and degenerative changes that result in slower-than-normal and fragmented conduction across the myocardium.

Hypertrophy is also associated with cellular forms of *electrical remodeling.* This includes biochemical changes in gap junctions and ion channels that alter the intensity of current flow. In addition, changes in myocyte branching patterns alter impulse propagation. The heterogeneous distribution of these abnormalities and scattered intramural scarring associated with hypertrophy can also disrupt smooth propagation of wavefronts to produce prolongation and notching of the QRS complex. Simulation studies have demonstrated that it is the combination of the anatomic abnormalities (i.e., increased muscle mass) and slowed and disordered conduction that leads to the observed ECG changes.

ST-T abnormalities reflect several interrelated phenomena These include primary disorders of repolarization that accompany the cellular processes of hypertrophy, the mechanical consequences of hypertrophy, and myocardial ischemia-related relative inadequacy of perfusion in relation to the increased oxygen demand caused by greater muscle mass and increased wall stress.

Diagnostic Criteria

Many sets of criteria to diagnose anatomic LVH have been developed based on these ECG abnormalities. Widely used criteria are listed in Table 14.4.

Most methods predict the presence or absence of LVH as a binary function, indicating that structural LVH either does or does not exist, based on an empirically determined set of criteria. For example, the widely used Sokolow-Lyon and Cornell voltage criteria require that voltages in specific leads exceed certain values. The Cornell voltage-duration method includes measurement of QRS duration as well as amplitudes. Other methods such as the Cornell regression equation seek to quantify LV mass as a continuum, with a diagnosis of LVH based on a computed mass that exceeds an independently determined threshold.

Diagnostic Accuracy. The accuracy of these criteria depends on the ultimate outcome being predicted. This reference standard may be, as most frequently practiced, the presence or absence of structural LVH. Alternatively, the ECG criteria may be used to predict clinical outcomes, as discussed later.

The reported diagnostic accuracies of these ECG criteria to detect structural LVH are highly variable, differing with the specific criteria tested, the imaging method used to determine anatomic measurements (e.g., echocardiography or CMR) and the population studied. Most studies have reported low sensitivities and high specificities. An analysis of the MESA study which used CMR imaging to establish anatomic standards, for example, demonstrated a sensitivity and specificity

TABLE 14.4 Common Diagnostic Criteria for Left Ventricular Hypertrophy

MEASUREMENT	CRITERIA
Sokolow-Lyon voltages	$SV_1 + RV_5 > 3.5$ mV
	$RaVL > 1.1$ mV
Romhilt-Estes point score system*	Any limb lead R wave or S wave >2.0 mV (3 points)
	or SV_1 or $SV_2 \geq 3.0$ mV (3 points)
	or RV_5 to $RV_6 \geq 3.0$ mV (3 points)
	ST-T wave abnormality, no digitalis therapy (3 points)
	ST-T wave abnormality, digitalis therapy (1 point)
	Left atrial abnormality (3 points)
	Left axis deviation ≥−30 degrees (2 points)
	QRS duration ≥90 msec (1 point)
	Intrinsicoid deflection in V_5 or V_6 ≥50 msec (1 point)
Cornell voltage criteria	$SV_3 + RaVL > 2.8$ mV (for men)
	$SV_3 + RaVL > 2.0$ mV (for women)
Cornell regression equation	Risk of LVH = $1 / (1 + e^{-exp})$†
Cornell voltage duration measurement	QRS duration × Cornell voltage >2436 mm-sec‡
	QRS duration × sum of voltages in all leads >1742 mm-sec

LVH, Left ventricular hypertrophy; *PTF,* P terminal force; *PTFV₁,* P terminal force in lead V_1.

*Probable LVH is diagnosed with totals of 4 points, and definite LVH is diagnosed with totals of 5 or more points.

†For persons in sinus rhythm, exp = 4.558 − 0.092 (SV_3 + RaVL) − 0.306 TV_1 − 0.212 QRS − 0.278 PTFV₁ − 0.559 (sex). Voltages are in mV, QRS is QRS duration in milliseconds, PTFV₁ is the area under the P terminal force in lead V_1 (in mm-sec), and sex = 1 for men and 2 for women. LVH is diagnosed as present if exp <−1.55.

‡For women, add 8 mm.

Reference: Hancock EW, Deal BJ, Mirvis DM, et al. AHA/ACCF/HRS recommendations for the standardization and interpretation of the electrocardiogram: part V: electrocardiogram changes associated with cardiac chamber hypertrophy: a scientific statement from the American Heart Association Electrocardiography and Arrhythmias Committee, Council on Clinical Cardiology; the American College of Cardiology Foundation; and the Heart Rhythm Society. Endorsed by the International Society for Computerized Electrocardiology. *J Am Coll Cardiol.* 2009;53:992–1002.

of 22.4% and 95.1%, respectively, for detecting CMR-determined LVH based upon having either a positive Sokolow-Lyon or Cornell voltage criterion.[21]

Because of the limited and variable accuracy of the various criteria from one trial to another, no single criterion can be established as the preferred method. The use of combined criteria, e.g., using both the Cornell product and the Sokolow-Lyon criteria, may result in a higher sensitivity (with a modest reduction in specificity), as well as an increase in the predicted risk of future cardiovascular events, than ECG diagnoses based on only one of the criteria.[22]

Accuracy in identifying anatomic LVH also varies with sex (with women having lower QRS amplitudes than men), race (with African Americans having higher QRS amplitudes than whites), age (with lower voltages with increasing age), and body habitus (with obesity reducing QRS amplitudes).

Clinical Significance

The low sensitivities of ECG measurements limit the value of these criteria as screening tools for structural LVH in both the general population and cohorts with a higher prevalence of LVH. The significance of an ECG diagnosis of LVH may also be measured by its ability to identify patients at high risk for future cardiac clinical events.[21,23] Thus, the presence of ECG criteria for LVH may identify a subset of the general population and of those with various cardiac diseases who have a significantly increased risk for cardiovascular morbidity, independent of the presence of anatomic hypertrophy. For example, in the ALLHAT
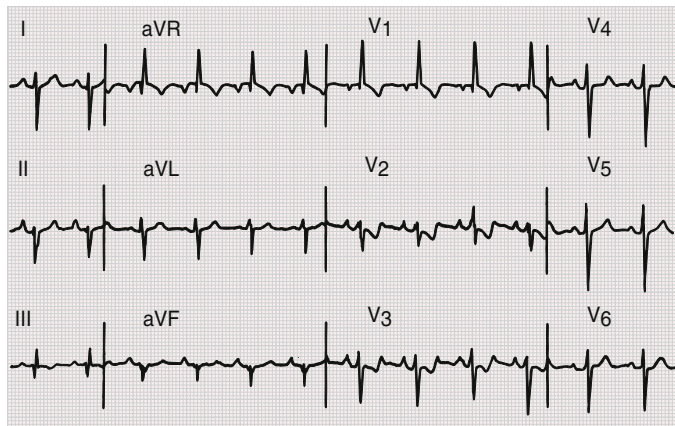
FIGURE 14.17 Right ventricular hypertrophy pattern most consistent with severe pressure overload of the right ventricle. Findings include (1) a tall R wave in V_1 (as part of the qR complex), (2) right axis deviation, (3) ST-segment depression and T wave inversion in V_1 through V_3, (4) delayed precordial transition zone (rS in V_6), (5) right atrial abnormality, and (6) an $S_1Q_3T_3$ pattern.

study, baseline LVH by Cornell criteria as well as higher absolute levels of Cornell voltage were associated with 29% to 98% increases in the risks of all-cause mortality, MI, coronary heart disease events, stroke, and heart failure during a 5-year follow-up.[23]

Studies have also documented the independent predictive value of LVH diagnoses by ECG and by imaging studies. For example, the risk of cardiovascular events in patients with LVH by ECG is independent of anatomic abnormalities on echocardiography.[24] Also, the risk of cardiovascular events in patients with ECG LVH is higher than in those without these findings, whether the findings represented a true- or false-positive finding based on anatomic measurements.[21] These reports and the common discrepancies between ECG and anatomic measures of LVH may relate to the different although overlapping pathophysiologic effects of hypertrophy described earlier, i.e., structural changes assessed by imaging and electrical dysfunction and remodeling assessed by the ECG.

The clinical significance of ST-T wave changes has been demonstrated in, for example, the MESA study.[25] The presence of ST-T strain patterns was associated with an increased risk of all-cause mortality, incidence of heart failure, MI, all cardiovascular disease events during the 10-year follow-up, with hazard ratios of 1.3 to 2.8. CMR imaging in this population demonstrated that the presence of these patterns is associated with the development of abnormal cardiac remodeling, concentric hypertrophy, and LV scarring.

In addition to these clinical impacts, the ECG changes of LVH may confound or obscure ECG changes of other common conditions. The widened and notched QRS complex may mimic intraventricular conduction defects, and the ST-T wave changes may suggest myocardial ischemia or infarction. Similarly, the ECG changes of other conditions such as left anterior fascicular block (LAFB), left bundle branch block (LBBB), and right bundle branch block (RBBB) may reduce the value of ECG criteria for LVH.

Right Ventricular Hypertrophy

Right ventricular hypertrophy (RVH) changes fundamental aspects of the QRS complex, whereas an enlarged LV produces predominantly quantitative changes in underlying normal waveforms. The abnormalities associated with moderate to severe concentric RVH most often include abnormally tall R waves in anteriorly and rightward-directed leads (e.g., leads aVR, V_1, and V_2), and abnormally deep S waves and small r waves in leftward-directed leads (e.g., I, aVL, and lateral precordial leads) (Fig. 14.17). The normal R wave progression in the precordial leads is reversed, the frontal plane QRS axis is shifted to the right, and S waves in leads I, II, and III are common (the $S_IS_{II}S_{III}$ *pattern*).

Less severe hypertrophy, especially when limited to the outflow tract of the RV that is activated late during the QRS complex, produces less marked changes. Abnormalities may be limited to an rSr′ pattern in

TABLE 14.5 Common Diagnostic Criteria for Right Ventricular Hypertrophy

Tall R in V_1 > 0.6 mV
Increased R/S in V_1 > 1
Deep S in V_5 > 1.0 mV
Deep S in V_6 > 0.3 mV
Tall R in aVR > 0.4 mV
Small S in V_1 < 0.2 mV
Small R in V_{5-6} < 0.3 mV
Reduced R/S ratio in V_5 < 0.75
Reduced R/S ratio in V_6 < 0.4
Reduced R/S in V_5 to R/S in V_1 < .04
$(R_I + S_{III}) - (S_I + R_{III})$ < 1.5 mV
Max R_{V1-2} + Max $S_{I, aVL} - S_{V1}$ > 0.6 mV
$RV_1 + S_{V5-6}$ > 1.05 mV
R peak V_1 > 0.035 msec
QR in V_1 present

Data from Hancock EW, et al. Deal BJ, Mirvis DM, et al. Recommendations for the standardization and interpretation of the electrocardiogram. Part V. ECG changes associated with cardiac chamber hypertrophy. *J Am Coll Cardiol.* 2009;53:992–1002.

V_1 and persistence of s (or S) waves in the left precordial leads. This pattern is typical of RV volume overload, such as produced by an atrial septal defect and may also be seen in persons without manifest cardiac abnormalities (see later).

Diagnostic Criteria

Commonly relied-on criteria for the ECG diagnosis of RVH are listed in Table 14.5. Right axis deviation is present in most cases of significant RVH, although it is not typically included as a diagnostic criterion. Other ECG findings that are supportive although not diagnostic of RVH include an RSR′ pattern in V_1 with a QRS duration longer than 120 msec; positive S/R ratio in leads I, II and III; an S_1Q_3 pattern; negative T waves in V_{1-3}; and evidence of RA abnormality.

Diagnostic Accuracy. Common criteria typically show low sensitivities and high specificities. In the MESA study comparing ECG and CMR diagnoses of RVH in subjects without cardiac disease and normal LV morphology, most criteria had sensitivities less than 10%.[1] Although specificities were high (85% to 99%), the low prevalence of RVH resulted in a post-test positive predictive value that was similar to the pre-test probability of having RVH. Higher sensitivities have been reported with congenital heart disease and in patients with pulmonary hypertension (see Chapters 82 and 88).

Several factors contribute to the limited accuracy of standard criteria. Because the magnitude of forces generated by the RV are much lower than those generated by the LV, RVH must be severe enough to overcome the masking effects of the LV forces to be manifest on the ECG. Also, most standard criteria were developed based on autopsy studies of patients with severe disease and, hence, may have limited applicability to other populations.

Mechanisms for the Electrocardiogram Abnormalities. As in LVH, RVH increases current fluxes between hypertrophied cells and increases the size of activation fronts moving through the enlarged and thickened RV to produce higher-than-normal voltages on the body surface. In addition, the activation time of the RV is prolonged. RV activation now ends after activation of the LV is completed. As a result, cancellation of RV forces by the more powerful LV forces is reduced, so that RV forces become manifest late in the QRS complex (e.g., generation of S waves in left precordial leads). Because the RV is located anteriorly and to the right of the LV, these changes are most prominent in leads directed anteriorly and to the right, that is, in the right precordial leads.

CMR imaging has also suggested that RV enlargement may cause changes in cardiac anatomy. The RV may be shifted in a clockwise direction so that it lies under more leftward precordial electrodes than normal. Hence, leads V_4 to V_6 are more affected by RV forces than normal to show delayed transition zones with lateral S waves.[26]
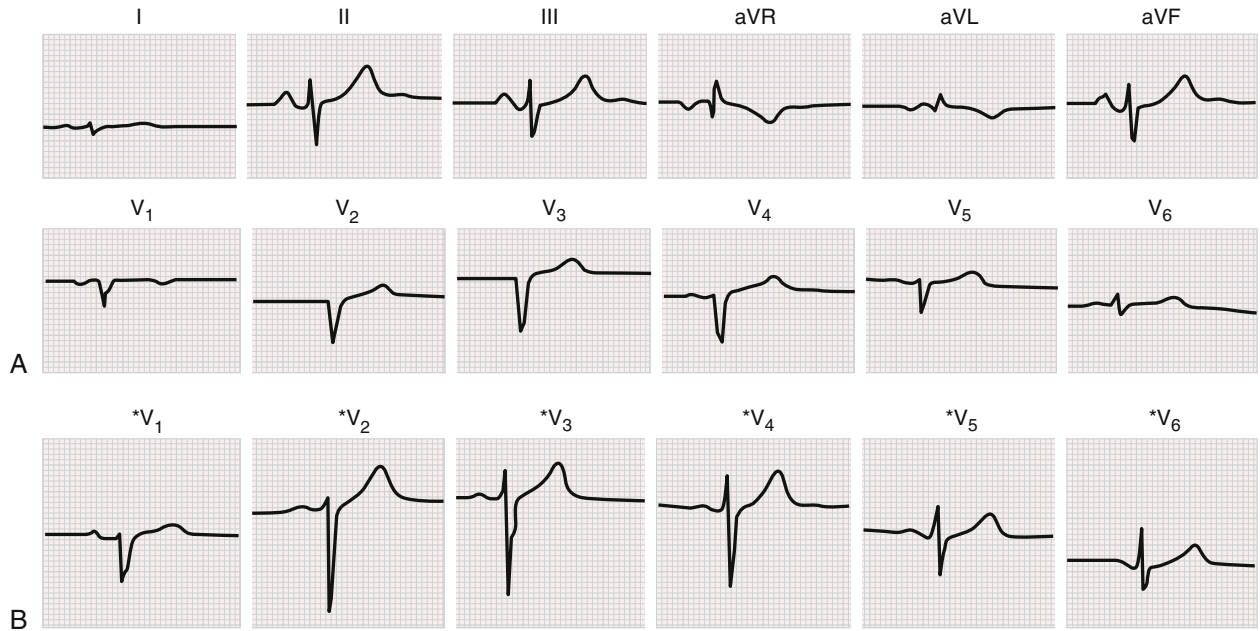
FIGURE 14.18 Pulmonary emphysema simulating anterior infarction in a 58-year-old man with no clinical evidence of coronary artery disease. **A,** Loss of anterior R waves in the precordial leads. **B,** Relative normalization of R wave progression with placement of the chest leads an interspace below their usual position (e.g., *V$_1$, *V$_2$). (Modified from Chou TC. Pseudo-infarction (noninfarction Q waves). In: Fisch C, ed. *Complex Electrocardiography*. Vol. 1. Philadelphia: FA Davis; 1973.)
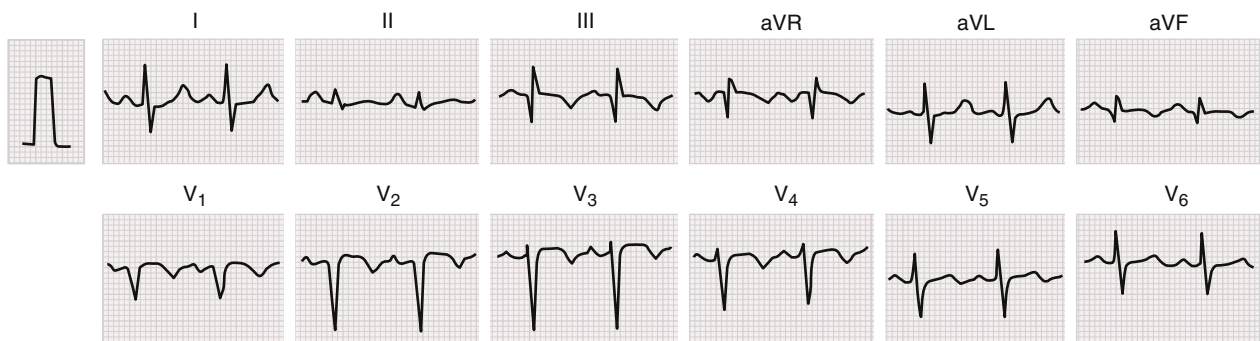
FIGURE 14.19 Acute cor pulmonale secondary to acute pulmonary embolism simulating inferior and anterior infarction. This tracing shows an $S_1Q_3T_3$ pattern, a QS in lead V$_1$ with slow R wave progression in the right precordial leads (clockwise rotation pattern), and right precordial to midprecordial ST elevation and T wave inversion (V$_1$ to V$_4$). (From Goldberger AL, Goldberger ZD, Shvilkin A. *Goldberger's Clinical Electrocardiography: A Simplified Approach*. 9th ed. Philadelphia: Elsevier; 2017.)

Clinical Significance

The prevalence of ECG-diagnosed RVH varies widely based on the criteria that are used. An analysis of 7857 patients in the third NHANES trial using 16 different criteria, the prevalence of diagnosed RVH varied from 0.9% to 20.7%.[27] A positive ECG diagnosis was associated with a significant increase in all-cause mortality with most criteria; mortality during the 14-year follow-up increased by 6% with each additional ECG criterion that was met.

Chronic obstructive pulmonary disease (see Chapter 88) can induce ECG changes by producing anatomic RVH, by changing the position of the heart within the chest, and by hyperinflation of the lungs (Fig. 14.18). The insulating and positional changes produced by pulmonary hyperinflation lead to reduced amplitude of the QRS complex, right axis deviation of both the P wave and QRS complex in the frontal plane, and delayed transition in the precordial leads. Evidence of true anatomic RVH includes right axis deviation, deep S waves in the lateral precordial leads, and an $S_1Q_3T_3$ *pattern*, with an S wave in lead I (as an RS or rS complex), an abnormal Q wave in lead III, and an inverted T wave in the inferior leads.

Pulmonary embolism causing acute RV pressure overload may generate characteristic ECG patterns (Fig. 14.19) (see Chapter 87). These include a QR or qR pattern in the right sided leads, an $S_1Q_3T_3$ pattern, ST-segment deviation and T wave inversions in leads V$_1$ to V$_3$,

and incomplete or complete RBBB. Massive embolization may also cause ST-segment elevation in the right to midprecordial leads, complete RBBB, and T wave inversions in leads V$_1$ to V$_4$. In one series, the presence of the $S_1Q_3T_3$ pattern was associated with an odds ratio (OR) of 2.5 for adverse events.[28] However, the sensitivity of these findings for detecting RV dysfunction is low even with major pulmonary artery obstruction.

Biventricular Hypertrophy

Hypertrophy of both ventricles produces complex ECG patterns. In contrast to biatrial abnormality or enlargement, the result is not the simple sum of the two sets of abnormalities. The effects of enlargement of one chamber may cancel the effects of enlargement of the other. The greater LV forces generated in LVH increase the degree of RVH needed to overcome the dominance of the LV, and the anterior forces produced by RVH may cancel the enhanced posterior forces generated by LVH.

Because of these factors, specific ECG criteria for either RVH or LVH are seldom observed with biventricular enlargement. Rather, ECG patterns usually are a modification of the features of LVH, and include tall R waves in the right and left precordial leads, or evidence of LVH along with right axis deviation, deep S waves in the left precordial leads, or a shift in the precordial transition zone to the left (Fig. 14.20).
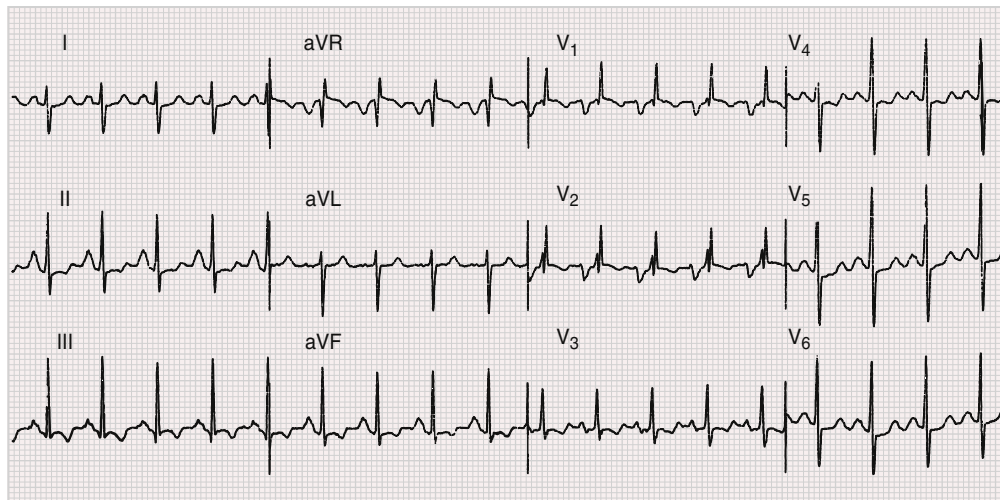
FIGURE 14.20 ECG from a 45-year-old woman with severe mitral stenosis showing right axis deviation and a tall R wave in lead V_1 consistent with right ventricular hypertrophy (RVH). The biphasic P wave in lead V_1 indicates left atrial abnormality and the tall P waves in lead II suggest concomitant right atrial abnormality. Nonspecific ST-T changes and incomplete right bundle branch block also are present. The combination of RVH and marked left or biatrial abnormality is highly suggestive of mitral stenosis. (From Goldberger AL, Goldberger ZD, Shvilkin A. *Goldberger's Clinical Electrocardiography: A Simplified Approach*. 9th ed. Philadelphia: Elsevier; 2017.)

Intraventricular Conduction Delays

Intraventricular conduction delays (IVCDs) may result from structural or functional abnormalities in the specialized conducting tissues of the LBB system, in the RBB system, or in cardiac muscle (see Chapters 65, 67, and 68). The hallmark of these disorders is significant alteration in the activation pattern of the ventricles and, hence, in the QRS complex.

Fascicular Blocks

Conduction delays in one or more of the fascicles of the LBB system result in abnormal sequences of early LV activation leading to characteristic ECG patterns of *fascicular block*. Only modest delays in conduction in one fascicle relative to that in the others are enough to alter ventricular activation sequences sufficiently to produce characteristic ECG patterns.

Left Anterior Fascicular Block

Delays in conduction through the left anterior fascicle result in delayed activation of the uppermost portion of septum, the anterosuperior portion of LV, and the left anterior papillary muscle. This results in unbalanced inferior and posterior forces early during ventricular activation (activated by the normal left posterior fascicle) followed by unopposed anterosuperior forces later during the QRS complex (the region activated late).

The diagnostic features of LAFB are listed in Table 14.6 and illustrated in Figure 14.21.[1,29] The most characteristic finding is marked left axis deviation, with a shift of the mean frontal plane QRS axis to between −45 and −90 degrees. Lower degrees of left axis deviation, with axis shifts to between −30 and −45 degrees, may be the result of less severe conduction delay or other conditions such as LVH.

The resulting QRS pattern in the inferior leads includes initial r waves (caused by early unopposed activation of the inferoposterior LV) followed by deep S waves (caused by unopposed late activation of the anterosuperior LV). Therefore, leads II, III, and aVF show rS patterns. Leads I and aVL may show exaggerated septal q waves followed by R waves (a qR pattern).

Precordial leads typically show the pattern of a delayed transition zone that is produced by the late activation of the anterosuperior LV. Leads V_4 through V_6 typically show deeper than normal S waves. The overall QRS duration is not prolonged; fascicular blocks alter the sequence but not the overall duration of LV activation.

LAFB may mask or mimic ECG changes from other conditions. The larger R waves in leads I and aVL and smaller R waves but deeper S waves in leads V_5 and V_6 make LVH criteria relying on R wave amplitude less accurate. Changes that may mimic or obscure patterns of MI are discussed later.

LAFB is common in persons without overt cardiac disease and in a variety of cardiac conditions, reflecting the delicate nature of the structure that lies in regions of turbulent blood flow near the LV outflow tract. Although generally considered to be a benign finding in the

TABLE 14.6 Common Diagnostic Criteria for Fascicular Blocks

Left Anterior Fascicular Block
Frontal plane mean QRS axis between −45 and −90 degrees
qR pattern in lead aVL
QRS duration <120 msec
Time to peak R wave in aVL ≥ 45 msec
Left Posterior Fascicular Block
Frontal plane mean QRS axis >90 degrees (or >110–120 degrees)
rS pattern in leads I and aVL with qR patterns in leads III and aVF
QRS duration <120 msec
Exclusion of other factors causing right axis deviation (e.g., normal variants, right ventricular overload patterns, lateral infarction)

Reference: Surawicz B, Childers R, Deal BJ, et al. AHA/ACCF/HRS Recommendations for the standardization and interpretation of the electrocardiogram. Part III. Intraventricular conduction disturbances. *J Am Coll Cardiol*. 2009;53:976–981.

absence of manifest cardiovascular disease, it has been associated with an increased mortality risk in patients with coronary artery or other cardiac disorders.

Left Posterior Fascicular Block

The ECG pattern of left posterior fascicular block (LPFB) is characterized by right axis deviation. Although this is traditionally defined as greater than +90 degrees, requiring an axis greater than +110 to 120 degrees may improve specificity. The QRS shows rS patterns in leads I and aVL, and qR complexes in the inferior leads (see Table 14.6 and Fig. 14.21). These changes are the result of early unopposed activation forces from the anterosuperior aspect of the LV (activated normally via the left anterior fascicle and producing the initial q and r waves) and late unopposed forces from the inferoposterior free wall (activated late via the left posterior fascicle and generating the late S and R waves). The QRS duration remains normal.

Damage to the left posterior fascicle of the LBB is less common than damage to the anterior branch because of its thicker structure and more protected location near the LV inflow tract. LPFB most often occurs with extensive cardiac disease and in association with RBBB; it is unusual in otherwise healthy persons. The specific diagnosis of LPFB, isolated or in combination with RBBB, requires first excluding other, more common causes of right axis deviation, e.g., normal variants (especially in young adults), RV overload syndromes, and extensive high or anterolateral infarction.

Other Forms of Fascicular Block

An estimated one-third of people have an anatomic third branch of the LBB system—the *left median* or *septal fascicle*—that arises most often
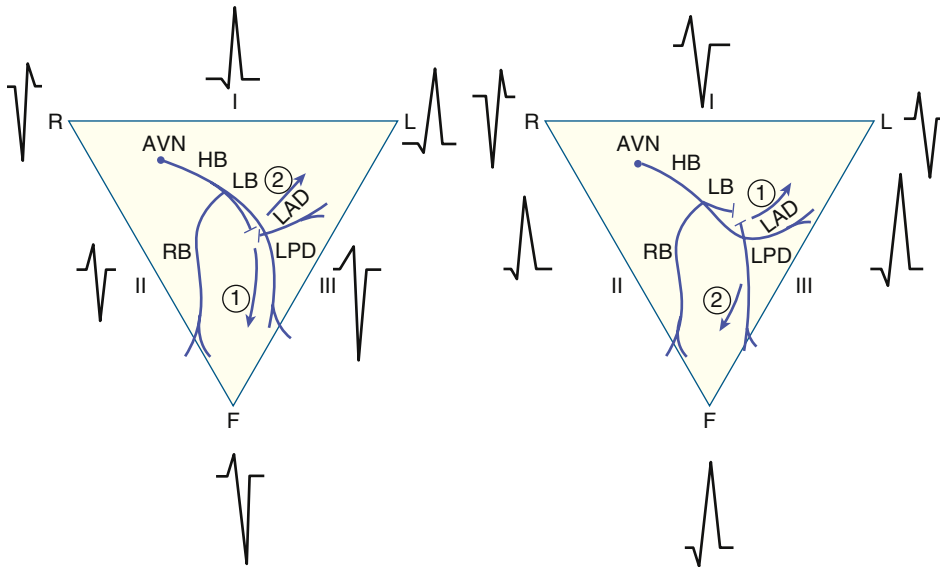
FIGURE 14.21 Diagrammatic representation of fascicular blocks in the left ventricle. **Left,** Interruption of the left anterior fascicle or division (here labeled *LAD*) results in an initial inferior (*1*) followed by a dominant superior (*2*) direction of activation. **Right,** Interruption of the left posterior fascicle or division (here labeled *LPD*) results in an initial superior (*1*) followed by a dominant inferior (*2*) direction of activation. *AVN,* Atrioventricular node; *HB,* His bundle; *LB,* left bundle; *RB,* right bundle. (Courtesy Dr. C. Fisch.)

from the left posterior fascicle and that contributes to initial left-to-right septal activation.[30] Conduction delay results in abnormal septal activation and the absence of septal q waves.

Left Bundle Branch Block

LBBB results from conduction delay or block in any of several sites in the left ventricular conduction system, including the fibers of the bundle of His that become the main LBB; the main LBB, in each of its two major fascicles; the distal conduction system of the LV, or in the ventricular myocardium. Recent mapping studies have suggested that the most common site of block may be within the bundle of His.[31] Simulation studies have also suggested that LBBB patterns may develop solely from disordered conduction within the ventricular walls even without disordered ventricular endocardial activation.[1]

Electrocardiogram Abnormalities

LBBB causes extensive reorganization of the activation and recovery patterns of the LV. The resulting ECG changes include a widened QRS complex with characteristic changes in its shape, as well as abnormalities of the ST-T wave. An example of the typical changes is shown in Figure 14.22 and the classical diagnostic criteria for LBBB are listed in Table 14.7.

Basic requirements include QRS duration of 120 msec or more; broad and, typically, notched R waves in leads I, aVL, and the left precordial leads; narrow r waves followed by broad and deep S waves in the right precordial leads; and, usually, the absence of septal q waves. The mean QRS axis may be normal, deviated to the left or, rarely, to the right.

Stricter criteria mandate a QRS duration of 140 msec or more and mid-QRS notching in left-facing leads.[1] These criteria may have better correlations with disordered endocardial activation patterns, abnormal LV mechanical function (see later), and greater benefit from resynchronization pacemaker therapy (see Chapters 58 and 69). Other criteria require a prolonged time to the peak of the R wave (≥60 msec) in the left precordial leads.

The ST segment and T wave are discordant with the QRS complex in most cases. The ST segments are depressed, and T waves are inverted in leads with positive QRS waves (e.g., leads I, aVL, V_5, and V_6). ST segments are elevated and T waves are typically upright in leads with predominantly negative QRS complexes (e.g., leads V_1 and V_2).

Incomplete LBBB (ILBBB) may result from lower degrees of conduction delay in the LBB system. Features include modest prolongation of the QRS complex (100 to 119 msec), slurring and notching of the upstroke of tall R waves, and delay in time to peak of the R wave in left precordial leads. Septal q waves may remain in many cases considered to have ILBBB. As many as one-third of patients with ILBBB develop full LBBB within 2 years.[32]
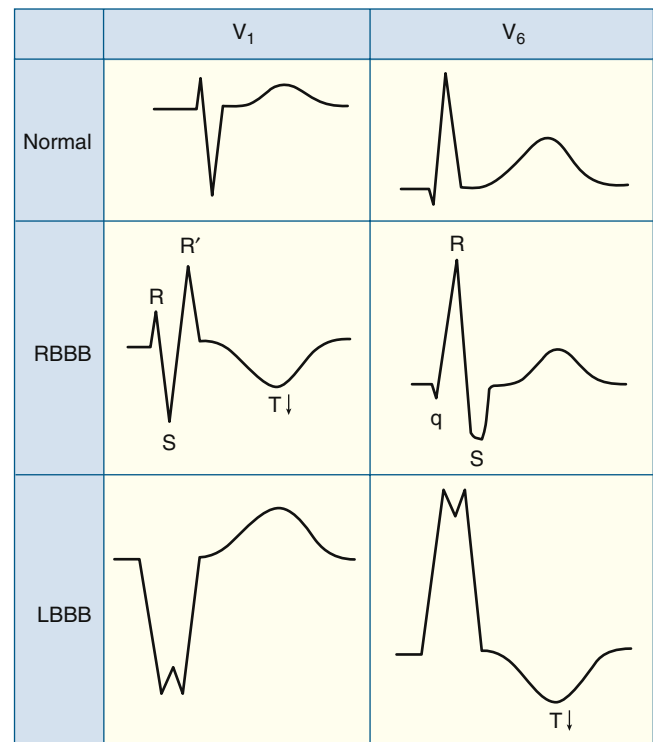
FIGURE 14.22 Comparison of typical QRS-T patterns in right bundle branch block (RBBB) (middle tracing) and left bundle branch block (LBBB) (bottom tracing) with the normal pattern (top tracing) in leads V_1 and V_6. Note the secondary T wave inversions (*arrows*) in leads with an rSR' complex with RBBB and in leads with a wide R wave with LBBB. (From Goldberger AL, Goldberger ZD, Shvilkin A. *Goldberger's Clinical Electrocardiography: A Simplified Approach.* 9th ed. Philadelphia: Elsevier; 2017.)

Mechanisms for the Electrocardiogram Abnormalities. LBBB causes extensive reorganization of left ventricular activation. Septal activation typically begins on the right rather than on the left septal surface, leading to right-to-left (rather than normal left-to-right) activation of the septum. As a result, normal septal q waves are absent. A delay of as little as 6 msec is sufficient to produce abnormal septal activation.

In as many as one-third of cases, however, earliest septal activation occurs in the left midseptal region. This suggests initial activation of the left side of the septum by the LBB rather than by transseptal spread. In such cases, septal q waves may persist. This LBBB pattern may reflect damage to the distal LBB system, a well-developed and spared septal branch of the LBB system, or delays primarily within the ventricular myocardium.

TABLE 14.7 Common Diagnostic Criteria for Bundle Branch Blocks

Complete Left Bundle Branch Block*
QRS duration ≥120 msec
Broad, notched, or slurred R waves in leads I, aVL, V_5, and V_6
Small or absent initial r waves in leads V_1 and V_2 followed by deep S waves
Absent septal q waves in leads I, V_5, and V_6
Prolonged time to peak R wave (>60 msec) in V_5 and V_6
Complete Right Bundle Branch Block
QRS duration ≥120 msec
rsr′, rsR′, or rSR′, patterns in leads V_1 and V_2
S waves in leads I and V_6 ≥40 msec wide
Normal time to peak R wave in leads V_5 and V_6 but >50 msec in V_1

*See text for discussion of criteria.
Reference: Surawicz B, Childers R, Deal BJ, et al. AHA/ACCF/HRS Recommendations for the standardization and interpretation of the electrocardiogram. Part III. Intraventricular conduction disturbances. *J Am Coll Cardiol.* 53:976–981.

LV activation follows slow transseptal spread from the RV side of the septum and is delayed by 40 to 80 msec. The pattern of activation of the LV free wall is highly variable, depending on the type, location, and extent of the underlying cardiac disease. Spread is disrupted by regions of block, especially in patients with infarction and scarring, forcing activation wavefronts to maneuver around the block through slowly conducting myocardium. This results in a prolonged QRS complex with prominent notching and slurring. Overall activation may require more than 180 msec. In contrast, among persons with LBBB but otherwise normal hearts, activation may proceed rapidly and in a more orderly fashion.

The discordant ST-T wave pattern reflects the altered pattern of ventricular activation. With LBBB, the RV is activated and recovers earlier than the LV so that recovery currents are directed toward the right and away from the LV. Therefore, positive ST-T waves will be registered in leads over the RV that show S waves and negative ones are detected over the left sided leads showing prominent R waves. These ST-T wave changes are referred to *secondary ST-T abnormalities* because they are generated predominantly by abnormalities in conduction. As discussed later, ST-T wave changes produced by direct abnormalities of the recovery process are referred to as *primary ST-T abnormalities*.

Clinical Significance
LBBB is uncommon in the general population. In the ARIC study of over 14,000 persons free of heart disease, LBBB was observed in 0.5%.[33] However, it occurs more often in older persons and in more than one-third of patients with heart failure. As many as 70% of persons in whom LBBB develops have preceding ECG evidence of LVH, and fewer than 10% of patients have no clinically demonstrable heart disease.

In persons with or without overt heart disease, LBBB is associated with a higher-than-normal risk of mortality and morbidity from infarction, heart failure, and arrhythmias including high-grade AV block. In the ARIC study, LBBB was associated with a fourfold increase in coronary artery disease death during a 21-year follow-up.[33] In the LIFE study, among patients with hypertension, LBBB was also associated with a fourfold increase in the likelihood of developing wall motion abnormalities during 5 years of follow-up.[34]

Hemodynamic abnormalities reflect the direct effects of the abnormal ventricular activation pattern of LBBB, the ventricular remodeling that may occur with prolonged disordering of activation, and the abnormalities caused by the underlying heart disease.[35] Although normal LV contraction is highly synchronized, the contraction pattern with LBBB is less coordinated and prolonged. Early septal contraction occurs while the LV lateral wall has not yet been activated. The activated septum balloons into the LV cavity and the as yet to be activated lateral wall is stretched. Once the LV free wall is finally activated, the septum has relaxed and the LV contraction forces the septum to balloon into the RV. These forms of mechanical dysfunction can be demonstrated in approximately 60% of patients with LBBB and is more common in those with the longest QRS durations.

These abnormalities reduce the contribution of the septum and of the free wall to stroke volume by approximately 10%, increase end

diastolic volume by approximately 15%, reduce cardiac efficiency, and increase myocardial work. Over time, these anomalous activation patterns likely contribute to structural remodeling, which when associated with hypertrophy of the lateral wall and thinning of the septum may cause or worsen mitral regurgitation. Such perturbations serve as a basis for resynchronization cardiac therapy (see Chapters 58 and 69).

Furthermore, the ECG changes of LBBB may obscure or simulate other ECG patterns. The diagnosis of LVH is complicated by the increased QRS amplitude intrinsic to LBBB, and the very high prevalence of anatomic LVH in patients with LBBB makes defining criteria with high specificity difficult. The diagnosis of MI may be obscured, as discussed in detail later. The impacts of the diffuse ST-T wave abnormalities related to altered activation patterns and changes in regional myocardial perfusion[1] due to disordered ventricular contraction also render unreliable the detection of ischemia on exercise ECG testing (see Chapter 15).

Right Bundle Branch Block
RBBB is a result of conduction delay in any portion of the right-sided intraventricular conduction system. The delay is most common in the distal branching portion of the bundle of His or in the main RBB; it may also occur in the more distal RV conduction system such as with damage to the RV moderator band after ventriculotomy.

Electrocardiogram Abnormalities
Major features of RBBB are illustrated in Figure 14.22, and common diagnostic criteria are listed in Table 14.7. As with LBBB, the QRS complex duration exceeds 120 msec. The right precordial leads show prominent and notched R waves with rsr′, rsR′, or rSR′ patterns, and leads I, aVL and the left precordial leads demonstrate S waves that are wider than the preceding R wave. The ST-T waves are discordant with the QRS complex; T waves are inverted in the right precordial leads and upright in the left precordial leads and in leads I and aVL. The mean QRS axis is not altered by RBBB; axis shifts can occur, however, as a result of the simultaneous occurrence of fascicular blocks along with RBBB (see later).

Incomplete RBBB may be produced by lesser delays in conduction in the RBB system or more distal damage to the RBB. It is characterized by an rSr′ pattern with a narrow r′ in lead V_1 and a QRS duration between 100 and 120 msec. These changes also may reflect underlying RVH (especially with a rightward QRS axis) without intrinsic dysfunction of the conduction system or may be a manifestation of the Brugada pattern (see Chapters 63 and 67). An rSr′ morphology in lead V_1 (and sometimes V_2) with a normal QRS duration is also a common finding in patients without cardiovascular disease, in association with pectus excavatum, and when the right precordial electrodes are placed too high in the chest.

> **Mechanisms for Electrocardiogram Abnormalities.** With delay in the proximal RBB system, activation of the right side of the septum is initiated only after slow transseptal spread of activation from the left septal surface. The activation of the septum and RV anterior free wall are delayed, and is followed by slow activation of the remaining RV.
>
> As a result, much or all of the RV is activated after depolarization of much of the LV has been completed. The late RV forces generated by the last areas of the RV to be activated—the right lateral wall and the outflow tract—are not cancelled by LV activation and generate increased anterior and rightward voltage observed in the latter half of the QRS in complete RBBB.
>
> Abnormal slow and disordered LV activation patterns similar to those seen with LBBB, accompanied by LV mechanical dyssynchrony, also occurs in patients with RBBB.[1] This likely reflects the extent of the underlying cardiac disease and the associated conduction system dysfunction.
>
> Discordant ST-T wave patterns are generated by the same mechanisms as for LBBB. With RBBB, recovery forces are directed away from the right and toward the earlier activated LV. The result is inverted T waves in the right precordial leads and positive ones in the left precordial leads.

Clinical Significance
RBBB is relatively common and is often detected as an incidental finding on routine testing. In the ARIC population-based study, RBBB was detected in 2.1% of enrollees.[33] The relatively high prevalence of RBBB

is attributable to the relative fragility of the RBB, as suggested by the development of RBBB after the minor trauma produced by right ventricular catheterization.

It is often found as an incidental finding in the absence of any demonstrable heart disease, may signal occult disease, or can develop in patients with any form of cardiovascular disorder. Although studies have reported variable effects of RBBB on prognosis, a meta-analysis of 19 studies including over 200,000 persons documented a small but significant increase in all-cause mortality (OR = 1.17) and an increase in cardiac death (OR = 1.43) in the general population.[36] Risks were similarly increased for patients with acute infarction, pulmonary embolism, and heart failure. Its frequent detection in athletes is discussed in Chapter 32.

RBBB, like LBBB, is associated with significant RV mechanical dysfunction, with higher RV end-systolic volumes and lower RV ejection fractions, especially in cases with R′ durations of over 100 msec.[37] This relation may reflect secondary damage to the RBB by mechanical stretch associated with marked RV dysfunction caused by the underlying condition. Alternatively, because of the delayed activation of the RV, peak RV contraction occurs significantly after that of the LV. These abnormalities may lead to mechanical dyssynchrony analogous to that seen with LBBB. In addition, as many as 40% of persons with RBBB (without LBBB) have abnormal LV mechanics.[38]

RBBB may also interfere with other ECG diagnoses. The diagnosis of RVH is more difficult to make with RBBB because of the accentuated positive potentials in lead V_1. RVH is suggested, although with limited accuracy, by the presence of an R wave in lead V_1 that exceeds 1.5 mV and a rightward shift of the mean QRS axis. An RBBB-like pattern with persistent ST-segment elevation in the right precordial leads may indicate the Brugada pattern, with susceptibility to ventricular tachyarrhythmias and sudden cardiac death (see Chapters 63 and 67).

The usual criteria for LVH have lower sensitivities than with normal conduction. RBBB reduces the amplitude of (or eliminates) the S wave in the right precordial leads and of the R waves in the left precordial leads, thus reducing the accuracy of ECG criteria for LVH. The combination of LAA or left axis deviation with RBBB does suggest underlying LVH.

Multifascicular Blocks

The term *multifascicular block* refers to conduction delay in more than one of the major structural components of the specialized conduction system. *Bifascicular block* involves delay or block in any two of these structures. It may have several forms depending on the sites of conduction delay. Delay in the RBBB and LAFB, the most common pattern, is characterized by a QRS pattern of RBBB plus left axis deviation beyond −45 degrees (Fig. 14.23). RBBB with LPFB produces a pattern of RBBB and a mean QRS axis deviation to the right of approximately +100 degrees (Fig. 14.24). LBBB alone, which may be caused by delay in both the anterior and the posterior fascicle, is also usually considered a form of bifascicular block even though the site or sites of delay are not known.

Trifascicular block involves conduction delay in the RBB plus delay in either the main LBB or in both the left anterior and the left posterior fascicle. The resulting ECG pattern depends on the relative degree of delay in the affected structures. If conduction delay exists in both the RBB and the main LBB and if the delay in the RBB is less than the delay in the LBB system, the QRS pattern will resemble that of LBBB. If the delay is greater in the RBB than in the LBB, the ECG pattern will be that of RBBB. Mixed patterns, for example, with LBBB patterns in the limb leads but RBBB patterns in the precordial leads, are also common.

A diagnosis of trifascicular block requires an ECG pattern of bifascicular block plus evidence of prolonged conduction *below* the AV node.
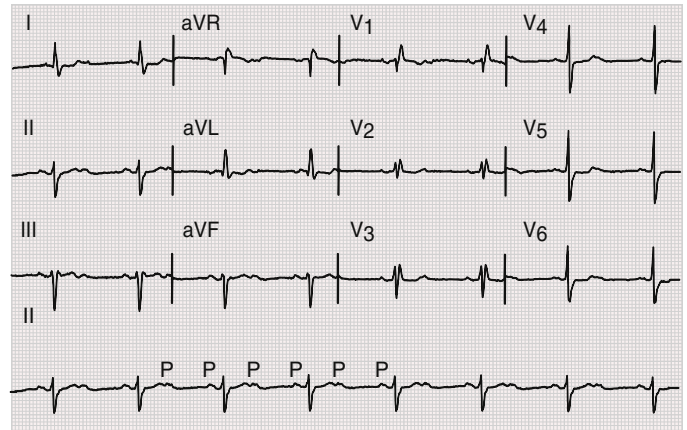
FIGURE 14.23 Sinus rhythm at 95 beats/min with 2:1 atrioventricular block. Conducted ventricular beats show a pattern consistent with bifascicular block with delay or block in the right bundle and left anterior fascicle. The patient underwent pacemaker implantation for presumed infra-Hisian block.
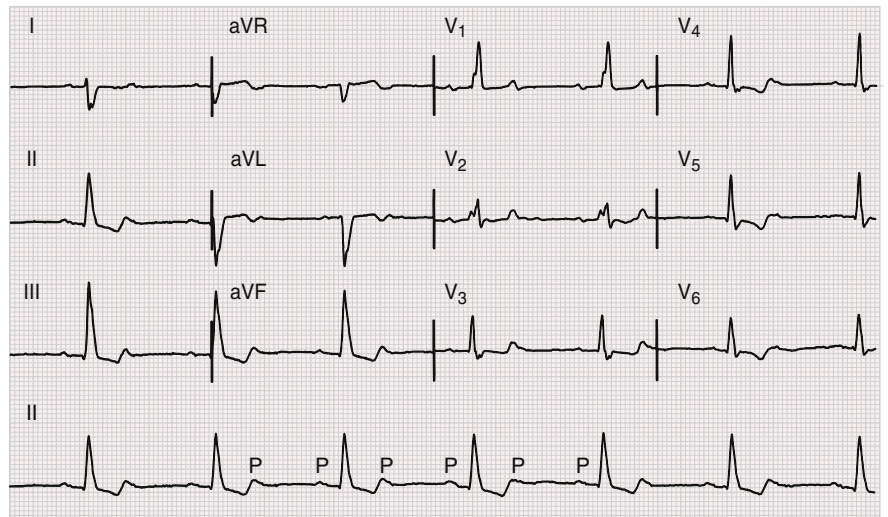
FIGURE 14.24 Sinus rhythm with 2:1 atrioventricular block. QRS morphology in the conducted beats is consistent with bifascicular block with delay or block in the right bundle and left posterior fascicle. Subsequently, complete heart block developed and the patient underwent pacemaker implantation.

In bifascicular block, conduction time through the unaffected fascicle is normal and the net conduction time from the AV node to ventricular muscle is normal. In trifascicular block, however, the delay in conduction through even the least affected path is abnormally prolonged so that the minimal conduction time from the AV node to the ventricular myocardium (and the HV interval on intracardiac recordings) (see Chapter 62) also is prolonged. Only delay, not block, of conduction in at least one of the conduction pathways is required; if complete block were present in the RBB and in the LBB or in both of its fascicles, conduction would fail, and complete heart block would result.

On the surface ECG, the delay in conduction may or may not be manifested as a prolonged PR interval. The PR interval is mostly determined by the conduction time through the AV node, with a lesser contribution by the conduction time in the infranodal conduction system. Prolonged intraventricular conduction may be insufficient to extend the PR interval beyond normal limits, whereas a greatly prolonged PR interval most often reflects delay in the AV node rather than in all three intraventricular fascicles. Thus, the finding of a prolonged PR interval in the presence of an ECG pattern of bifascicular block is consistent with but is not diagnostic of trifascicular block; similarly, the presence of a normal PR interval does not exclude it.

In some cases, the path that has the longest delay can vary with the cycle length. In these cases, conduction patterns vary or alternate between two or more IVCD types to produce *alternating bundle branch block* (Fig. 14.25). This suggests severe conduction system disease and is associated with a high risk of progression to heart block.

The major clinical implication of a multifascicular block is its relation to advanced conduction system as well as advanced underlying myocardial disease. It may identify patients at risk for heart block (see Fig. 14.23 and Chapter 68), although the incidence of progression appears to be low, especially with bifascicular block.[39]

Other Forms of Conduction Abnormalities

Rate-Dependent Conduction Blocks. Rate-dependent block usually occurs as a transient IVCD pattern (see Chapter 62). In *acceleration (tachycardia)-dependent block,* conduction delay occurs when the heart rate exceeds a critical value. This form of rate-related block is relatively common and can have the ECG pattern of RBBB or LBBB (Fig. 14.26). In *deceleration (bradycardia)-dependent block,* conduction delay occurs when the heart rate falls below a critical level. Deceleration-dependent block is less common than acceleration-dependent block and usually is seen only in patients with advanced conduction system disease (Fig. 14.27). The electrophysiologic bases for these patterns are discussed in Chapter 62.

Other mechanisms of ventricular aberration are discussed in Chapters 62 and 65, and Table 14.8 summarizes the major causes of a wide QRS occurring at physiologic heart rates. The more specific topic of wide complex tachycardias is discussed in Chapters 65 and 67.

Nonspecific Intraventricular Conduction Defects. This term is often used to refer to patterns with a widened QRS complex (110 to 130 msec) but without the specific pattern characteristic of RBBB or LBBB. It may represent any of a series of conditions including LBBB whose typical features are obscured by infarction, *intraventricular parietal block* (i.e., block in the distal conducting system beyond the bundle branches), or *peri-infarction block* (i.e., wide QRS complexes caused by delayed and disordered conduction around an area of infarction or scarring).[40] This term may also be applied to cases in which the limb leads have RBBB patterns but the precordial leads suggest LBBB, or vice versa.

Fragmentation of the QRS Complex. Fragmented QRS complexes represent disordered activation paths around or through areas of infarction, ischemia, or scar. They include patterns with a variety of RSR morphologies, notching in an R or S wave, or the presence of more than one r′ wave in the absence of typical LBBB or IRBB patterns. These deformities are common in patients with various cardiac disorders and are associated with an increased risk of mortality and complex arrhythmias.[41]

Myocardial Ischemia and Infarction

The ECG remains a key test for the diagnosis and management of acute and chronic coronary syndromes.[42–45] The waveform findings vary considerably depending on at least five major factors: (1) the duration of the ischemic process (acute versus evolving versus chronic), (2) its severity (ischemia with or without infarction), (3) its extent (size and degree of transmural involvement), (4) its topography (anterior versus inferior-posterior-lateral or right ventricular), and (5) the presence of other underlying abnormalities (e.g., prior infarction, LBBB, Wolff-Parkinson-White [WPW] syndrome, or pacemaker patterns) that can alter or mask the classic patterns. A critical clinical distinction is between *ST-segment elevation myocardial infarction* (or ischemia) (STEMI) and *non-STEMI infarction* (or ischemia) syndromes. With STEMI, an invasive approach aimed toward immediate reperfusion therapy with a percutaneous coronary intervention is the goal, unless contraindicated. With non-STEMI, urgent diagnostic angiography with revascularization, if feasible, is indicated by the presence of refractory angina, or hemodynamic or electrical instability (see Chapters 38 and 39).
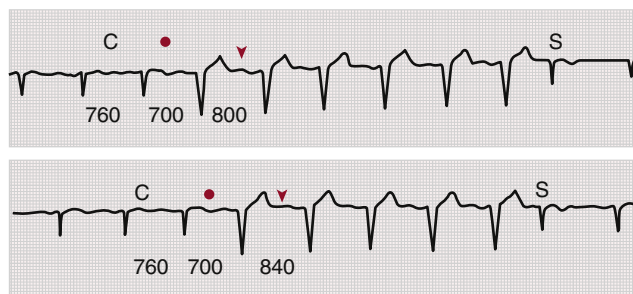
FIGURE 14.26 Acceleration-dependent QRS aberration with the persistence at a longer cycle length and normalization at a shorter cycle length than that initiating the aberration, indicating conduction hysteresis in the conduction system. The basic duration of the basic cycle (*C*) is 760 msec. LBBB appears at a cycle length of 700 msec (*dot*) and is perpetuated at cycle lengths (*arrowhead*) of 800 and 840 msec; conduction normalizes after a cycle length of 600 msec (S). (From Fisch C, Zipes DP, McHenry PL. Rate dependent aberrancy. *Circulation.* 1973;48:714.)

FIGURE 14.27 Deceleration-dependent aberration. The basic rhythm is sinus with a Wenckebach (type I) atrioventricular block. With 1:1 atrioventricular conduction, the QRS complexes are normal in duration; with a 2:1 atrioventricular block or after the longer pause of a Wenckebach sequence, left bundle branch block appears. (Courtesy Dr. C. Fisch.)

FIGURE 14.25 Multifascicular block manifested by alternating bundle branch blocks and PR intervals (sections *A–C*), recorded on separate days. *A,* Lead V₁ recording shows a right bundle branch block (RBBB) with a prolonged PR interval of 280 msec. *B,* Lead V₁ shows left bundle branch block (LBBB) with a PR of 180 msec. *C,* Leads I, II, III, and V₁ show alternating RBBB and LBBB patterns, along with PR alternation. The limb leads also show left anterior fascicular block (with subtle alternation of the QRS morphology). (From Fisch C. *Electrocardiography of Arrhythmias.* Philadelphia: Lea & Febiger; 1990.)

TABLE 14.8 **Major Causes of a Wide QRS (at Physiologic Rates)**

Chronic (intrinsic) intraventricular conduction delays or defects (IVCDs)
Right bundle branch block (RBBB)
Left bundle branch block (LBBB)
Nonspecific IVCDs
"Toxic" (extrinsic) conduction delays
Hyperkalemia
Drugs (especially those with class I activity)
Transient IVCDs
Rate related
Acceleration dependent
Deceleration dependent
Retrograde (transseptal) activation
Ashman type IVCD
Ventricular-originating complexes
Premature ventricular complexes (PVCs)
Ventricular escape beats
Ventricular paced beats
Ventricular preexcitation (WPW and related patterns)

WPW, Wolff-Parkinson-White syndrome.
For causes of wide-complex tachycardias, see Chapters 62 and 67.

Repolarization (ST-T Wave) Abnormalities

The earliest and most consistent ECG findings during acute severe ischemia/ischemia are deviation of the ST segment occurring as a result of complicated current of injury mechanisms (see Chapter 38). Repolarization changes, including ST elevations, often precede elevation of cardiac serum biomarkers and, therefore, the ECG plays an essential role in the emergency management of acute coronary syndromes (see Chapter 38).

Under normal conditions, the ST segment usually is nearly isoelectric, because almost all healthy myocardial cells attain approximately the same potential during the plateau phase of the ventricular action potential. Ischemia, however, produces complex time-dependent effects on the electrical properties of myocardial cells. Severe acute ischemia can reduce the resting membrane potential, shorten the duration of the action potential, and decrease the rate of rise and amplitude of phase 0 in the ischemic area (Fig. 14.28). The key concept is that these perturbations cause a *voltage gradient* between normal and ischemic zones that leads to current flow between these regions. The resulting *injury currents* are represented on the surface ECG as deviations of the ST segment.

The precise electrophysiologic mechanisms underlying injury currents and their directionality with ischemia and related conditions remain an area of active research and some controversy even after decades of study. Both "diastolic" and "systolic" injury currents have been proposed, based primarily on animal studies, to explain ischemic ST-segment elevations (Fig. 14.29). According to the "diastolic current of injury" hypothesis, ischemic ST-segment elevation is attributable to negative (downward) displacement of the electrical diastolic baseline (the TQ segment of the ECG). Ischemic cells remain relatively depolarized, probably related importantly to potassium ion leakage, during phase 4 of the ventricular action potential (i.e., lower membrane resting potential; see Fig. 14.28), and depolarized muscle carries a negative extracellular charge relative to repolarized muscle. Therefore, during electrical diastole, current (the diastolic current of injury) will flow between the partly or completely depolarized ischemic myocardium and the neighboring, normally repolarized, uninjured myocardium. The injury current vector will be directed away from the more negative ischemic zone toward the more positive normal myocardium. As a result, leads overlying the ischemic zone will record a negative deflection during electrical diastole and produce depression of the TQ segment.

TQ-segment depression appears as ST-segment elevation, because the ECG recorders in clinical practice use AC-coupled amplifiers that automatically "compensate" or adjust for any negative baseline shift, including in the TQ segment. As a result of this electronic effect, the ST segment will be proportionately elevated. Therefore, according to the diastolic current of injury theory, ST-segment elevation represents an apparent shift. The true shift, observable only with DC-coupled ECG amplifiers, is the negative displacement of the TQ baseline.

Evidence also suggests that ischemic ST-segment elevations (and hyperacute T waves) may also be related to systolic injury currents. Three pathologic factors may make acutely ischemic myocardial cells relatively positive compared with normal cells in regard to their extracellular charge during electrical systole (QT interval): (1) abbreviation of action potential duration, (2) decreased action potential upstroke velocity, and (3) decreased action potential amplitude (see Fig. 14.28). The presence of one or more of these effects will establish a voltage gradient between normal and ischemic zones during the QT interval such that the current of injury vector will be directed toward the ischemic region. This systolic current of injury mechanism, also probably related in part to potassium leakage, will result in primary ST-segment elevation, sometimes with tall positive (*hyperacute*) T waves. However, inspection of the surface ECG, with either ST elevation or ST depression ischemia, cannot differentiate between the contributions of systolic and diastolic currents of injury.

When acute ischemia is transmural (or nearly so), the overall ST vector (whether caused by diastolic or systolic injury currents, or both) usually is shifted in the direction of the outer (epicardial) layers, and ST-segment elevation and sometimes tall, positive (hyperacute) T waves are recorded over the ischemic zone (Fig. 14.30). Reciprocal ST-segment depression commonly appears in leads reflecting the contralateral surface of the heart. Occasionally, the reciprocal changes can be more apparent than the primary ST-segment elevations, leading to diagnostic confusion.

When ischemia is confined primarily to the subendocardium (approximately the inner half of the ventricular wall), the overall ST vector
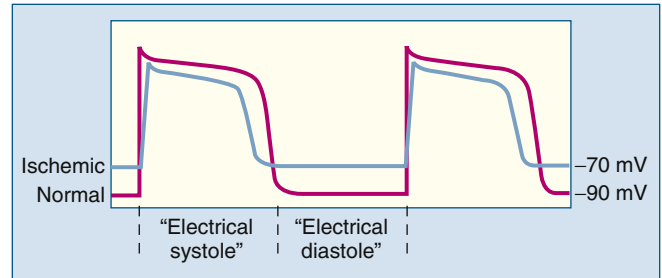
FIGURE 14.28 Acute ischemia may alter ventricular action potentials in a number of ways that result in lower resting membrane potential, decreased amplitude and velocity of phase 0, and an abbreviated action potential duration. These electrophysiologic effects, singly or in combination, create a voltage gradient between ischemic and normal cells during different phases of the cardiac electrical cycle. The resulting currents of injury are reflected on the surface ECG by deviation of the ST segment (see Fig. 14.29).
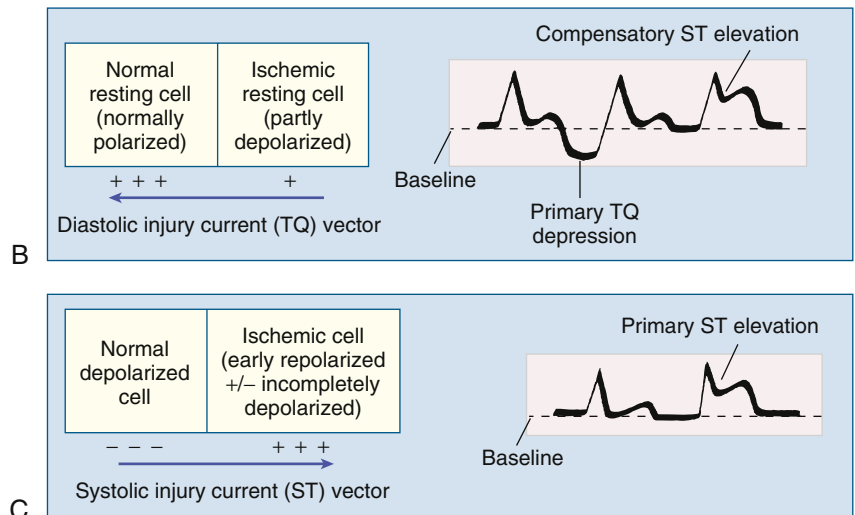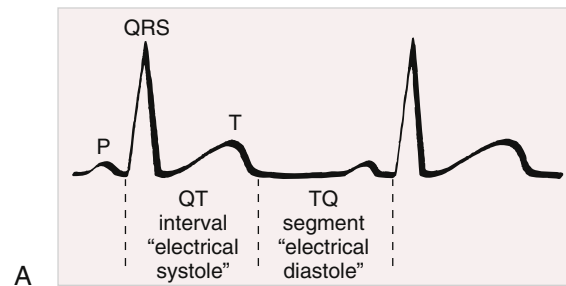
FIGURE 14.29 A simplified scheme of the pathophysiology of ischemic ST elevation. Two basic mechanisms have been advanced to explain the ST elevation seen with acute myocardial injury (**A**) based on currents of injury during ventricular electrical systole or diastole. **B,** Diastolic current of injury. In this case (first QRS-T complex), the ST vector will be directed away from the relatively negative, partly depolarized ischemic region during electrical diastole (TQ segment), and the result will be primary TQ depression. Conventional alternating current ECGs "compensate" for the baseline shift, and apparent ST-segment elevation (second QRS-T complex) results. **C,** Systolic current of injury. In this scenario, the ischemic zone will be relatively positive during electrical systole because the cells are repolarized early, and the amplitude and upstroke velocity of their action potentials may be decreased. This so-called systolic injury current vector will be oriented toward the electropositive zone, and the result will be primary ST-segment elevation. In clinical recordings, the contributions of diastolic and systolic injury currents to the observed ST-segment elevation cannot be determined (see text).

typically shifts toward the inner ventricular layer and the ventricular cavity such that the overlying (e.g., anterior precordial) leads show ST-segment depression, with ST-segment elevation in lead aVR (see Fig. 14.30). This subendocardial ischemia pattern is the typical finding during spontaneous episodes of angina pectoris or during symptomatic or asymptomatic (silent) ischemia induced by exercise or pharmacologic stress tests (see Chapter 15). Furthermore, associated alterations in myocardial conduction and action potential properties may contribute to the ST deviations observed on the ECG.[42]

Multiple factors can affect the amplitude of acute ischemic ST-segment deviations. Profound ST-segment elevation or depression in multiple leads usually indicates very severe or widespread ischemia. Conversely, prompt resolution of ST-segment elevation after reperfusion with percutaneous coronary interventions or thrombolytic therapy is a useful marker of successful reperfusion.

However, these relationships are not universal. Severe ischemia or even infarction can occur with slight or absent ST-T changes. Furthermore, a relative increase in T wave amplitude (hyperacute T waves) can accompany or precede ischemic ST-segment elevations with or without actual infarction (Fig. 14.31). Occasionally the ECG in acute coronary syndromes involving the occlusion of the left anterior descending (LAD) coronary will show a paradoxical combination of ST depressions and prominent T waves, especially in the precordial leads, sometimes now referred to as DeWinter's sign.[42] Finally, with evolving ischemia, ST-segment elevations usually become isoelectric, accompanied by T wave inversions. This evolutionary finding may lead to misclassification of an evolving ST-segment elevation MI as a non-ST elevation event.

QRS Changes

With actual infarction, depolarization (QRS) changes often accompany repolarization (ST-T) abnormalities (Fig. 14.32). Necrosis of sufficient myocardial tissue can lead to decreased R wave amplitude or frank Q waves (typically >30 to 40 msec in duration in multiple leads) a result of loss of electromotive forces in the infarcted area. Abnormal Q waves were once considered markers of transmural MI, whereas subendocardial (*nontransmural*) infarcts were thought not to produce Q waves. However, careful experimental and correlative studies based on necropsy and imaging findings have convincingly indicated that transmural infarcts can occur without Q waves and that subendocardial or other nontransmural infarcts can be associated with Q waves. Local conduction delays caused by acute ischemia also can contribute to Q wave pathogenesis in selected cases. Accordingly, evolving or chronic infarcts are more appropriately designated by ECG as *Q wave* or *non–Q wave*, rather than as "transmural" or "nontransmural."

The QRS findings may also be somewhat different with posterior or lateral infarction (Fig. 14.33). Loss of depolarization forces in these regions can reciprocally increase R wave amplitude in lead V_1 and sometimes V_2, occasionally without causing diagnostic Q waves in any of the conventional leads. The differential diagnosis for major causes of prominent right precordial R waves is presented in Table 14.9. In certain patients, fragmentation of the QRS complex, even without Q waves, may be a marker of myocardial scarring from ischemic or non-ischemic causes.[41,44]

Evolution of Electrocardiogram Changes

Ischemic ST-segment elevation and hyperacute T wave changes may occur as the earliest ECG manifestations of STEMI. These are

FIGURE 14.30 Directionality of current of injury patterns (ST vectors) with acute ischemia. **A,** With predominant subendocardial ischemia, the resultant ST vector is directed toward the inner layer of the affected ventricle and the ventricular cavity. Overlying leads therefore record ST depression, as may be seen during abnormal exercise stress tests or with spontaneous angina pectoris. **B,** With ischemia involving the outer ventricular layer (transmural or epicardial injury), the ST vector is directed outward. Overlying leads record ST-segment elevation.

FIGURE 14.31 Hyperacute phase of extensive anterolateral myocardial infarction. Marked ST-segment elevation melding with prominent T waves is present across the precordium, as well as in leads I and aVL. ST-segment depression, consistent with a reciprocal change, is seen in leads III and aVF. Q waves are present in leads V_3 through V_6. Marked ST-segment elevations with tall T waves caused by severe ischemia are sometimes referred to as a *monophasic current of injury pattern*. A paradoxical increase in R wave amplitude (V_2 and V_3) may accompany this pattern. This tracing also shows left axis deviation with small or absent inferior R waves, possibly from a previous inferior infarct.

typically followed within hours to days by evolving T wave inversion and sometimes Q waves in the same lead distribution (see Fig. 14.32 and Chapter 38). T wave inversion from evolving or chronic ischemia correlates with increased ventricular action potential duration, and these ischemic changes are often associated with QT prolongation. The T wave inversions can resolve after days or weeks or may persist indefinitely.

In the days to weeks or longer after infarction, the QRS changes can persist or begin to resolve. Complete normalization of the ECG after Q wave infarction is uncommon but can occur, particularly with smaller infarcts, and is associated with subsequent improvement of the LV ejection fraction and regional wall motion. This development usually reflects spontaneous recanalization or good collateral circulation and is a positive prognostic sign. By contrast, persistent Q waves and ST-segment elevation seen several weeks or more after infarction correlate strongly with severe underlying wall motion disorders (akinetic or dyskinetic zone), although not necessarily a frank ventricular aneurysm. The presence of an rSr′ pattern or similar type of multiphasic complex

in the mid-left chest leads or lead I is another reported marker of an LV aneurysm.[42]

Other Ischemic ST-T Patterns

Reversible transmural ischemia, such as that caused by coronary vasospasm, may result in transient ST-segment elevation (Fig. 14.34).[42] This pattern is the classic ECG marker of *Prinzmetal's variant (vasospastic) angina* (see Chapter 39). Depending on the severity and duration of such noninfarction ischemia, the ST-segment elevation either can resolve within minutes or can be followed by T wave inversions that can persist for hours or even days.

Some patients with ischemic chest pain exhibit deep coronary T wave inversions in multiple precordial leads (e.g., V_1 through V_4, I, and aVL), with or without cardiac biomarker level elevations. This finding typically is the result of severe ischemia associated with a high-grade stenosis in the proximal LAD coronary artery system (referred to as the LAD–T wave or *Wellens' pattern*).[42,45] These T wave inversions may be preceded by transient ST-segment elevations that resolve by the time

ECG sequence with anterior-lateral Q wave infarction

ECG sequence with inferior Q wave infarction
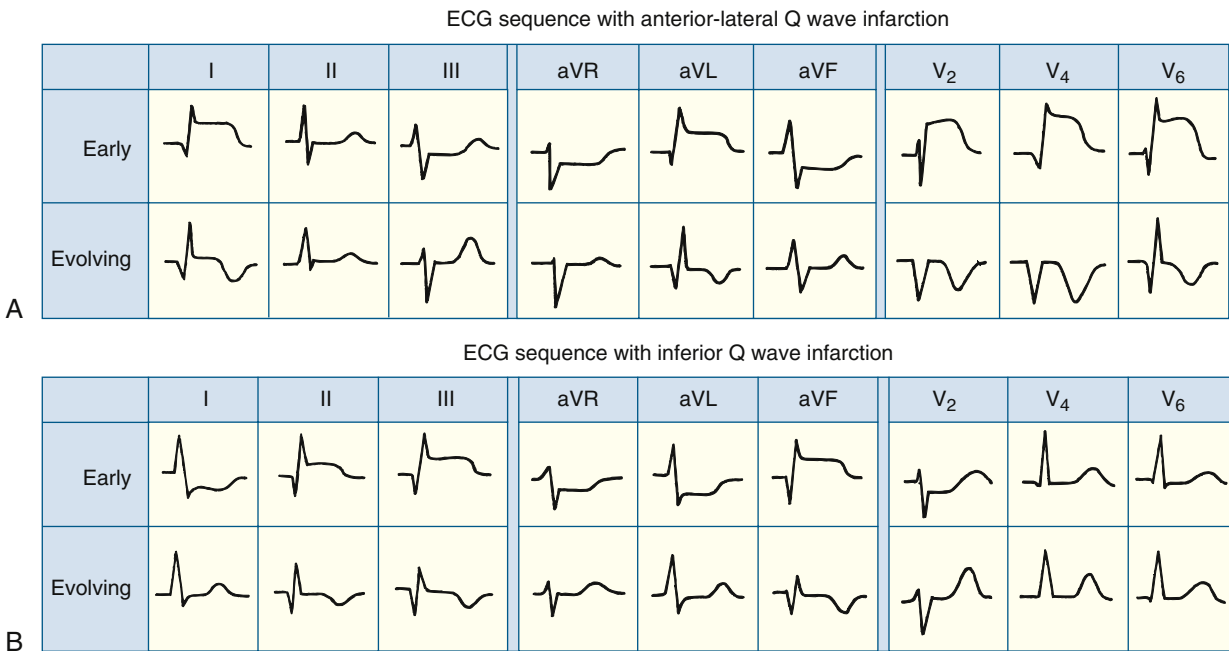
FIGURE 14.32 Sequence of depolarization and repolarization changes with acute anterior-lateral and inferior wall Q wave infarctions. **A,** With anterior-lateral infarcts, ST-segment elevation in leads I, aVL, and the precordial leads can be accompanied by reciprocal ST-segment depression in leads II, III, and aVF. **B,** Conversely, acute inferior (or posterior) infarcts can be associated with reciprocal ST-segment depression in leads V_1 to V_3. (From Goldberger AL, Goldberger ZD, Shvilkin A. *Goldberger's Clinical Electrocardiography: A Simplified Approach*. 9th ed. Philadelphia: Elsevier; 2017.)
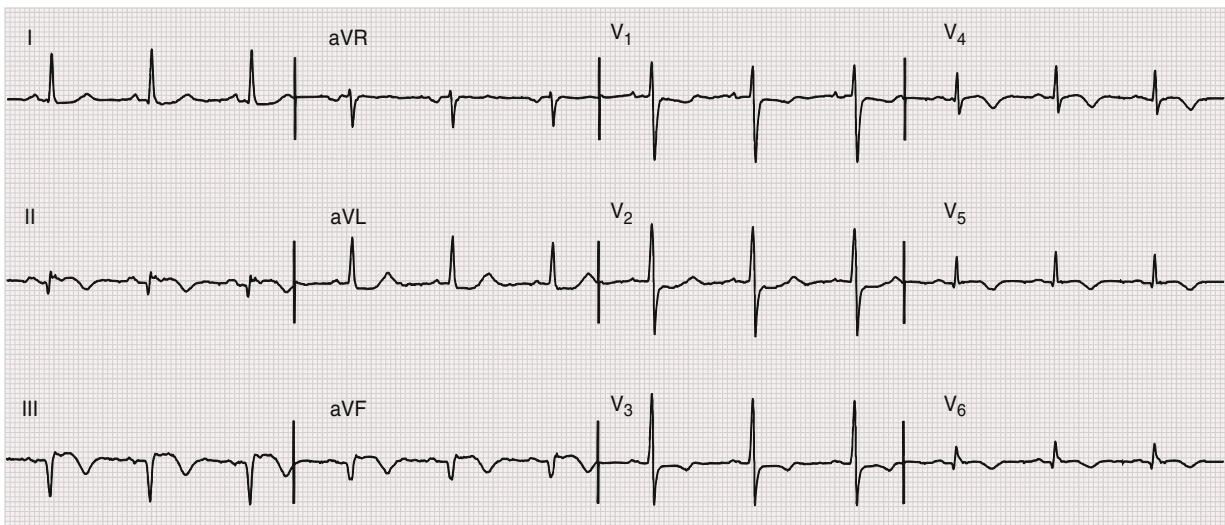
FIGURE 14.33 Evolving infero-posterolateral infarction. Note the prominent Q waves in II, III, and aVF, along with ST-segment elevation and T wave inversion in these leads, as well as V_3 through V_6. ST depression in I, aVL, V_1, and V_2 is consistent with a reciprocal change. Relatively tall R waves also are present in V_1 and V_2.

TABLE 14.9 Differential Diagnosis of Tall R Waves in Leads V$_1$ and V$_2$

Physiologic and Positional Factors
Misplacement of chest leads
Normal variants
Displacement of heart toward right side of chest (dextroversion), congenital or acquired
Myocardial Injury
Lateral or "true posterior" myocardial infarction
Duchenne muscular dystrophy (see Chapter 100)
Ventricular Enlargement
RVH (usually with right axis deviation)
Hypertrophic cardiomyopathy
Altered Ventricular Depolarization
Right ventricular conduction abnormalities
WPW patterns (caused by posterior or lateral wall preexcitation)

RVH, Right ventricular hypertrophy; *WPW,* Wolff-Parkinson-White syndrome.
Modified from Goldberger AL, Goldberger ZD, Shvilkin A. *Goldberger's Clinical Electrocardiography: A Simplified Approach*. 9th ed. Philadelphia: Elsevier; 2017.
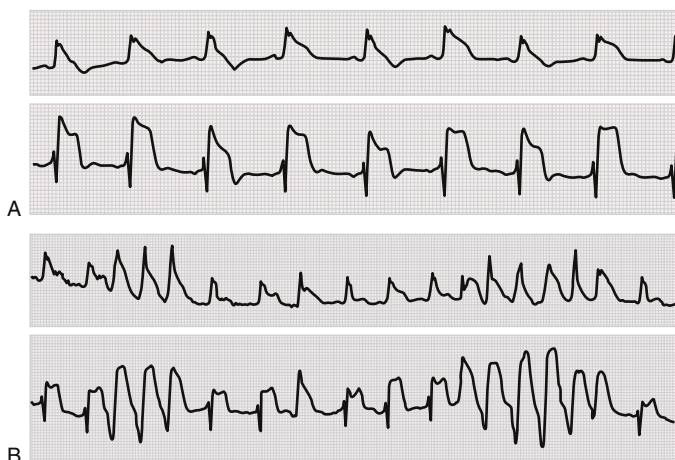
FIGURE 14.34 A, ECG tracing from a patient with Prinzmetal angina with ST-segment elevation and ST-T wave (repolarization) alternans. **B,** ECG shows ST segment elevation and T wave alternans associated with nonsustained ventricular tachycardia. (Courtesy Dr. C. Fisch.)

the patient has their initial ECG. Furthermore, T wave inversions of this type, especially in the setting of an acute coronary syndrome, can correlate with segmental hypokinesis of the anterior wall and suggest a myocardial stunning syndrome (see Chapter 39). The natural history of this syndrome is unfavorable, with a high incidence of recurrent angina and MI.[42,45]

On the other hand, patients whose baseline ECG shows abnormal T wave inversion can experience paradoxical T wave normalization (*pseudonormalization*) during episodes of acute transmural ischemia (Fig. 14.35). In summary, there are four major classes of acute coronary artery syndromes in which myocardial ischemia is associated with distinct ECG findings, as shown in Figure 14.36.

Alterations in U wave amplitude or polarity have been reported with acute ischemia or infarction. For example, exercise-induced transient inversion of precordial U waves has been correlated with severe stenosis of the LAD coronary artery. Rarely, U wave inversion can be the earliest ECG sign of an acute coronary syndrome.

Electrocardiogram Localization of Myocardial Ischemia and Infarction

The ECG leads are more helpful in localizing regions associated with ST-segment elevation than with ST-segment depression. ST-segment
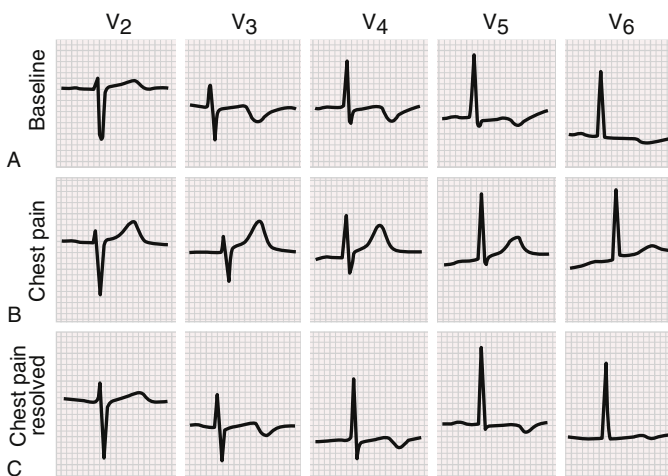
FIGURE 14.35 Pseudo– (paradoxical) T wave normalization. **A,** Baseline ECG of a patient with coronary artery disease shows ischemic T wave inversion. **B,** T wave "normalization" during an episode of ischemic chest pain. **C,** Following resolution of the chest pain, the T waves reverted to their baseline appearance. (From Goldberger AL. *Myocardial Infarction: Electrocardiographic Differential Diagnosis*. 4th ed. St Louis: Mosby–Year Book; 1991.)

FIGURE 14.36 Variability of ECG patterns with acute myocardial ischemia. The ECG also may be normal or nonspecifically abnormal. Furthermore, these categorizations are not mutually exclusive. For example, a non–Q-wave infarct can evolve into a Q wave infarct, ST-segment elevation can be followed by a non–Q-wave infarct or ST-segment depression, and T wave inversion can be followed by a Q wave infarct. *May exactly mimic acute infarction. (From Goldberger AL, Goldberger ZD, Shvilkin A. *Goldberger's Clinical Electrocardiography: A Simplified Approach*. 9th ed. Philadelphia: Elsevier; 2017.)
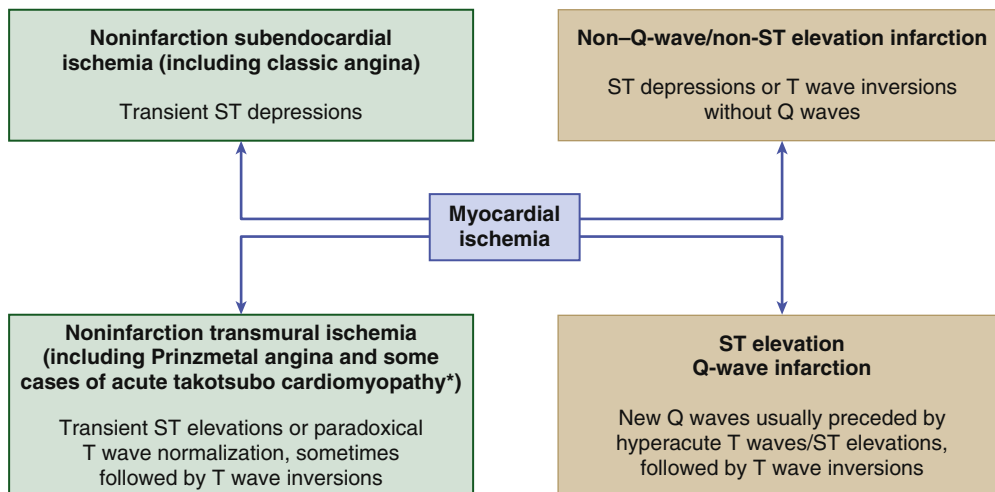
elevation and hyperacute T waves are seen in the following: (1) two or more contiguous precordial leads (V_1 through V_6) and/or in leads I and aVL with acute transmural anterior or severe anterolateral wall ischemia; (2) leads V_1 to V_3 with anteroseptal or apical ischemia; (3) leads V_4 to V_6 with apical or lateral ischemia; (4) leads II, III, and aVF with inferior wall ischemia; and (5) right-sided precordial leads with RV ischemia.

In addition, posterior or posterolateral wall infarction can produce ST-segment elevation in leads placed over the back of the heart, such as leads V_7 to V_9 (see Table 14.1), associated with occlusion of the right coronary artery (RCA) or the left circumflex artery (LCA). Such blockages can produce both inferior and posterolateral injuries, which may be indirectly recognized by reciprocal ST-segment depression in leads V_1 to V_3. Similar ST changes also can be the primary ECG manifestation of anterior subendocardial ischemia.

The ECG also can also suggest more specific information about the location of an acute occlusion within the coronary system (the *culprit lesion*).[42] For example, with an acute inferior wall MI, ST-segment elevation in lead III exceeding that in lead II, particularly combined with ST-elevation in lead V_1 (and additional right-sided chest leads), is a reliable predictor of occlusion in the proximal to midportion of the RCA (Fig. 14.37). By contrast, the presence of ST-segment elevation in lead II equal to or exceeding that in lead III, especially in concert with ST-segment depressions in leads V_1 to V_3 or ST-segment elevation in leads I and aVL, suggests occlusion of the LCA or a distal occlusion of a dominant RCA.

Right-sided ST-segment elevation is indicative of acute RV injury and usually indicates occlusion of the proximal RCA. Of note is the finding that acute right ventricular infarction can project an injury current pattern in leads V_1 through V_3 or even V_4, thus simulating anterior infarction. In other cases, simultaneous ST-segment elevation in V_1 (V_2R) and ST-segment depression in V_2 (V_1R) can occur (see Fig. 14.37).

Lead aVR[46] may provide important clues to the location of artery occlusion in acute MI. Left main (or severe multivessel) coronary artery disease should be considered when leads aVR and V_1 show ST-segment elevation, especially in concert with diffuse prominent ST-segment depression in other leads.

Of note, current and future criteria to identifying the precise location of the culprit occlusion will always be subject to limitations and exceptions based on interindividual variations in coronary anatomy, the dynamic nature of acute ECG changes, the presence of multivessel involvement, collateral flow, and ventricular conduction delays. For example, in some cases, ischemia can affect more than one region of the myocardium, such as infero-posterolateral MI (see Fig. 14.33). In such cases, the ECG may show the characteristic features of involvement in each region. Sometimes, however, partial normalization can result from cancellation of opposing vectoral forces. Similarly, inferior lead ST-segment elevation accompanying acute anterior wall infarction suggests either occlusion of an LAD artery that extends onto the inferior wall of the LV (the "wraparound" vessel) or multivessel disease with jeopardized collaterals.

Clinicians should also be aware that ECG localization of the topography of infarction may not correspond to that observed with imaging studies. Distinctions between posterior, basal, and lateral regions may not map to an expected ECG designation. A noteworthy example is that the ECG label of acute anteroseptal infarction (based on changes in V_1 to V_3) may underestimate the extent of lateral or apical involvment.[42]

Electrocardiogram Diagnosis of Myocardial Infarction with Bundle Branch Blocks

The diagnosis of MI often is more difficult when the baseline ECG shows a bundle branch block pattern or when bundle branch block develops as a complication of the MI. The diagnosis of Q wave infarction usually is not impeded by the presence of RBBB, which affects primarily the terminal phase of ventricular depolarization (see earlier). The net effect is that the criteria for the diagnosis of a Q wave infarct in a patient with RBBB are the same as in patients with normal conduction (Fig. 14.38).

The diagnosis of infarction in the presence of LBBB is considerably more complicated and confusing, because LBBB alters the early and the late phases of ventricular depolarization and produces secondary ST-T changes. These changes may mask or mimic MI findings. As a result, considerable attention has been directed to the problem of diagnosing acute and chronic MI in patients with LBBB (Fig. 14.39).[47]

Infarction of the LV free (or lateral) wall ordinarily results in abnormal Q waves in the midprecordial to lateral precordial leads and in selected limb leads. However, the initial septal depolarization forces with LBBB are directed from right to left. These leftward forces produce an initial R wave in the midprecordial to lateral precordial leads, usually masking the loss of electrical potential (Q waves) caused by the MI. Therefore, acute or chronic LV free wall infarction by itself will not usually produce diagnostic Q waves in the presence of LBBB. Acute or chronic MI involving both the free wall and septum (or the septum itself) may produce abnormal Q waves (usually as part of QR-type complexes) in leads V_4 to V_6. These initial Q waves probably reflect posterior and superior forces from the spared basal portion of the septum (Fig. 14.40). Thus, a wide Q wave (>30 to 40 msec) in two or more of these leads is usually a reliable sign of underlying MI. The sequence of repolarization also is altered in LBBB, as described earlier,
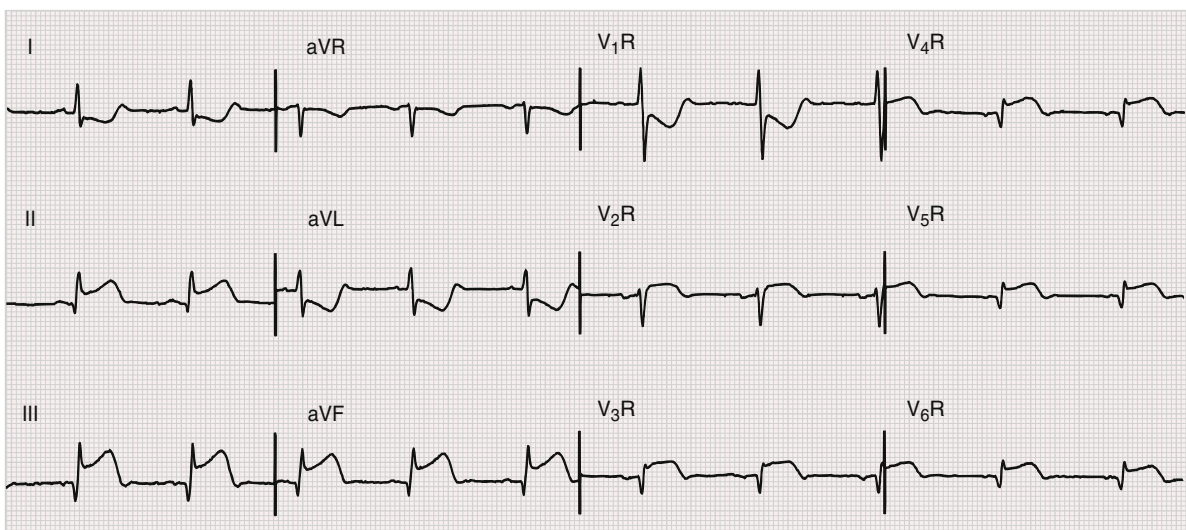
FIGURE 14.37 Acute right ventricular infarction in concert with an acute inferior wall ST-segment elevation infarction. Note the ST-segment elevation in the right precordial leads, as well as in leads II, III, and aVF, with reciprocal changes in leads I and aVL. ST-segment elevation in lead III greater than in lead II and right precordial ST-segment elevation are consistent with proximal to middle occlusion of the right coronary artery. The combination of ST-segment elevation in conventional lead V_1 (i.e., V_2R here) juxtaposed with ST-segment depression in lead V_2 (i.e., lead V_1R here) also has been reported with acute right ventricular ischemia or infarction.
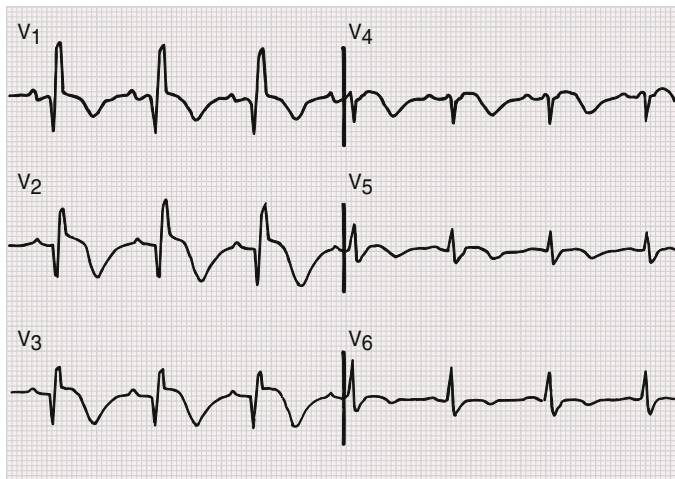
FIGURE 14.38 Right bundle branch block with acute anterior infarction. Loss of anterior depolarization forces results in QR-type complexes in the right precordial to midprecordial leads, with ST-segment elevations and evolving T wave inversions (V_1 through V_6).
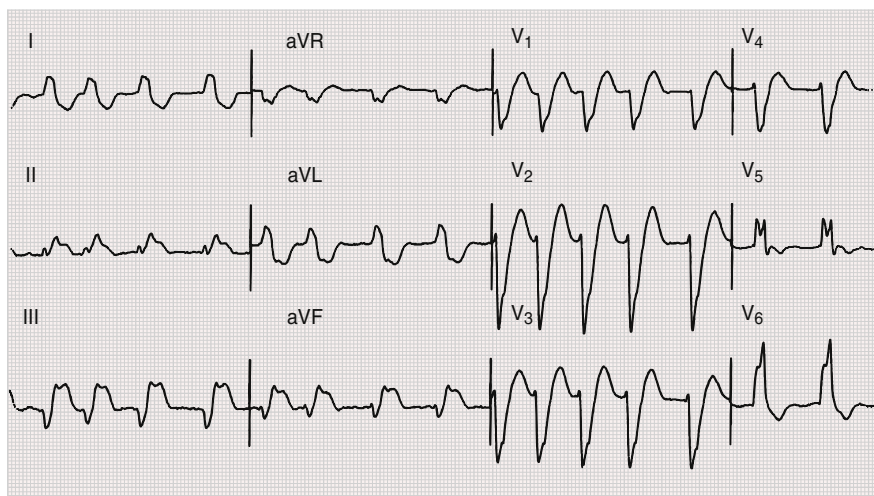
FIGURE 14.39 Complete left bundle branch block with acute inferior myocardial infarction. Note the prominent ST-segment elevation in leads II, III, and aVF, with reciprocal ST-segment depression in leads I and aVL superimposed on secondary ST-T changes. The underlying rhythm is atrial fibrillation.

and these changes can mask or simulate the ST-segment changes of actual ischemia.

The following points summarize the ECG signs of MI in LBBB:

1. ST-segment elevation with tall, positive T waves frequently is seen in the right precordial leads with uncomplicated LBBB. Secondary T wave inversions are characteristically seen in the lateral precordial leads. However, the appearance of ST-segment elevations in the lateral leads or ST-segment depressions or deep T wave inversions in leads V_1 to V_3 strongly suggests underlying ischemia. More marked ST-segment elevations (>0.5 mV) in leads with QS or rS waves also may be caused by acute ischemia, but false-positive findings occur, especially with large-amplitude negative QRS complexes. Use of the ratio of the *absolute amplitude* of the ST segment to S wave, determined in any relevant lead, of greater than 0.25 has been reported to have greater accuracy than that of the original Sgarbossa criterion.[47]
2. The presence of QR complexes in leads I, V_5, or V_6 or in II, III, and aVF with LBBB strongly suggests underlying MI.
3. Chronic MI also is suggested by notching of the ascending part of a wide S wave in the midprecordial leads or the ascending limb of a wide R wave in lead I, aVL, V_5, or V_6.

Similar principles can apply to the diagnosis of acute and chronic MI in the presence of RV pacing. Comparison between an ECG exhibiting the LBBB before the infarction and the present ECG often is helpful to show these changes.

The diagnosis of concomitant LAFB and inferior wall MI also can pose challenges. This combination can result in loss of the small r waves in the inferior leads, so leads II, III, and aVF show QS, not rS, complexes.

However, LAFB may also hide the diagnosis of inferior wall MI. The inferior orientation of the initial QRS forces caused by the fascicular block can mask inferior Q waves, with resultant rS complexes in leads II, III, and aVF. In other cases, the combination of LAFB and inferior wall MI will produce qrS complexes in the inferior limb leads, with the initial q wave the result of the infarct and the minuscule r wave the result of the fascicular block.

Atrial Infarction

A number of ECG clues to the diagnosis of atrial infarction have been suggested.[48,49] These include localized deviations of the PR segment, such as PR elevation in lead V_5 or V_6 or the inferior leads, changes in P wave morphology, and atrial arrhythmias. However, the sensitivity and specificity of these signs are limited.

Electrocardiogram Differential Diagnosis of Ischemia and Infarction

The ECG has important limitations in sensitivity and specificity in the diagnosis of coronary syndromes.[42] A normal or nondiagnostic ECG does not exclude ischemia or even acute infarction. If the initial ECG is not diagnostic, but the patient remains symptomatic, with a clinical picture strongly suggestive of acute ischemia, the ECG should be repeated at 15- to 30-minute intervals or shorter. However, a normal ECG throughout the course of an acute infarction is distinctly uncommon. As a result, prolonged chest pain without suggestive or diagnostic ECG changes on repeat ECGs should always prompt a careful search for noncoronary causes of chest pain (see Chapter 35).

Noninfarction Q Waves and Related Depolarization Changes

Q waves simulating the ECG pattern of coronary artery disease can be related to one (or a combination) of the following four factors[42] (Table 14.10): (1) physiologic or positional variants, (2) altered ventricular conduction, (3) ventricular enlargement/hypertrophy, and (4) myocardial damage or replacement. The latter category includes necrosis due to classic atherosclerotic coronary disease and nonatherosclerotic causes (see Chapter 52).

1. Prominent Q waves can be associated with a variety of positional factors that alter the orientation of the heart vis-à-vis a specific lead axis. Depending on the electrical axis, prominent Q waves (as part of QS- or QR-type complexes) can appear in the limb leads (aVL with a vertical axis and III and aVF with a horizontal axis). A QS complex can appear in lead V_1 as a normal variant but rarely in leads V_1 and V_2. Slow R wave progression, sometimes with actual QS waves, can be caused solely by improper placement of chest electrodes above their usual position. With dextrocardia (see Chapter 82), in the absence of underlying structural abnormalities, normal R wave progression can be restored by recording leads V_2 to V_6 on the right side of the chest (with lead V_1 placed in the V_2 position). A rightward mediastinal shift with left pneumothorax can contribute to the apparent loss of left precordial R waves. Other positional factors associated with slow R wave progression include pectus excavatum and congenitally corrected transposition of the great vessels.
2. An intrinsic change in the sequence of ventricular depolarization can lead to pathologic, noninfarct Q waves. The two most important conduction disturbances associated with pseudoinfarction Q waves are LBBB and the WPW preexcitation patterns (Chapter 65). With LBBB, QS complexes can appear in the right precordial to midprecordial leads and occasionally in leads II, III, and/or aVF. Depending on the location of the bypass tract, WPW preexcitation can mimic anteroseptal, lateral, or inferior-posterior infarction.

Left bundle branch block

A

Left bundle branch block with septal infarct

B

C
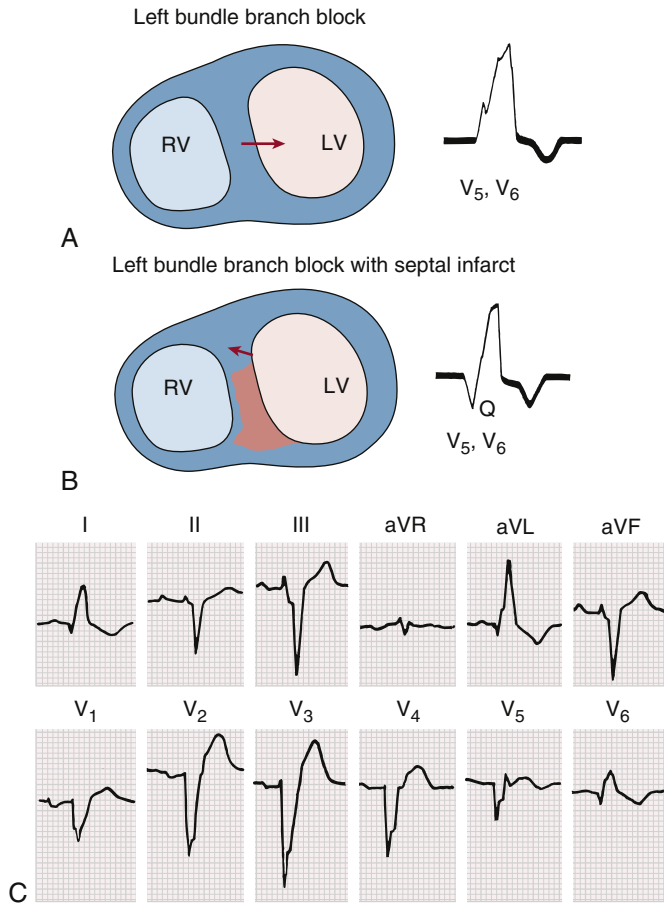
FIGURE 14.40 **A,** In uncomplicated (pure) left bundle branch block (LBBB), early septal forces are directed to the left (*arrow*). Therefore, no Q waves will be seen in V_5 and V_6 on the ECG tracing. **B,** With LBBB complicated by anteroseptal infarction, early septal forces can be directed posteriorly and rightward (*arrow*). Therefore, prominent Q waves may appear in leads V_5 and V_6 as a paradoxical marker of septal infarction. **C,** ECG from patient with anterior wall infarction (involving septum) with LBBB. Note the presence of QR complexes in leads I, aVL, V_5, and V_6. *LV,* Left ventricle; *RV,* right ventricle. (**A** and **B** modified from Dunn MI, Lipman BS. *Lipman-Massie Clinical Electrocardiography*. 8th ed. Chicago: Year Book; 1989.)

LAFB is sometimes cited as a cause of anteroseptal infarct patterns; however, LAFB usually has only minor effects on the QRS complex in horizontal plane leads. Probably the most common findings are relatively prominent S waves in leads V_5 and V_6. Slow R wave progression is not a consistent feature of LAFB, although minuscule q waves in leads V_1 to V_3 have been reported in this setting. These small (e.g., ≤20 msec duration) q waves can become more apparent if the leads are recorded one interspace above their usual position and disappear in leads that are one interspace below their usual position.

3. Slow ("poor") R wave progression is a nonspecific finding and is frequently observed with LVH, with acute or chronic RV overload (as well as in normal persons). Frank QS waves (e.g., in $V_1 – V_2 /V_3$) associated with ventricular overload syndromes (left, right, or biventricular) can reflect a variety of mechanisms, including a change in the balance of early ventricular depolarization forces, altered cardiac geometry and position, and electrode locations. A marked loss of R wave voltage, sometimes with frank Q waves from lead V_1 to the lateral chest leads, can be seen with severe chronic obstructive pulmonary disease (see Fig. 14.18). The presence of low limb voltage and signs of RA abnormality ("P pulmonale") can serve as additional diagnostic clues. This loss of R wave progression in part may be related to RV dilation and downward displacement of the heart in an emphysematous chest, as discussed earlier. Partial or complete normalization of R wave progression can be achieved in some of these cases by recording the chest leads an interspace lower than usual.

TABLE 14.10 **Differential Diagnosis of Noninfarction Q Waves (With Select Examples)**

Physiologic or Positional Factors
Normal variant "septal" Q waves
Normal variant Q waves in V_1–V_2, III, and aVF
Left pneumothorax or dextrocardia—loss of lateral R wave progression
Myocardial Injury or Infiltration
Acute processes—myocardial ischemia without infarction, takotsubo cardiomyopathy myocarditis, hyperkalemia (rare cause of transient Q waves)
Chronic myocardial processes—idiopathic cardiomyopathies, myocarditis, amyloid, tumor, sarcoid
Ventricular Hypertrophy or Enlargement
Left ventricular (slow R wave progression)*
Right ventricular (reversed R wave progression[†] or slow R wave progression, particularly with chronic obstructive lung disease)
Hypertrophic cardiomyopathy (can simulate anterior, inferior, posterior, or lateral infarcts
Conduction Abnormalities
LBBB (slow R wave progression*)
WPW patterns

LBBB, Left bundle branch block; *WPW,* Wolff-Parkinson-White syndrome.
*Small or absent R waves in the right precordial to midprecordial leads.
[†]Progressive decrease in R wave amplitude from V_1 to the midlateral precordial leads.
Modified from Goldberger AL, Goldberger ZD, Shvilkin A. *Goldberger's Clinical Electrocardiography: A Simplified Approach*. 9th ed. Philadelphia: Elsevier; 2017.

Other ventricular overload syndromes, acute or chronic, can also mimic ischemia and infarction. Acute cor pulmonale caused by pulmonary thromboembolism (see Chapter 87) can cause a variety of pseudoinfarct patterns. Acute RV overload in this setting can cause slow R wave progression and sometimes right precordial to midprecordial T wave inversion (sometimes still referred to as right ventricular "strain"), mimicking anterior ischemia or infarction. The classic $S_1Q_3T_3$ pattern can occur but, as noted, is neither sensitive nor specific. A prominent Q wave (usually as part of a QR complex) also can occur in lead aVF along with this pattern (see Fig. 14.19). However, acute right overload by itself does not cause a pathologic Q wave in lead II. Right-sided heart overload, acute or chronic, also may be associated with a QR complex in lead V_1, simulating anteroseptal infarction.

Pseudoinfarction patterns are also important findings in patients with hypertrophic cardiomyopathy (see Chapter 54), and the ECG changes can simulate those in anterior, inferior, posterior, or lateral infarction. The pathogenesis of depolarization abnormalities in this cardiomyopathy is not certain. Prominent inferolateral Q waves (leads II, III, aVF, and V_4 to V_6) and tall, right precordial R waves probably are related to increased depolarization forces generated by the markedly hypertrophied septum (Fig. 14.41). Abnormal septal depolarization also can contribute to bizarre QRS complexes.

4. Loss of electromotive force associated with myocardial necrosis contributes to R wave loss and Q wave formation in MI. This mechanism of Q wave pathogenesis, however, is not specific for coronary artery disease with infarction. Any process, acute or chronic, that causes sufficient loss of regional electromotive potential can result in Q waves. For example, replacement of myocardial tissue by electrically inert material such as amyloid, sarcoid, or tumor can cause noninfarction Q waves (see Chapters 52, 53, and 98). Q waves caused by myocardial injury, whether ischemic or nonischemic in origin, can appear transiently and do not necessarily signify irreversible heart muscle damage. Severe ischemia can cause regional loss of electromotive potential without actual cell death (*electrical stunning* phenomenon). Transient conduction disturbances also can cause alterations in ventricular activation and result in noninfarctional Q waves. In some cases, transient Q waves may represent unmasking of a previous Q wave infarct. New but transient

Q waves have been described in patients with severe hypotension from a variety of causes, as well as with tachyarrhythmias, acute myocarditis, Prinzmetal angina, protracted hypoglycemia, and hyperkalemia.[42]

ST-T Changes Simulating Ischemia and Infarction

The differential diagnosis of STEMI (or ischemia)[42] due to obstructive coronary disease encompasses a wide variety of clinical entities, including acute pericarditis (Fig. 14.42) (see Chapter 86), acute myocarditis (Chapter 55), normal variants (including classic "early repolarization" patterns, see Fig. 14.11), takotsubo (stress) cardiomyopathy, Brugada patterns (Chapters 63 and 67), and other conditions (Table 14.11). Acute pericarditis, unlike MI, typically induces diffuse ST-segment elevation, usually in most of the chest leads and also in leads I, aVL, II, and aVF. Reciprocal ST-segment depression is seen in lead aVR. An important clue to acute pericarditis, in addition to the diffuse nature of the ST-segment elevation, is the frequent presence of PR-segment elevation in aVR, with reciprocal PR-segment depression

in other leads, caused by an atrial current of injury (see Fig. 14.42). Abnormal Q waves do not occur with acute pericarditis, and the ST-segment elevation may be followed by T wave inversion after a variable period. In addition, the J point in patients with pericarditis is typically sharp rather than slurred as in acute ischemic injury. Severe acute myocarditis can produce identical ECG patterns of acute myocardial infarction (AMI), including ST-segment elevations and Q waves. These findings can be associated with a rapidly progressive course and increased mortality. A fulminant myopericarditis-like syndrome has been reported with the COVID-19 infection, including ST elevations mimicking AMI.[50,51]

The novel SARS coronavirus may present diagnostic challenges to acute care clinicians (Chapter 94). Ischemic appearing ST-T changes may also be due to one or a combination of other pathogenetic mechanisms, including: classic "type 1" infarction precipitated by the infection (Chapter 37); takotsubo (stress) cardiomyopathy described later, Brugada pattern unmasked by fever (Chapter 63), coronary vascular injury (immune or infectious-mediated), acute right ventricular overload due to pneumonitis or pulmonary thromboembolic events (Chapter 87), and so forth.

Takotsubo cardiomyopathy (see Chapter 52), also called *transient left ventricular apical ballooning syndrome* or *stress cardiomyopathy*, is characterized by reversible wall motion abnormalities of the LV apex and midventricle.[52,53] Patients, usually postmenopausal women, may present with chest pain, ST-segment elevations, and elevated cardiac enzyme levels, mimicking AMI caused by obstructive coronary disease. The syndrome typically is reported in the setting of emotional or physiologic stress. Fixed epicardial coronary disease is absent. The exact pathophysiology is not known but may relate to coronary vasospasm or adrenergically mediated myocardial damage resulting in a variety of ST-T elevation (or
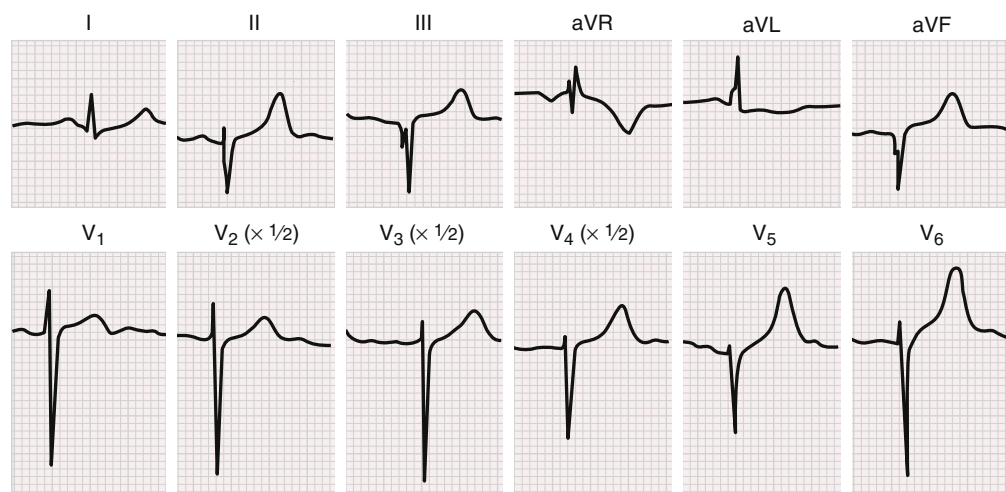
FIGURE 14.41 Hypertrophic cardiomyopathy simulating inferolateral infarction. This ECG was obtained in an 11-year-old girl who had a family history of hypertrophic cardiomyopathy. Note the W-shaped QS waves and the QRS complexes in the inferior and lateral precordial leads. (From Goldberger AL, Goldberger ZD, Shvilkin A. *Goldberger's Clinical Electrocardiography: A Simplified Approach*. 9th ed. Philadelphia: Elsevier; 2017.)
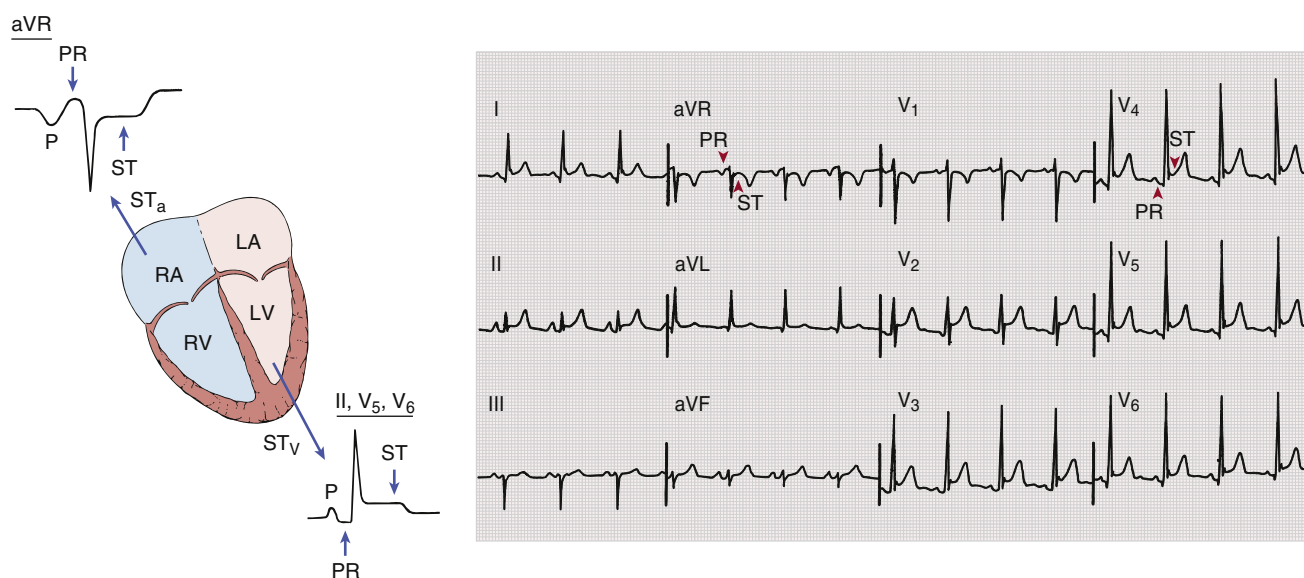
FIGURE 14.42 Acute pericarditis often is characterized by two apparent injury currents, one atrial and the other ventricular. The atrial injury current vector (ST_a) usually is directed upward and to the right (see diagram at *left*) and produces PR-segment elevation in aVR, with reciprocal PR depression in II, V_5, and V_6. The ventricular injury current (ST_V) is directed downward and to the left, associated with ST-segment elevation in leads II, V_5, and V_6. This characteristic PR-ST segment discordance is illustrated in the bottommost tracing. Note the diffuse distribution of ST-segment elevation in acute pericarditis (e.g., I, II, and V_2 through V_6, with reciprocal changes in aVR and perhaps minimally in V_1). *LA,* Left atrium; *LV,* left ventricle; *RA,* right atrium; *RV,* right ventricle. (From Goldberger AL. *Myocardial Infarction: Electrocardiographic Differential Diagnosis*. 4th ed. St Louis: Mosby–Year Book; 1991.)

depression) changes simulating coronary occlusion. Criteria for differentiating takotsubo syndrome from MI due to obstructive coronary disease have been proposed.[54]

A number of factors, such as digitalis, ventricular hypertrophy, hypokalemia, secondary ST-T changes, and hyperventilation, can cause *ST-segment depression* mimicking that in non–ST-segment elevation ischemic syndromes. Similarly, *tall positive T waves* do not invariably represent hyperacute ischemic changes but can reflect normal variants, hyperkalemia, cerebrovascular injury, and LV volume overloads resulting from mitral or aortic regurgitation (see Fig. 14.16), among other causes. ST-segment elevation, J point elevations, and tall positive T waves also are common chronic findings in leads V_1 and V_2 with LBBB or LVH patterns, which may simulate acute ischemia.

As noted, a variety of other factors, pathologic and sometimes physiologic, can alter repolarization, causing prominent T wave inversion, sometimes simulating ischemia or evolving MI. For example, prominent primary T wave inversions also are a well-described feature of the ECG in CVAs, particularly with subarachnoid hemorrhage. The so-called *cerebrovascular accident (CVA) T wave pattern* characteristically is seen in multiple leads, with a widely splayed appearance usually associated with marked QT prolongation (Fig. 14.43). Some studies have implicated structural damage (termed *myocytolysis*) in the hearts of patients with such T wave changes, probably induced by excessive sympathetic stimulation mediated through the hypothalamus. A role for concomitant vagal hyperactivation has also been postulated in the pathogenesis of such T wave changes, which usually are associated with bradycardia. In addition, the massive diffuse T wave inversion seen in some patients after Stokes-Adams syncope may be related to a similar neurocardiogenic mechanism. Patients with subarachnoid hemorrhage also can show transient ST-segment elevation, as well as arrhythmias including torsades de pointes. Ventricular dysfunction can even occur and may be related to takotsubo cardiomyopathy[52–54] or neurogenic stress–type syndromes (see Chapters 45 and 102).

In contrast to these primary ST-T wave abnormalities, secondary ST-T wave changes are caused by altered ventricular activation, without changes in action potential characteristics (discussed earlier). Examples include bundle branch block, WPW preexcitation, and ventricular ectopic or paced beats. In addition, transiently altered ventricular activation (associated with QRS interval prolongation) can induce T wave changes, which can persist for hours to days after normal ventricular depolarization has resumed. The term *cardiac memory T wave changes* has been used in this context to describe repolarization changes after depolarization changes caused by ventricular pacing, intermittent LBBB, intermittent WPW preexcitation, and other alterations of ventricular activation.[55,56] T wave inversions also may occur. The term *idiopathic global T wave inversion* has been applied in cases in which no identifiable cause for prominent diffuse repolarization abnormalities can be found. Some of these cases may represent unrecognized takotsubo cardiomyopathy.

When caused by physiologic variants, T wave inversion is sometimes mistaken for ischemia. T waves in the right precordial leads can be slightly inverted, particularly in leads V_1 and V_2. Some adults show persistence of the juvenile T wave pattern (see Fig. 14.10), with more prominent T wave inversion in right precordial to midprecordial leads showing an rS or RS morphology. Such patterns, especially associated with ventricular ectopy with LBBB-morphology or relevant family history, also raise strong consideration of *arrhythmogenic right ventricular cardiomyopathy* (formerly referred to as *dysplasia;* see Chapter 52).[57] The other major normal variant that can be associated with notable T wave inversion is the so-called benign *early repolarization pattern* (see Fig. 14.11). As described earlier, some persons, especially athletes, with this variant have prominent, biphasic T wave inversion in association with the ST-segment elevation. This pattern, which may simulate the initial stages of an evolving infarct, is most prevalent in young Black men and endurance athletes. These functional ST-T changes probably are the result of regional

TABLE 14.11 Differential Diagnosis of ST-Segment Elevation

Myocardial ischemia or infarction

    Noninfarction, transmural ischemia (e.g., Prinzmetal angina pattern, takotsubo syndrome)

    Acute myocardial infarction (caused by obstructive coronary occlusion or other causes)

    Post–myocardial infarction (ventricular aneurysm pattern)

Acute pericarditis

Normal variants (including the classic "early repolarization" pattern)

LVH, LBBB (V_1,V_2 or V_3 only)

Other (rarer) causes

    Acute pulmonary embolism (right to mid-chest leads)

    Brugada pattern (RBBB-like pattern and ST-segment elevations in right precordial leads)*

    Class IC antiarrhythmic drugs*

    Hypercalcemia*

    DC cardioversion (immediately after procedure)

    Hyperkalemia*

    Hypothermia (J or Osborn wave)

    Intracranial hemorrhage

    Myocardial injury (e.g., caused by trauma)

    Myocarditis (may resemble myocardial infarction or pericarditis)

    "Spiked-helmet" sign†

    Tumor invading the left ventricle

DC, Direct current; *LVH,* left ventricular hypertrophy; *LBBB,* left bundle branch block; *RBBB,* right bundle branch block.
*Usually most apparent in leads V_1 to V_2.
†Crinion D, Abdollah H, Baranchuk A. An ominous ECG sign in critical care. *Circulation.* 2020;14:2106–2109.
Modified from Mirvis DM, Goldberger AL. Electrocardiography. In *Braunwald's Heart Disease,* 11th ed. Philadelphia: Elsevier;2019; and Goldberger AL, Goldberger ZD, Shvilkin A. *Goldberger's Clinical Electrocardiography: A Simplified Approach.* 9th ed. Philadelphia: Elsevier; 2017.
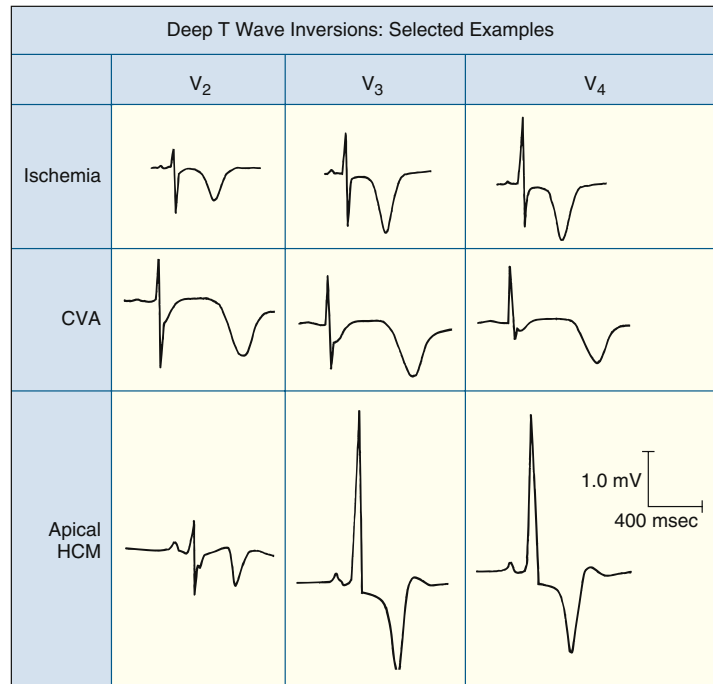
FIGURE 14.43 Deep T wave inversion can have various causes. In the *middle* tracing, note the marked QT prolongation in conjunction with the cerebrovascular accident (*CVA*) T wave pattern, caused here by subarachnoid hemorrhage. Apical hypertrophic cardiomyopathy (*HCM*), "memory T waves," and takotsubo syndrome are other causes of deep T wave inversion that can be mistaken for ischemia from acute/evolving or chronic obstructive coronary disease. (From Goldberger AL. Deep T wave inversions. *ACC Curr J Rev.* 1996;5:28–29.)

disparities in repolarization and usually can be normalized by exercise. An important consideration in the differential diagnosis for such changes, especially in athletes, is apical hypertrophic cardiomyopathy (see Chapter 54).

Drug Effects

Numerous drugs can affect the ECG and often are associated with nonspecific ST-T alterations.[1] More marked changes, as well as AV and intraventricular conduction disturbances, can occur with select agents (see Chapters 63 and 64).

The term *digitalis effect* refers to the relatively distinctive "scooped" appearance of the ST-T complex and shortening of the QT interval, which correlates with abbreviation of the ventricular action potential duration (Fig. 14.44). Digitalis-related ST-T changes can be accentuated by an increased heart rate during exercise, with consequent false-positive results on stress testing (see Chapter 15), and can occur with either therapeutic or toxic doses of the drug. *Digitalis toxicity* refers specifically to systemic effects (e.g., nausea, anorexia) or conduction disturbances and arrhythmias caused by drug excess or increased sensitivity.

The ECG effects and toxicities of other cardioactive agents can be anticipated in part from ion channel effects (see Chapter 62). Inactivation of sodium channels by class I agents (e.g., quinidine, procainamide, disopyramide, flecainide) can cause QRS prolongation. Class IA (e.g., quinidine) and class III (e.g., amiodarone, dronedarone, dofetilide, ibutilide, sotalol) agents can induce an *acquired long QT(U) syndrome* (see Chapters 63 and 67). Psychotropic drugs (e.g., tricyclic antidepressants, phenothiazines), which have class IA–like properties, also can lead to QRS and QT(U) prolongation (see Chapter 99). Toxicity can produce asystole or torsades de pointes. Right axis shift of the terminal 40 msec frontal plane QRS axis may be a helpful additional marker of tricyclic antidepressant overdose. QT prolongation has been reported with multiple other drugs, including methadone, and hydroxychloroquine (especially in combination with azithromycin) in some of the initial attempts to treat COVID-19.[58] Finally, cocaine (see Chapter 28) can cause a variety of ECG changes, including those of STEMI, as well as life-threatening arrhythmias.

Electrolyte and Metabolic Abnormalities

In addition to the structural and functional cardiac conditions already discussed, numerous systemic metabolic aberrations may affect the ECG, including electrolyte abnormalities and acid-base disorders, as well as systemic hypothermia.[7,42]

Calcium

Hypercalcemia and hypocalcemia predominantly alter the action potential duration. An increased

extracellular calcium concentration shortens the ventricular action potential duration by shortening phase 2. By contrast, hypocalcemia prolongs phase 2. These cellular changes are reflected in abbreviation or prolongation of the ST segment portion of the QT interval with hypercalcemia or hypocalcemia, respectively (Fig. 14.45). Severe hypercalcemia (e.g., serum Ca^{2+} >15 mg/dL) also can be associated with decreased T wave amplitude, sometimes with T wave notching or
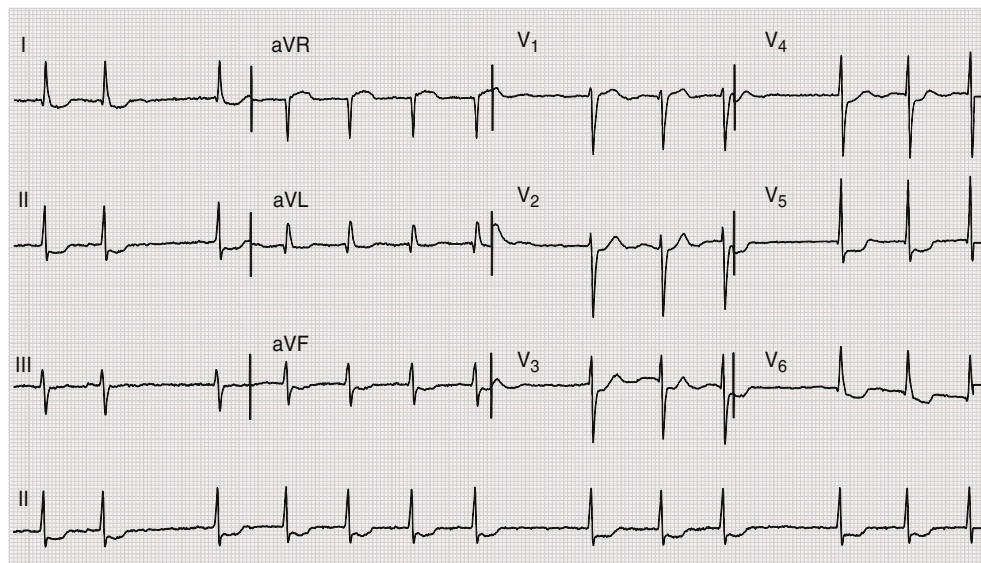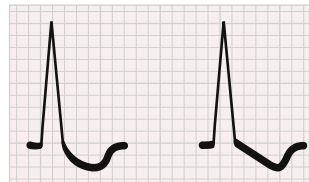
FIGURE 14.44 Top, Digitalis effect. Digitalis glycosides characteristically produce shortening of the QT interval with a scooped or downsloping ST-T complex. **Bottom,** Digitalis effect in combination with digitalis toxicity. The underlying rhythm is atrial fibrillation. A group beating pattern of QRS complexes with shortening of the R-R intervals is consistent with nonparoxysmal junctional tachycardia with probable exit block (atrioventricular Wenckebach) variant. ST-segment depression and scooping (lead V_6) are consistent with the digitalis effect, although ischemia or left ventricular hypertrophy cannot be excluded. These ECG findings are strongly suggestive of digitalis excess; the serum digoxin level was over 3 ng/mL. (**Top** from Goldberger AL, Goldberger ZD, Shvilkin A. *Goldberger's Clinical Electrocardiography: A Simplified Approach.* 9th ed. Philadelphia: Elsevier; 2017.)

Hypocalcemia	Normal	Hypercalcemia
QT 0.48 sec	QT 0.36 sec	QT 0.26 sec
QTc 0.52 sec	QTc 0.41 sec	QTc 0.36 sec
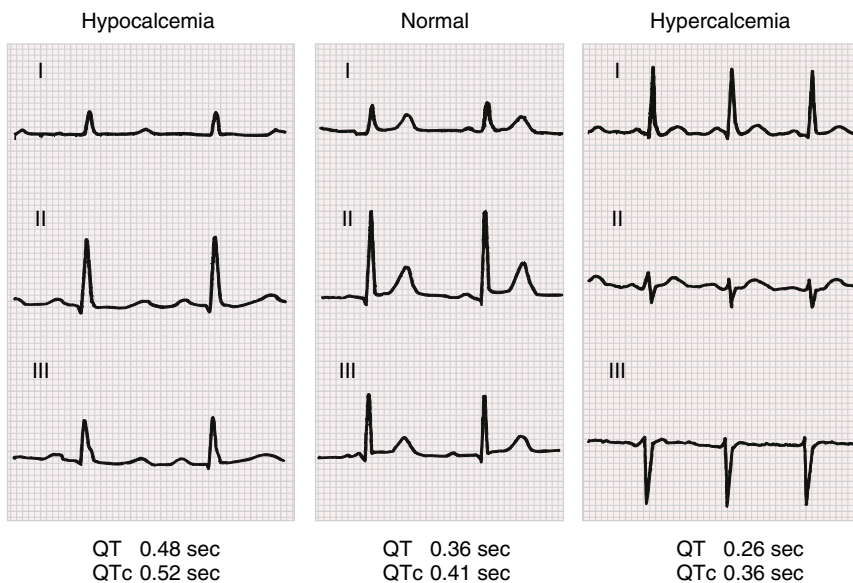
FIGURE 14.45 Prolongation of the QT interval (ST-segment portion) is typical of hypocalcemia. Hypercalcemia may cause abbreviation of the ST segment and shortening of the QT interval. (From Goldberger AL, Goldberger ZD, Shvilkin A. *Goldberger's Clinical Electrocardiography: A Simplified Approach.* 9th ed. Philadelphia: Elsevier; 2017.)

inversion. Hypercalcemia sometimes produces a high takeoff of the J point/ST segment in leads V_1 and V_2 and can thus simulate acute ischemia (see Table 14.11).

Potassium

Hyperkalemia is associated with a distinctive sequence of ECG changes (Fig. 14.46A). The earliest effect usually is narrowing and peaking (or *tenting*) of the T wave. The QT interval is shortened at this stage, reflecting a decreased action potential duration.

Progressive extracellular hyperkalemia reduces atrial and ventricular resting membrane potentials, thereby inactivating sodium channels, which decreases Vmax and conduction velocity. The QRS begins to widen, and P wave amplitude decreases. PR interval prolongation can occur, followed sometimes by second- or third-degree AV block. Complete loss of P waves may be associated with a junctional escape rhythm or putative *sinoventricular rhythm*. In the latter, sinus rhythm persists with conduction (possibly over internodal tracts or muscle bundles) between the sinoatrial and AV nodes but without producing an overt P wave.

Moderate to severe hyperkalemia occasionally induces ST elevations in the right precordial leads (V_1 and V_2), simulating an ischemic current of injury or Brugada-type patterns. Even severe hyperkalemia, however, can be associated with atypical or nondiagnostic ECG findings. Marked hyperkalemia leads to eventual asystole, sometimes preceded by a slow undulatory (or *sine wave*) ventricular flutter-like pattern. The ECG triad of peaked T waves (from hyperkalemia), QT (ST portion) prolongation (from hypocalcemia), and LVH (from hypertension) is strongly suggestive of chronic renal failure (see Chapter 101).

Electrophysiologic changes associated with hypokalemia, by contrast, include hyperpolarization of myocardial cell membranes and increased action potential duration. The major ECG manifestations are ST depression with flattened T waves and increased U wave prominence (see Fig. 14.46B). U waves can exceed the amplitude of T waves, and distinguishing T waves from U waves can be difficult or impossible from the surface ECG. Indeed, apparent U waves in hypokalemia and other pathologic settings may actually be part of T waves whose morphology is altered by the effects of voltage gradients between M, or midmyocardial, cells and adjacent myocardial layers.[6,7] The prolongation of repolarization with hypokalemia, as part of an acquired long QT(U) syndrome, predisposes to the development of torsades de pointes (see Chapter 63) and to tachyarrhythmias during digitalis therapy.

Magnesium. Specific ECG effects of mild to moderate isolated abnormalities in magnesium ion concentration are not well characterized. Severe hypermagnesemia (e.g., serum Mg^{2+} >15 mEq/L) can cause AV and intraventricular conduction disturbances that may culminate in complete heart block and cardiac arrest. Hypomagnesemia usually is associated with hypocalcemia or hypokalemia and can potentiate certain digitalis toxic arrhythmias. The role of magnesium deficiency in the pathogenesis and treatment of the acquired long QT(U) syndrome with torsades de pointes is discussed in Chapters 63 and 67.

Other Factors. Isolated hypernatremia or hyponatremia does not produce consistent effects on the ECG. Acidemia and alkalemia are often associated with hyperkalemia and hypokalemia, respectively. Systemic hypothermia may be associated with the appearance of a distinctive convex elevation at the junction (J point) of the ST segment and QRS complex (J wave or Osborn wave) (Fig. 14.47).[7] The cellular mechanism of this type of pathologic J wave appears to be related to an epicardial-endocardial voltage gradient associated with the localized appearance of a prominent epicardial action potential notch.

Nonspecific QRS and ST-T Changes

Low QRS voltage is considered to be present when the total (positive-to-negative peak) amplitude of the QRS complexes in each of the six extremity leads is 0.5 mV or less or 1.0 mV or less in leads V_1 through V_6. Low QRS voltage, as described earlier, can be caused by a variety of mechanisms, including increased insulation of the heart by air (chronic obstructive pulmonary disease) or adipose tissue (obesity); replacement
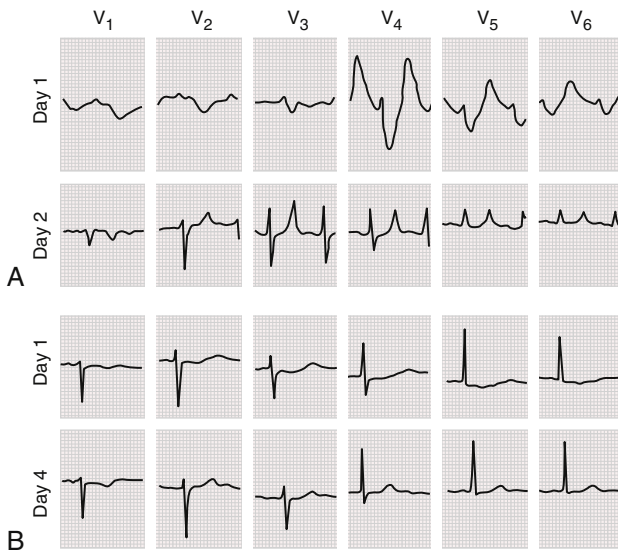
FIGURE 14.46 ECG changes in hyperkalemia (**A**) and hypokalemia (**B**). **A,** On day 1, at a K⁺ level of 8.6 mEq/liter, the P wave is no longer recognizable and the QRS complex is diffusely prolonged. Initial and terminal QRS delays are characteristic of K⁺-induced intraventricular conduction slowing and are best illustrated in leads V_2 and V_6. On day 2, at a K⁺ level of 5.8 mEq/liter, the P wave is recognizable, with a PR interval of 0.24 second; the duration of the QRS complex is approximately 0.10 second, and the T waves are characteristically "tented." **B,** On day 1, at a K⁺ level of 1.5 mEq/liter, the T and U waves are merged. The U wave is prominent and the QU interval is prolonged. On day 4, at a K⁺ level of 3.7 mEq/liter, the tracing is normal. (Courtesy Dr. C. Fisch.)
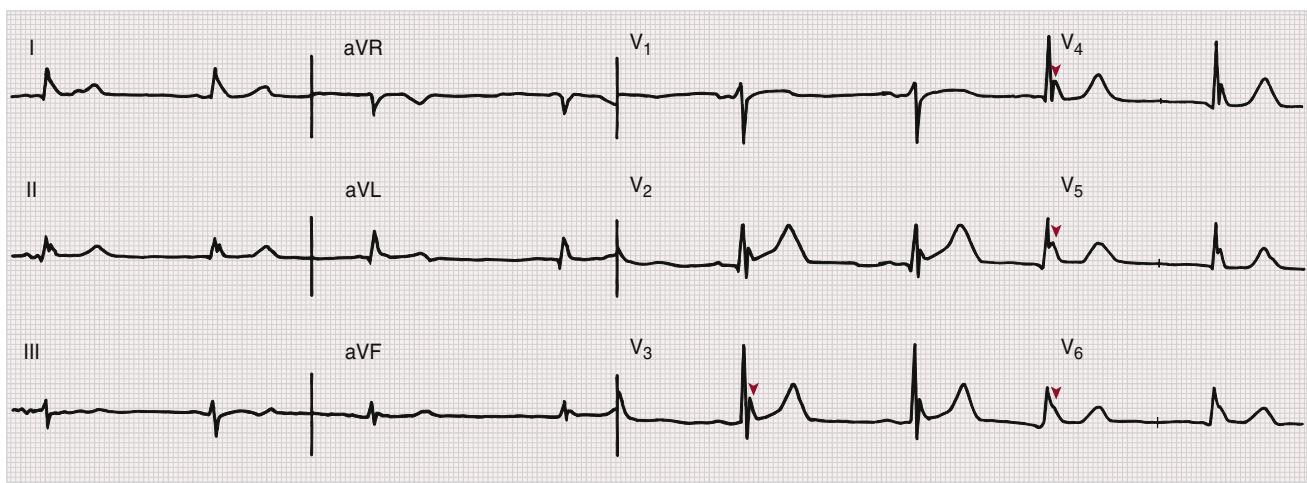
FIGURE 14.47 Systemic hypothermia. *Arrowheads* (leads V_3 through V_6) point to the characteristic convex J waves, termed *Osborn waves.* Prominent sinus bradycardia is also present, along with QT prolongation.
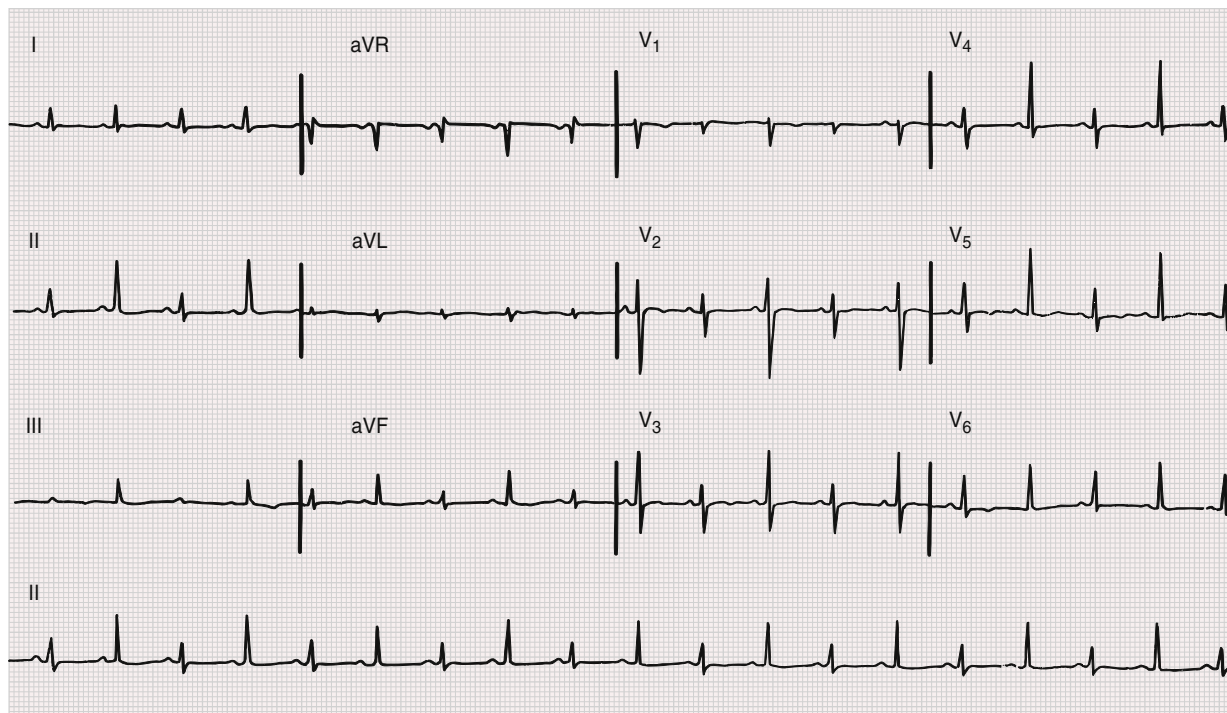
FIGURE 14.48 Total electrical alternans (P-QRS-T) caused by pericardial effusion with tamponade. This finding, particularly in concert with sinus tachycardia and relatively low voltage, is a highly specific, although not sensitive, marker of cardiac tamponade.

of myocardium by fibrous tissue (ischemic or nonischemic cardiomyopathy), amyloid, or tumor; and possibly to short-circuiting (shunting) effects resulting from low resistance of fluids (especially with pericardial or pleural effusions, or anasarca). The combination of relatively low limb voltage (QRS voltage <0.8 mV in each of the limb leads), relatively prominent QRS voltage in the chest leads (S_{V1} or S_{V2} + R_{V5} or R_{V6} >3.5 mV), and slow R wave progression (R wave < S wave amplitude in V_1 through V_4) has been reported as a relatively specific but not sensitive sign of dilated-type cardiomyopathies (initially referred to as the ECG "congestive heart failure triad").[42]

Ventricular repolarization is particularly sensitive to the effects of many factors in addition to ischemia (e.g., postural changes, meals, drugs, hypertrophy, electrolyte and metabolic disorders, central nervous system lesions, infections, pulmonary diseases) that can lead to a variety of *nonspecific ST-T changes*. The term usually is applied to slight ST-segment depression or T wave inversion or to T wave flattening without evident specific cause. Care must be taken not to over interpret such changes, especially in persons with a low prior probability of heart disease. At the same time, subtle repolarization abnormalities can be markers of coronary or hypertensive heart disease or other types of structural heart disease; these probably account for the association of relatively minor but persistent nonspecific ST-T changes with increased cardiovascular mortality in middle-aged and older men and women.

Alternans Patterns

The term *alternans* applies to conditions characterized by the sudden appearance of a periodic beat-to-beat change in some property of cardiac electrical or mechanical behavior. These abrupt changes (AAAA→ABAB pattern) are reminiscent of a generic class of patterns observed in perturbed nonlinear control systems. Many different forms of electrical alternans have been described clinically. Most familiar is total electrical alternans with sinus tachycardia, a specific but not highly sensitive marker of pericardial effusion with tamponade physiology (Fig. 14.48) (see Chapter 86). This finding is associated with an abrupt transition from a 1:1 to a 2:1 pattern in the "to-and-fro" swinging motion of the heart in the effusion.

Other alternans patterns have primary electrical rather than mechanical causes. QRS (and sometimes R-R) amplitude alternans may occur with a number of different types of supraventricular tachycardias.[1] Alternans has long been recognized as a marker of electrical instability of repolarization in cases of acute ischemia, in which it may precede ventricular tachyarrhythmia (see Fig. 14.34). Therefore, considerable interest continues to be directed at the detection of microvolt T wave (or ST-T)
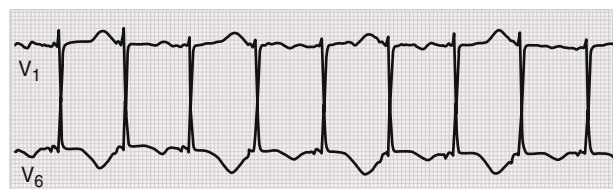
FIGURE 14.49 The QT(U) interval is prolonged (approximately 600 msec) with T-U wave alternans. The tracing was recorded in a patient with chronic renal disease shortly after dialysis. This type of repolarization alternans may be a precursor to torsades de pointes. The underlying rhythm appears to be an ectopic atrial tachycardia. (Courtesy Dr. C. Fisch.)

alternans and its variants[59] as a noninvasive marker for increased risk of ventricular tachyarrhythmias in patients with chronic heart disease (see Chapter 67). Similarly, T-U wave alternans (Fig. 14.49) may be a marker of imminent risk of torsades de pointes in hereditary or acquired long QT syndromes (see Chapter 63). Finally, with aging and advancing cardiovascular disease, fluctuations in heart rate faster than and decoupled from respiration may emerge, including sinoatrial alternans and its variants, under the proposed rubric of heart rate fragmentation.[60]

Clinical Issues in Electrocardiographic Interpretation

The clinical value of the ECG is maximized when an appropriately ordered and technically adequate recording is interpreted by a skilled professional. Key factors include reader competency, technical issues in ECG recording that impact reliability and consistency, and the appropriate application of computer technology and interpretation.

Indications

Numerous professional organizations, including the AHA, the ACC, the American College of Physicians (ACP), the U.S. Preventive Services Task Force (USPSTF), and the American College of Preventive Medicine (ACPM), have proposed appropriateness guidelines for recording an ECG[1] that have been periodically updated on their websites (Section e14.7). These include recommendations for several different populations, including persons with known or suspected heart disease, those without evidence of heart disease, and those in more specific

Monitor lead

A

II

B

FIGURE 14.50 Artifacts simulating serious arrhythmias. **A,** Motion artifact mimicking ventricular tachyarrhythmia. Partly obscured normal QRS complexes (*arrowheads*) can be seen with a heart rate of approximately 100 beats/min. **B,** Parkinsonian tremor causing baseline oscillations mimicking atrial fibrillation. The regularity of QRS complexes may provide a clue to the source of this artifact.

results in an inverted P and QRS waveforms in lead I but not in lead V_6, two leads that would normally be expected to have similar polarities.

The most common precordial electrode errors are placing V_1 and V_2 electrodes in the second or third rather than in the fourth intercostal place and the placement of the V_5 and V_6 electrodes above or below the horizontal line of V_4 or too far laterally. These misplacements may result in changes in R wave progression, accentuation of r′ waves, and ST-segment elevation in the right precordial leads simulating IVCDs or MI. In addition, variation in placement of electrodes between recordings, even small changes, may cause diagnostically confusing changes when relying on serial tracings.

As noted earlier, ECGs recorded using nonstandard electrode locations or altered filter settings such as those used for exercise testing or in intensive care settings are significantly different from those recorded using standard electrode sets. These should not be used for diagnostic purposes.[1]

groups including preoperative patients (see Chapter 23), persons with dangerous occupations, athletes (see Chapter 32), and patients taking medications with electrophysiologic effects.

Reading Competency

Developing and maintaining ECG interpretation are critical to successful clinical practice. It has been reported, however, that as many as one-third of ECG interpretations contain clinically meaningful errors and that over 10% of these lead to inappropriate management decisions.[61] Error rates are higher among noncardiologists than with cardiologists, although error rates among cardiologists as high as 40% have been reported.

A related issue is the common differences in diagnoses even among expert readers, that is, *interreader variability*. One recent study reported that, based on a test set of 20 ECGs read by 21 experts, agreement occurred in only 79% of tracings with evidence of STEMI and in only 37% of cases showing chamber hypertrophy.[1]

Professional organizations have made recommendations to aide in achieving adequate competency. The ACC recommends supervised and documented interpretation of a minimum of 3000 to 3500 ECGs covering a broad spectrum of diagnoses and clinical settings, over a 3-year training period for cardiology fellows.[62] However, the actual adequacy of training and the level of competency of trainees remain limited. In one study, cardiology fellows at an academic institution correctly interpreted only 58% of a test set of ECGs and missed 36% of potentially life-threatening abnormalities.[1] The challenge of adequate training is compounded by the number of physician specialties as well as non-physician professionals with various levels of training performing ECG interpretation.

Technical Errors

Technical errors can lead to clinically significant diagnostic mistakes. Artifacts that interfere with interpretation can result from movement of the patient, poorly secured electrodes, electrical disturbances related to current leakage and grounding failure, and external interference from nearby electrical sources such as stimulators or cauteries. Electrical or motion (e.g., Parkinsonian tremor) artifacts can simulate life-threatening arrhythmias (Fig. 14.50). Body motion can cause excessive baseline wander that may simulate or obscure ST-segment shifts of myocardial ischemia or injury.

Misplacement of one or more electrodes is a common cause for errors. Many limb lead switches produce ECG patterns that can aid in their identification. Reversal of the two arm electrodes, for example,

Computer Interpretation

Computerized interpretation systems have the advantages of reducing analysis and reporting times, providing diagnostic prompts to clinicians to reduce overlooked abnormalities, standardizing criteria and report terminology, and increasing the ability to archive recordings to enhance serial comparisons and population studies.[63,64] The performance of these systems in identifying normal tracings is generally excellent. However, accuracy is lower for specific abnormalities including rhythm disturbances, conduction defects, and paced rhythms. Error rates as high as 30% for pattern-based diagnoses and as high as 40% for arrhythmias have been reported.

Although differences in measurements between manufacturers are clinically small, the differences increase with increasing abnormality in the ECG tracing[65] and differences may be substantial for certain diagnoses, e.g., myocardial ischemia and infarction.[66] Some of these differences may relate to differences between the information provided by analog and digital recordings and variations in methods to determine, for example, the ends of the QRS complex and T wave.[63]

An ongoing concern is common overreliance on computerized interpretations. There is a general consensus that, although computerized diagnostic algorithms have become more accurate and serve as important adjuncts to the clinical interpretation of ECGs, such systems are currently not sufficiently accurate to be relied on in critical clinical environments without expert review.

FUTURE PERSPECTIVES

Clinical electrocardiography represents a mature methodology based on extensive electrophysiologic study and clinical correlations that have evolved over more than a century of study. Several areas for expanded knowledge and clinical relevance may be suggested. These include, as examples, the application of artificial intelligence[67] and "big data"[68] approaches to interpretation and analysis, further development of clinically useful approaches to estimate epicardial potentials from body surface recordings,[69] and enhanced understanding of the genetic and cellular bases for ECG patterns (see Chapters 11 and 62).

GUIDELINES

The Guidelines for Electrocardiography are presented in the online chapter.

REFERENCES

Fundamental Principles

1. Mirvis DM, Goldberger AL. *Electrocardiography. Braunwald's Heart Disease.* 11th ed. Philadelphia, PA: Elsevier Saunders; 2019.
2. Young B, Schmidt JJ. Updates to IEC/AAMI ECG standards: a new hybrid standard. *J Electrocardiol.* 2018;51:S103–S105.
3. Lindow T, Birnbaum Y, Nikus K, et al. Why complicate an important task? An orderly display of the limb leads in the 12-lead electrocardiogram and its implications for recognition of acute coronary syndrome. *BMC Cardiovasc Dis.* 2019;19:13–20.

The Normal Electrocardiogram

4. Rautaharju PM, Zhang Z-M, Haisty WK, et al. Race- and sex-associated differences in rate-adjusted QT, QT$_{peak}$, ST elevation and other regional measures of repolarization: the Atherosclerosis Risk in Communities (ARIC) study. *J Electrocardiol.* 2014;47:342–350.
5. Costa MD, Davis RB, Goldberger AL. Heart rate fragmentation: a new approach to the analysis of cardiac interbeat interval dynamics. *Front Physiol.* 2017;8:255.
6. Opthof T, Janse MJ, Meijborg VM, et al. Dispersion in ventricular repolarization in human, canine and porcine heart. *Prog Biophys Mol Biol.* 2016;120:222–235.
7. Antzelevitch C, Yan GX, Ackerman MJ, et al. J-wave syndromes expert consensus conference report: emerging concepts and gaps in knowledge. *Europace.* 2017;19:665–694.
8. Vink AS, Neumann B, Lieve KVV, et al. Determination and interpretation of the QT interval. *Circulation.* 2018;138:2345–2358.
9. Beinart R, Zhang Y, Lima JC, et al. The QT interval is associated with incident cardiovascular events: the MESA study in the multi-ethnic study of atherosclerosis. *J Am Coll Cardiol.* 2014;65:2111–2119.
10. Waks JW, Sitlani CM, Soliman EZ, et al. Global electrical heterogeneity risk score for prediction of sudden cardiac death in the general population. *Circulation.* 2016;133:2222–2234.
11. Ghadban R, Alpert MA, Dohrmann ML, et al. A QS pattern in leads V_1 and V_2 is associated with septal scarring independent of etiology – a cardiac magnetic resonance imaging study. *J Electrocardiol.* 2018;51:577–582.
12. Patton K, Ellinor PT, Ezekowitz M, et al. Electrocardiographic early repolarization. A scientific statement from the American Heart Association. *Circulation.* 2016;13:1520–1529.
13. Zhang J, Hocini M, Strom M, et al. The electrophysiological substrate of early repolarization syndrome: noninvasive mapping in patients. *JACC Clin Electrophysiol.* 2017;3:894–904.
14. Sharma S, Drezner JA, Baggish A, et al. International recommendations for electrocardiographic interpretation in athletes. *J Am Coll Cardiol.* 2017;69:1057–1075.

The Abnormal Electrocardiogram

15. Soliman EZ, Zhang Z-M, Chen LY, et al. Usefulness of maintaining a normal electrocardiogram over time for predicting cardiovascular health. *Am J Cardiol.* 2017;119:249–255.
16. Bayes de Luna A, Baranchuk A, Robledo LA, et al. Diagnosis of interatrial block. *J Geriatric Cardiol.* 2017;14:161–165.
17. O'Neal WT, Zhang Z-M, Loehr LR, et al. Electrocardiographic advanced intra-atrial block and atrial fibrillation risk in the general population. *Am J Cardiol.* 216; 117:1755-1759.
18. Lacalzada-Almeida J, Izquierdo-Gomez M, Belleyo-Belkasem C, et al. Interatrial block and atrial remodeling assessed using speckled tracking echocardiography. *BMC Cardiovasc Dis.* 2018;18:38–45.
19. Kamel H, O'Neal WT, Okin PM, et al. Electrocardiographic left atrial abnormality and stroke subtype in ARIC. *Ann Neurol.* 2015;78:670–678.
20. Bacharova L. Missing link between molecular aspects of ventricular arrhythmias and QRS complex morphology in left ventricular hypertrophy. *Intern J Molec Sci.* 2019;21:48–65.
21. Bacharova L, Chen H, Estes EH, et al. Determinants of discrepancies and comparison of the prognostic significance of left ventricular hypertrophy by electrocardiographic and cardiac magnetic resonance imaging. *Am J Cardiol.* 2015;115:515–522.
22. Okin PM, Hille DA, Kjeldsen SE, Devereux RB. Combining ECG criteria for left ventricular hypertrophy improves risk prediction in patients with hypertension. *J Am Heart Assoc.* 2017;6:e007564–e007572.
23. Bang CN, Soliman EZ, Simpson LM, et al. Electrocardiographic left ventricular hypertrophy predicts cardiovascular morbidity and mortality in hypertensive patients: the ALLHAT Study. *Am J Hypertension.* 2017;30:914-822.
24. Leigh JA, O'Neal WT, Soliman EZ. Electrocardiographic left ventricular hypertrophy as a predictor of cardiovascular disease independent of left ventricular anatomy in subjects >65 years. *Am J Cardiol.* 2016;117:1831–1835.
25. Inoue YY, Soliman EZ, Yoneyama K, et al. Electrocardiographic strain pattern is associated with left ventricular concentric remodeling, scar, and mortality over 10 years: the Multi-ethnic Study of Atherosclerosis. *J Am Heart Assoc.* 2017;6:e006624–e0006632.
26. De Lazzari M, Zorzi A, Cipriani A, et al. Relationship between electrocardiographic findings and cardiac magnetic resonance phenotypes in arrhythmogenic cardiomyopathy. *J Am Heart J.* 2018;7:e009855–e009865.
27. Kowal J, Ahmad MI, Li Y, Soliman EZ. Prognostic significance of electrocardiographic right ventricular hypertrophy in the general population. *J Electrocardiol.* 2019;54:49–53.
28. Carroll BJ, Heidinger BH, Dabreo DC, et al. Multimodality assessment of right ventricular strain in patients with acute pulmonary embolism. *Am J Cardiol.* 2018;122:175–181.
29. Kusumoto FM, Schoenfeld MH, Barrett C, et al. 2018 ACC/AHA/HRS guidelines on the evaluation and management of patients with bradycardia and cardiac conduction delay. *Heart Rhythm.* 2019;16:e128–e153.
30. Elizari MV. The normal variants in the left bundle branch system. *J Electrocardiol.* 2017;50:389–399.
31. Upadhyay GA, Cherlan T, Shatz DY, et al. Intracardiac delineation of septal conduction in left bundle branch block. *Circulation.* 2019;139:1876–1888.
32. Senesael E, Calle S, Kamoen V, et al. Progression of incomplete toward complete left bundle branch block: a clinical and electrocardiographic analysis. *Ann Noninvasive Electrocardiol.* 2020;25:e12732.
33. Zhang ZM, Rautaharju PM, Prineas RJ, et al. Bundle branch blocks and the risk of mortality in the Atherosclerosis Risk in Communities study. *J Cardiovasc Med.* 2016;17:411–417.
34. Stokke IM, Li B, Cicala S, et al. Association of left bundle branch block with new onset abnormal wall motion in treated hypertensive patients with left ventricular hypertrophy: the LIFE Echo Sub-Study. *Blood Press.* 2019;28:84–92.

35. Smiseth OA, Aalen JM. Mechanism of harm from left bundle branch block. *Trends Cardiovasc Med.* 2019;29:335–342.
36. Xiong Y, Wang L, Liu W, et al. The prognostic significance of right bundle branch block: a meta-analysis of prospective cohort studies. *Clin Cardiol.* 2015;38:604–613.
37. Devarapally SR, Arora S, Ahmad S, et al. Right ventricular failure predicted from right bundle branch block: cardiac magnetic resonance imaging validation. *Cardiovasc Diagn Ther.* 2016;6:432–438.
38. Sillanmaki S, Gimelli A, Ahmad S, et al. Mechanisms of left ventricular dyssynchrony: a multinational SPECT study of patients with bundle branch block. *J Nucl Cardiol.* 2020. Feb 14. doi: 10.1007/s12350-020-02054-y. Epub ahead of print .
39. Palmisano P, Ziachhi M, Ammendola E, et al. Long-term progression of rhythm and conduction disturbances in pacemaker recipients: findings from the pacemaker expert programming study. *J Cardiovasc Med.* 2018;19:357–365.
40. Eschaller R, Ploux S, Ritter P, et al. Nonspecific intraventricular conduction delay: definitions, prognosis and implications for cardiac resynchronization therapy. *Heart Rhythm.* 2015;12:1071–1079.
41. Rattanawong P, Riangwiwat T, Kanitsoraphan C, et al. Baseline fragmented QRS increases the risk of major arrhythmic events in hypertrophic cardiomyopathy: systematic review and meta-analysis. *Ann Noninvasive Electrocardiol.* 2018;23:e12533–e12540.
42. Goldberger AL, Goldberger ZD, Shvilkin A. *Goldberger's Clinical Electrocardiography: A Simplified Approach.* 9th ed. Philadelphia: Elsevier; 2017.
43. AHA/ACC clinical performance and quality measures for adults with ST-elevation and non-ST-elevation myocardial infarction: a report of the American College of Cardiology/American Heart Association task force on performance measures. *Circulation.* 2017;10:2048–2090.
44. Chew DS, Wilton SB, Kavanagh K, et al. Fragmented QRS complexes after acute myocardial infarction are independently associated with unfavorable left ventricular remodeling. *J Electrocardiol.* 2018;51:607–612.
45. Thygesen K, Alpert JS, Jaffe AS, et al. Fourth universal definition of myocardial infarction. *J Am Coll Cardiol.* 2018;72:2231–2264.
46. Barrabés JA, Figueras J, Moure C, et al. Prognostic value of lead aVR in patients with a first non–ST-segment elevation acute myocardial infarction. *Circulation.* 2016;108:814–819.
47. Meyers HP, Limkakeng Jr AT, Jaffa EJ, et al. Validation of the modified Sgarbossa criteria for acute coronary occlusion in the setting of left bundle branch block: a retrospective case-control study. *Am Heart J.* 2015;170:1255–1264.
48. Lu ML, Nwakile C, Bhalla V, et al. Prognostic significance of abnormal P wave morphology and PR-segment displacement after ST-elevation myocardial infarction. *Int J Cardiol.* 2015;197:216–221.
49. Lu ML, De Venecia T, Patnaik S, et al. Atrial myocardial infarction: a tale of the forgotten chamber. *Int J Cardiol.* 2016;202:904–909.
50. Hendren NS, Drazner MH, Bozkurt B, Cooper Jr LT. Description and proposed management of the acute COVID-19 cardiovascular syndrome. *Circulation.* 2020;141:1903–1914.
51. Clerkin KJ, Fried JA, Raikhelkar J, et al. COVID-19 and cardiovascular disease. *Circulation.* 2020;19:1648–1655.
52. Templin C, Ghadri JR, Diekmann J, et al. Clinical features and outcomes of takotsubo (stress) cardiomyopathy. *N Engl J Med.* 2015;373:929–938.
53. de Chazal HM, Del Buono MG, Keyser-Marcus L, et al. Stress cardiomyopathy diagnosis and treatment: JACC state-of-the-art review. *J Am Coll Cardiol.* 2018;72:1955–1971.
54. Frangieh AH, Obeid S, Ghadri JR, et al. ECG criteria to differentiate between Takotsubo (stress) cardiomyopathy and myocardial infarction. *J Am Heart Assoc.* 2016;5:e003418.
55. Shvilkin A, Huang HD, Josephson ME. Cardiac memory: diagnostic tool in the making. *Circ Arrhythm Electrophysiol.* 2015;8:475–482.
56. Siontis KC, Wen S, Asirvatham SJ. Cardiac memory for the clinical electrophysiologist. *J Cardiovasc Electrophysiol.* 2019;30:2140–2143.
57. Corrado D, van Tintelen PJ, McKenna WJ, et al. Arrhythmogenic right ventricular cardiomyopathy: evaluation of the current diagnostic criteria and differential diagnosis. *Eur Heart J.* 2020;41:1414–1429.
58. Saleh M, Gabriels J, Chang D, et al. Effect of chloroquine, hydroxychloroquine and azithromycin on the corrected QT interval in patients with SARS-CoV-2 infection. *Circ Arrhythm Electrophysiol.* 2020;13:e008662.
59. Krokhaleva Y, Patel D, Shah H, et al. Increased nonalternans repolarization variability precedes ventricular tachycardia onset in patients with implantable defibrillators. *Pacing Clin Electrophysiol.* 2016;39:140–148.
60. Costa MD, Goldberger AL. Heart rate fragmentation: using cardiac pacemaker dynamics to probe the pace of biological aging. *Am J Physiol Heart Circ Physiol.* 2019;316:H1341–H1344.

Clinical Issues in Electrocardiographic Interpretation

61. Breen CJ, Kelly GP, Kernohan WC. ECG interpretation skill acquisition: a review of learning, teaching and assessment. *J Electrocardiol.* 2019;S0022–0736(18):30641–1.
62. Balady GJ, Bufalino VJ, Gulati M, et al. COCATS 4 Task Force 3: training in electrocardiography, ambulatory electrocardiography, and exercise testing. *J Am Coll Cardiol.* 65:1763–1777.
63. Macfarlane PW, Mason JW, Kligfield P, et al. Debatable issues in automated ECG reporting. *J Electrocardiol.* 2017;50:833–840.
64. Schlepfer J, Willens HJ. Computer-interpreted electrocardiograms. Benefits and limitations. *J Am Coll Cardiol.* 2017;70:1183–1192.
65. Kligfield P, Badilini F, Denjoy I, et al. Comparison of automated interval measurements by widely used algorithms in digital electrocardiography. *Am Heart J.* 2018;200:1–10.
66. Garvey JL, Zegre-Hemey J, Gregg R, Studnek JR. Electrocardiographic diagnosis of ST segment elevation myocardial infarction: an evaluation of three standard interpretation algorithms. *J Electrocardiol.* 2016;49:728–732.

Future Perspectives

67. Lyon A, Minchole A, Martinez JP, et al. Computational techniques for ECG analysis and interpretation in light of their contribution to medical advances. *J R Soc Interface.* 2018;15:20170821–21070829.
68. Estes EH. Big data and the electrocardiogram. *J Electrocardiol.* 2015;48:29–30.
69. Rudy Y. Noninvasive ECG mapping (ECGI): mapping the arrhythmic substrate of the human heart. *Int J Cardiol.* 2017;237:13–14.

GUIDELINES: ELECTROCARDIOGRAPHY

David M. Mirvis and Ary L. Goldberger

Numerous professional organizations have proposed appropriateness guidelines for recording an ECG. These may be considered for several different populations—persons with known or suspected heart disease, those without evidence of heart disease, and those in more specific groups including preoperative patients, persons with dangerous occupations, athletes, and patients taking medications with electrophysiologic effects.

PATIENTS WITHOUT KNOWN OR SUSPECTED CARDIOVASCULAR DISEASE

The goals of ECG screening of asymptomatic persons with an ECG include identifying occult disorders, providing better risk assessment that may guide further testing and treatment, possibly providing a baseline for future tracings, and ultimately reducing cardiovascular morbidity and mortality. Establishing guidelines for this group, whether at low, intermediate, or high risk by other assessment tools, has been hampered by the limited number of studies specifically assessing the efficacy of the screening ECG in meeting these goals. This limitation has been acknowledged by several professional organizations including the American Heart Association (AHA) and the American College of Cardiology (ACC),[1,2] the American College of Physicians (ACP),[3] the U.S. Preventive Services Task Force (USPSTF),[4] and the American College of Preventive Medicine (ACPM).[5]

These organizations recognize that ECG abnormalities are common among asymptomatic persons, that certain ECG findings do have prognostic value, and that some reports have presented evidence of small improvements in risk stratification.[2,4] However, they also concluded that the available data that screening can improve management or outcomes is inadequate to make sound recommendations for screening for this very large population.

Thus, professional organizations, including the ACP, USPSTF and ACPM, recommend against routine screening of asymptomatic, low-risk populations. Likewise, the USPSTF[4] concluded that the existing data are insufficient to make a definitive recommendation about the relative benefits and risks of a routine screening ECG for asymptomatic persons with moderate to high risk of events (>10% likelihood of a major cardiac event within 10 years, based on other risk factor analyses).

The ACC/AHA guidelines[2] (Table 14G.1) suggest that an ECG "is reasonable" for cardiovascular risk assessment in asymptomatic persons with diabetes or hypertension. For those at low risk, they recommend that a screening ECG "may be considered." Both recommendations are based primarily on consensus opinion and current practice standards rather than on controlled trials.

In addition to limited evidence of benefit, possible negative effects of routine screening exist. These include high rates of false-positive results that may lead to unnecessary, expensive, and potentially hazardous noninvasive and invasive diagnostic testing, overtreatment, psychological stress, and labeling that may impact employment, insurance coverage, and athletic participation.[6] For example, in one series of over 36 million low-risk subjects, persons who had a routine ECG were five times more likely to have subsequent referrals or testing with no difference in clinical outcomes.[6] In addition, initiating screening programs also requires provisions for follow-up and management of any abnormality that is found.

PATIENTS WITH KNOWN OR SUSPECTED CARDIOVASCULAR DISEASE

Guidelines published jointly by the ACC and the AHA[1] for patients with known or suspected cardiovascular disease are summarized in Table 14G.2. They support the use of ECGs as part of the baseline evaluation of all patients with known or clinically suspected cardiovascular disease and during follow-up for assessment of changes in signs, symptoms, or laboratory testing.

Follow-up ECGs were not considered appropriate for patients with mild chronic cardiovascular conditions that are not deemed likely to progress (e.g., mild mitral valve prolapse) and are not considered to be appropriate at each visit for patients with stable heart disease who are seen frequently (e.g., within 4 months) without evidence of clinical change. ECGs may be appropriate after significant intervals (usually 1 year or longer) in the absence of clinical changes. The use of the ECG in these cases is based largely on clinical impressions and judgement.

Tracings are also appropriate after initiating therapy known to produce ECG changes that correlate with therapeutic responses or progression of disease, or that may cause adverse effects detected or predicted by the ECG, e.g., antiarrhythmic therapy and treatments with drugs known to prolong the QT interval. Serial tracings may also be appropriate until the response to therapy has stabilized.

SPECIAL POPULATIONS

Persons with Dangerous or Physically Demanding Occupations

Professional groups, including USPSTF[4] and AHA,[1] recognize the potential for benefit for screening persons with jobs that endanger themselves or others (such as airline pilots and bus drivers) or that require an unusual level of physical exertion (such as firefighters). Although no specific data defining the value of routine screening are available, a screening ECG with appropriate follow-up is considered reasonable. For example, the U.S. Federal Aviation Administration currently requires an ECG at age 35 and annually after age 40 for first-class commercial airplane pilots.

Preoperative Evaluation

The common practice of routinely recording an ECG before noncardiac surgery in patients without other indications has been based on the putative value of the ECG in predicting intraoperative or postoperative events and as a baseline for comparison if a later event occurs. However, most (although not all) studies have documented the absence of or limited value of the routine preoperative ECG in identifying patients with coronary artery disease and in predicting postoperative outcomes.[7–9] In observational studies, for example, abnormal preoperative ECGs resulted in cancellation or changes in management in only 0.46% to 2.6% of cases.[7]

Thus the ACC/AHA[8] concluded that a routine preoperative ECG is "reasonable" based on limited randomized or nonrandomized studies for patients with known coronary heart, peripheral vascular, or cerebrovascular disease, with significant arrhythmias, or with other structural heart diseases, except for those undergoing low-risk procedures. For asymptomatic persons, the ACC/AHA indicated that an ECG "may be considered" except for low-risk surgeries. For those undergoing low-risk surgeries, a preoperative ECG was found to have no benefit. However, for each recommendation, the level of evidence was limited.

Likewise, the European Society of Cardiology[9] and the American Society of Anesthesiologists Task Force on Preanesthesia Evaluation[7] have concluded that a preoperative ECG is not indicated for patients undergoing low-risk procedures who do not have risk factors. They do suggest that preoperative testing may be performed on a selective basis based on the clinical features of individual patients. Important clinical characteristics may include cardiovascular or respiratory disease, known cardiovascular risk factors, or risk factors and the patient's age. One study suggested that adhering to guidelines in low-risk operations would result in an annual reduction in U.S. health care costs of over $1.8 billion.[10]

Screening of Athletes

The requirement for an ECG as part of the preparticipation clinical evaluation of competitive athletes remains very controversial; this issue is treated more fully in Chapter 32. The European Society of Cardiology[11] recommends including the ECG as part of required, routine preparticipation medical assessment. This recommendation is based on studies that have reported an added diagnostic value of the ECG for detecting the most common underlying causes of athlete deaths, and the experience of the 30-year national screening program in Italy to prospectively identify these abnormalities and that greatly reduced the occurrence of sudden death by facilitating the disqualification of high-risk affected persons.[12,13] For example, Williams et. al. reported substantially higher sensitivity, specificity, and positive predictive values with ECG screening than with history and physical examination.[14] The Canadian Cardiovascular Society[15] as well as other international organizations have supported and implemented these recommendations for mandatory screening, and they have been followed by international professional and amateur sport leagues and associations.[12]

The AHA and the ACC, in contrast, have consistently argued against routine preparticipation ECG screening.[16] Rather, they recommend a complete 14-point clinical evaluation based on history and physical examination with a follow-up ECG only if suggestive abnormalities are discovered. Reasons for this position include the limited and conflicting data on the benefits and reductions in cardiovascular mortality; the significant false-positive

TABLE 14G.1 ACC/AHA Guidelines for Electrocardiography in Patients with No Apparent or Suspected Heart Disease or Dysfunction*

SETTING	CLASS I (SHOULD BE PERFORMED)[†]	CLASS II (REASONABLE TO PERFORM {CLASS IIA} OR MAY BE CONSIDERED {CLASS IIB})	CLASS III (NO BENEFIT)
Baseline or initial evaluation	Before administration of pharmacologic agents known to be associated with a high incidence of cardiovascular effects (e.g., antineoplastic agents). People of any age in special occupations that require very high cardiovascular performance (e.g., firefighters, police officers) or whose cardiovascular performance is linked to public safety (e.g., pilots, air traffic controllers, critical process operators, bus or truck drivers, railroad engineers)	Initial evaluation of patients with risk factors such as diabetes and hypertension	Routine screening, risk assessment, or as a baseline in asymptomatic, low-risk persons
Response to therapy	To evaluate patients in whom prescribed therapy is known to produce cardiovascular effects	None	To assess treatment not known to produce any cardiovascular effects
Follow-up	To evaluate interval changes in symptoms or signs	None	To evaluate asymptomatic adults who have had no interval change in symptoms, signs, or risk factors
Before surgery	Patients being evaluated as donor for heart transplantation or as recipient of noncardiopulmonary transplant	Patients undergoing vascular or other high-risk procedures	Asymptomatic persons undergoing low-risk procedures

*Based on published recommendations of the American College of Cardiology/American Heart Association (ACC/AHA) as described in the text.[1,2]
[†]Classifications are based on those used by Greenland and colleagues.[2]

TABLE 14G.2 ACC/AHA Guidelines for Electrocardiography in Patients with Known or Suspected Cardiovascular Disease or Dysfunction*

INDICATION	CLASS I (SHOULD BE PERFORMED)	CLASS II (REASONABLE TO PERFORM {CLASS IIA} OR MAY BE CONSIDERED {CLASS IIB})	CLASS III (NO BENEFIT)
Baseline or initial evaluation	All patients	None	None
Response to therapy	Patients in whom prescribed therapy is known to produce changes in the ECG that correlate with therapeutic responses or progression of disease or adverse effects	Patients prescribed drugs known to alter serum electrolyte concentrations	Patients receiving pharmacologic or nonpharmacologic therapy not known to produce changes in the ECG or to affect conditions that may be associated with such changes.
Follow-up evaluation	Patients with a new or a change in symptoms, signs, or laboratory findings related to cardiovascular status. Patients with an implanted pacemaker device. Patients with cardiovascular disease in the absence of new symptoms or signs after an interval of time appropriate for the condition or disease.	None	Adult patients whose cardiovascular condition is usually benign, stable, and unlikely to progress. Adult patients with chronic stable heart disease seen at frequent intervals (e.g., 4 months) without unexplained findings.

*Based on published recommendations of the American College of Cardiology/American Heart Association (ACC/AHA).[1,2]
[†]Classifications are based on those used by Greenland and colleagues.[2]

rate due to the common occurrence of ECG abnormalities in athletes that mimic but that are not caused by various disorders, leading to the inappropriate disqualification of many athletes and the need for unnecessary secondary testing; the significant false-negative rate related to common congenital and acquired disorders related to sudden death that do not cause resting ECG abnormalities; the substantial interobserver variability in interpretation that limits the reproducibility and reliability of findings: the differences in diagnoses among various interpretive criteria; and the financial and resource limitations to implement routine screening.[12] The U.S. national football, baseball, hockey leagues[12] as well as the National Collegiate Athletic Association (NCAA)[17] and the American Medical Society for Sports Medicine[18] do not mandate screening ECG recordings.

The NCAA, the AHA, and other groups that do and do not support mandatory screening do suggest that local, community, or institutional programs may institute screening ECGs if (1) athletes are well informed about the potential benefits and limits of the test, (2) tests are performed by adequately trained staff and interpreted based on accepted criteria for abnormalities in athletic hearts, and (3) appropriate cardiologic oversight and backup provide secondary testing if ECG abnormalities are found.

Recommendations may support a standard 12-lead ECG as part of routine evaluation for all athletes older than 40 seeking to engage in competitive sports. No conclusive data exist on the value of ECG screening for recreational athletes of any age.

Cardioactive Drug Administration

Numerous cardiac and noncardiac drugs have potentially harmful electrophysiologic effects that may be associated with ECG changes. These include, among many others, antiarrhythmic agents, antineoplastic agents, methadone, tricyclic antidepressants and other psychotropic agents, stimulants, and illicit drugs.[1] As indicated earlier (see Table 14G.1), recording an ECG prior to initiating drugs with possible electrophysiologic effects is appropriate.[1]

More specific guidelines have been published for selected agents. These include methadone treatment[19]; treatment for schizophrenia, bipolar and depressive syndromes[20,21]; and therapy for attention-deficit hyperactivity disorder.[22]

REFERENCES

1. Schlant RC, Adolph RJ, DiMarco JP, et al. Guidelines for electrocardiography. a report of the ACC/AHA task force on assessment of diagnostic and therapeutic cardiovascular procedures (committee on electrocardiography). *Circulation*. 1992;85:1221–1228.
2. Greenland P, Alpert JS, Beller GA, et al. 2010 ACCF/AHA guidelines for assessment of cardiovascular risk in asymptomatic adults. *Circulation*. 2010;122(25):e584–636.
3. Chou R. For the High Value Care Task Force of the American College of Physicians. Cardiac screening with electrocardiography, stress echocardiography, or myocardial perfusion imaging: advice for High-Value Care from the American College of Physicians. *Ann Intern Med*. 2015;162:438–447.
4. US Preventive Services Task Force (USPSTF). Screening for coronary heart disease with electrocardiography: USPSTF recommendation statement. *J Am Med Assoc*. 2018;319:2308–2314.
5. Lim LS, Haq M, Mahmood S, et al. Atherosclerotic cardiovascular disease screening in adults. American college of preventive medicine position statement on preventive medicine. *Am J Prev Med*. 2011;40:380–381.
6. Batia RS, Bouck Z, Ivers NM, et al. Electrocardiograms in low-risk patients undergoing an annual health examination. *JAMA Intern Med*. 2017;177:1326–1333.
7. Pasternak LR, Arens JF, Caplan RA, et al. Practice advisory for preanesthesia evaluation. An updated report by the American Society of Anesthesiologists Task Force on preanesthesia evaluation. *Anesthesiology*. 2012;116:522–538.
8. Fleisher LA, Fleischman KE, Auerbach AD, et al. 2014 ACC/AHA guideline on perioperative cardiovascular evaluation and care for noncardiac surgery. *J Am Coll Cardiol*. 2014;64:e778–e333.
9. Joint Task Force on Non-Cardiac Surgery 2014 ESC/ESA guidelines on non-cardiac surgery: cardiovascular assessment and management. *Eur Heart J*. 2014;35:2381–2431.
10. Langell JT, Bledsoe A, Vijaykumar S, et al. Implementation of national practice guidelines to reduce waste and optimize patient value. *J Surg Res*. 2016;203:287–292.
11. Corrado D, Pellicia A, Bjornstad HH, et al. Cardiovascular pre-participation screening of young competitive athletes for prevention of sudden death: proposal for a common European protocol. *Eur Heart J*. 2005;26:516–524.
12. Mont L, Pellicia A, Sharma S, et al. Pre-participation cardiovascular evaluation for athletic participants to prevent sudden death. *Europace*. 2017;19:139–163.
13. Pellicia A, Maron BJ. Preparticipation cardiovascular evaluation of the competitive athlete: perspectives from the 30-year Italian experience. *Am J Cardiol*. 1995;75:827–829.
14. Williams EA, Pelto HF, Toresdahl BG, et al. Performance of the American Heart Association (AHA) 14-point evaluation versus electrocardiography for the cardiovascular screening of high school athletes: a prospective study. *J Amer Heart Assoc*. 2019;8:e012235–e012243.
15. McKinney J, Johri AM, Poirer P, et al. Canadian Cardiovascular Society cardiovascular screening of competitive athletes: the utility of the screening electrocardiogram to predict sudden cardiac death. *Canadian Heart J*. 2019;35:1557–1566.
16. Maron BJ, Friedman RA, Kligfield P, et al. Assessment of the 12-lead ECG as a screening test for detection of cardiovascular disease in healthy general populations of young people (12-25 years of age). *Circulation*. 2014;130:1303–1304.
17. Hainline B, Drezner JA, Baggish A, et al. Inter-association consensus statement on cardiovascular care of college student-athletes. *J Am Coll Cardiol*. 2016;67:2981.
18. Drezner JA, O'Connor FG, Harmon KG, et al. AMSSM position statement on cardiovascular preparticipation screening in athletes: current evidence, knowledge gaps, recommendations and future directions. *Br J Sports Med*. 2017;51:153–167.
19. Chou R, Cruciani RA, Fiellin DA, et al. Methadone safety: a clinical practice guideline from the American Pain Society and College on Problems of Drug Dependence, in collaboration with the Heart Rhythm Society. *J Pain*. 2014;15:321–337.
20. Gutgesell H, Atkins D, Barst R, et al. Cardiovascular monitoring of children and adolescents receiving psychotropic drugs. *Circulation*. 1999;99:972–982.
21. Brouillette J, Nattel S. A practical approach to avoiding cardiovascular adverse effects of psychoactive medications. *Can J Cardiol*. 2017;33:1577–1586.
22. Vetter VL, Elia J, Erickson C, et al. Cardiovascular monitoring of children and adolescents with heart disease receiving medications for attention deficit/hyperactivity disorder. *Circulation*. 2008;117:2407–2423.